US Army Corps of Engineers

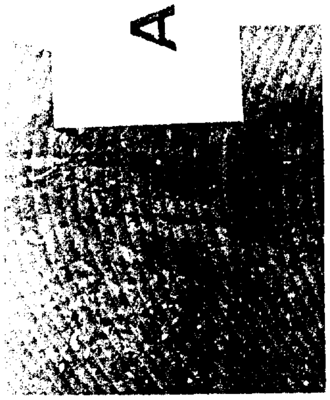

REPAIR, EVALUATION, MAINTENANCE, AND REHABILITATION RESEARCH PROGRAM

TECHNICAL REPORT REMR-GT-3

GEOTECHNICAL ASPECTS OF ROCK EROSION IN EMERGENCY SPILLWAY CHANNELS

Report 4

GEOLOGIC AND HYDRODYNAMIC CONTROLS ON THE MECHANICS OF KNICKPOINT MIGRATION

by

James H. May

Geotechnical Laboratory

DEPARTMENT OF THE ARMY
Waterways Experiment Station, Corps of Engineers
3909 Halls Ferry Road, Vicksburg, Mississippi 39180-6199

December 1989

Report 4 of a Series

Approved For Public Release; Distribution Unlimited

Prepared for DEPARTMENT OF THE ARMY
US Army Corps of Engineers
Washington, DC 20314-1000

Under Civil Works Work Unit 32317

The following two letters used as part of the number designating technical reports of research published under the Repair, Evaluation, Maintenance, and Rehabilitation (REMR) Research Program identify the problem area under which the report was prepared:

	Problem Area		Problem Area
CS	Concrete and Steel Structures	EM	Electrical and Mechanical
GT	Geotechnical	EI	Environmental Impacts
HY	Hydraulics	OM	Operations Management
CO	Coastal		

COVER PHOTOS:

TOP — Accelerated erosion at a knickpoint produced by relatively low discharge and unventing beneath waterfall.

MIDDLE — Knickpoint in emergency spillway at Brownwood, Texas.

BOTTOM — Failure of DMAD spillway (Utah) due to knickpoint migration.

Unclassified

SECURITY CLASSIFICATION OF THIS PAGE

REPORT DOCUMENTATION PAGE

Form Approved OMB No. 0704-0188

1a. REPORT SECURITY CLASSIFICATION: Unclassified	1b. RESTRICTIVE MARKINGS
2a. SECURITY CLASSIFICATION AUTHORITY	3. DISTRIBUTION/AVAILABILITY OF REPORT: Approved for public release; distribution unlimited
2b. DECLASSIFICATION/DOWNGRADING SCHEDULE	
4. PERFORMING ORGANIZATION REPORT NUMBER(S): Technical Report REMR-GT-3	5. MONITORING ORGANIZATION REPORT NUMBER(S)
6a. NAME OF PERFORMING ORGANIZATION: USAEWES Geotechnical Laboratory; 6b. OFFICE SYMBOL (If applicable)	7a. NAME OF MONITORING ORGANIZATION
6c. ADDRESS (City, State, and ZIP Code): 3909 Halls Ferry Road, Vicksburg, MS 39180-6199	7b. ADDRESS (City, State, and ZIP Code)
8a. NAME OF FUNDING/SPONSORING ORGANIZATION: US Army Corps of Engineers; 8b. OFFICE SYMBOL (If applicable)	9. PROCUREMENT INSTRUMENT IDENTIFICATION NUMBER
8c. ADDRESS (City, State, and ZIP Code): Washington, DC 20314-1000	10. SOURCE OF FUNDING NUMBERS: PROGRAM ELEMENT NO. / PROJECT NO. / TASK NO. / WORK UNIT ACCESSION NO.

11. TITLE (Include Security Classification)
Geotechnical Aspects of Rock Erosion in Emergency Spillway Channels; Report 4: Geologic and Hydrodynamic Controls on the Mechanics of Knickpoint Migration

12. PERSONAL AUTHOR(S)
May, James H.

13a. TYPE OF REPORT	13b. TIME COVERED	14. DATE OF REPORT (Year, Month, Day)	15. PAGE COUNT
Final report	FROM ____ TO ____	December 1989	138

16. SUPPLEMENTARY NOTATION
See reverse

17. COSATI CODES			18. SUBJECT TERMS (Continue on reverse if necessary and identify by block number)		
FIELD	GROUP	SUB-GROUP	Rock	Knickpoint	Hydraulic structures
			Rock mass	Headcutting	
			Erosion	Spillways	

19. ABSTRACT (Continue on reverse if necessary and identify by block number)

During the last decade, occurrences of emergency spillway discharges at Soil Conservation Service, Corps of Engineers, and private reservoirs have increased and, in certain circumstances, resulted in erosional damages to the spillways. Rapid headward erosion in unlined emergency spillways at Corps of Engineers reservoirs including Grapevine, Saylorville, and Black Butte caused the Corps to take a serious look at the available methods used to predict erosion damage in unlined emergency spillways. The catastrophic loss of private and Soil Conservation Service reservoirs because of knickpoint migration in emergency spillway channels was additional evidence that the mechanics of knickpoint erosion were not clearly understood. Severe erosion was documented at several Corps spillways where the flow was less than one-tenth of the designed capacity.

(Continued)

20. DISTRIBUTION/AVAILABILITY OF ABSTRACT: ☒ UNCLASSIFIED/UNLIMITED ☐ SAME AS RPT ☐ DTIC USERS	21. ABSTRACT SECURITY CLASSIFICATION: Unclassified	
22a. NAME OF RESPONSIBLE INDIVIDUAL	22b. TELEPHONE (Include Area Code)	22c. OFFICE SYMBOL

16. SUPPLEMENTARY NOTATION (Continued).

A report of the Geotechnical problem area of the Repair, Evaluation, Maintenance, and Rehabilitation (REMR) Research Program. This report is available from the National Technical Information Service, 5285 Port Royal Road, Springfield, VA 22161.

19. ABSTRACT (Continued).

Preliminary research revealed that the severe cases of knickpoint erosion were usually caused by the mass failure of large blocks of material and not by the tractive force scour of individual grains. The details of the mechanisms which actually caused the mass failures were largely unknown. Without an understanding of these mechanisms it would not be possible to develop scale hydraulic models or computer models.

The purpose of this research was to study knickpoint erosion phenomena with respect to the combined effects of the geologic and hydrodynamic controls. In order to study the mechanisms working at the knickpoint, several obstacles had to be overcome. First a material had to be developed which would erode like rock but would keep the eroding water clear so that the failure mechanisms could be observed. Sodium silicate and gelatin-cemented gravel in combination with Plexiglass were used to simulate knickpoints in layered rock. Next, a hydraulic flume had to be modified to accommodate layered samples.

The designed drop structure, which is constructed in streams or channels to dissipate erosive energy, was used as an analog to study the knickpoint phenomena. The research revealed that the potential for headward knickpoint erosion is controlled by the geometry of the knickpoint, the velocity of eroding water, and the pressure underneath the nappe. The geometry of the knickpoint is in turn controlled by the site-specific geology. The erosion rate was found to increase significantly when the thickness of the erodible lower layer in a two-layer model exceeded the diameter of the back roller at the toe of the knickpoint.

It was found that headward erosion in the flume could be controlled or completely stopped by controlling the pressure underneath the nappe. Headward erosion was orders of magnitude greater when the area underneath the nappe was not vented to the atmosphere. The development of an unvented condition was found to cause rapid headward erosion at flow conditions well below the maximum discharge.

PREFACE

This study addresses rock erosion in emergency spillway channels, a problem area of the Repair, Evaluation, Maintenance, and Rehabilitation (REMR) Research Program being conducted by the US Army Engineer Waterways Experiment Station (WES).

This fourth report of a series summarizes work performed during FY 88. Results of work currently in progress and ongoing research programs will be topics of a final report to be completed during FY 89. This study was under the direct supervision of Mr. J. S. Huie, the Problem Area Leader, and Dr. James H. May, the Principal Investigator, Engineering Geology and Rock Mechanics Division (EGRMD), Geotechnical Laboratory (GL). General supervision was provided by Dr. Lawson M. Smith, Chief, Engineering Geology Applications Group (EGAG), EGRMD; Dr. D. C. Banks, Chief, EGRMD; and Dr. W. F. Marcuson III, Chief, GL. The REMR Program Manager was William F. McCleese, Structures Laboratory.

This report was written by Dr. May and represents a portion of the writer's doctoral dissertation at the Center for Engineering Geosciences, Texas A&M University (TAMU). Appreciation is extended to the doctoral committee chairman, Dr. Christopher C. Mathewson; and to the committee members, Drs. Robert R. Berg, Patrick A. Domenico, Earl R. Hoskins, Wayne A. Dunlap, and Thomas N. Adair. Recognition is given to Mr. Garrett Jackson, University of Arizona, who served as laboratory assistant during much of the testing. The technical contributions of Mr. John B. Palmerton and Mr. Dale Barefoot, GL, Mr. Kerry D. Cato, TAMU, and Drs. David M. Patrick and Christopher P. Cameron, University of Southern Mississippi, are also acknowledged. Mr. Randy Oswalt and Mr. Bobby Fletcher of the Hydraulics Laboratory; and Dr. Robert H. Denson, Mr. John Boa, Mr. Ken Loyd, and Mr. Donald Walley of the Structures Laboratory helped develop the materials used to simulate rock and provided technical assistance for the flume tests. This report was edited by Mrs. J. Walker, Information Technology Laboratory.

WES gratefully acknowledges the helpful suggestions, constructive criticisms, and information provided by the Soil Conservation Service, US Department of Agriculture, and the Corps of Engineers Districts and Divisions.

Commander and Director of WES during preparation of this report was COL Larry B. Fulton, EN. Dr. Robert W. Whalin was the Technical Director during this study.

A-1

CONTENTS

CONVERSION FACTORS, NON-SI TO SI (METRIC)
UNITS OF MEASUREMENT

Non-SI units of measurement used in this report can be converted to SI (metric) units as follows:

Multiply	By	To Obtain
acres	4,046.873	square metres
acre-feet	1,233.489	cubic metres
cubic feet	0.02831685	cubic metres
cubic yards	0.7645549	cubic metres
degrees (angle)	0.01745329	radians
feet	0.3048	metres
feet per mile	0.1893935	metres per kilometre
miles (US statute)	1.609347	kilometres
tons (2,000 pounds, mass)	907.1847	kilograms
yards	0.9144	metres

GEOTECHNICAL ASPECTS OF ROCK EROSION IN EMERGENCY SPILLWAY CHANNELS

GEOLOGIC AND HYDRODYNAMIC CONTROLS ON THE MECHANICS OF KNICKPOINT MIGRATION

PART I: INTRODUCTION

Background

1. Prediction of initiation, rate, and intensity of erosion in earth materials is not a precise science, and a significant amount of erosion-induced damage has occurred in unlined emergency spillway channels at flood-control and water-storage projects built and managed by the US Army Corps of Engineers (CE), other Federal Agencies, state, and local interests (Cameron et al. 1986, 1988a, and 1988b). The potential for severe erosion of the bedrock (and associated soils) in unlined emergency spillways to cause undermining or failure of spillway structures and catastrophic release of reservoir waters, damage to dam embankments, spillway channel bank failure, and sedimentation in the spillway exit and main channel prompted the CE to include this problem as a work unit in the Repair, Evaluation, Maintenance, and Rehabilitation (REMR) Research Program being conducted by the US Army Engineer Waterways Experiment Station (WES).

Work Unit Objectives

2. The objectives of this work unit include the following:

- a. To identify and document the geotechnical and hydraulic parameters influencing the rate and mechanisms of erosion in unlined emergency spillway channels.
- b. To identify and document channel response to emergency spillway flow and to assess the nature, magnitude, and severity of downstream impacts.
- c. To develop methods of predicting erosion in unlined emergency spillway channels.

d. To develop cost-effective remedial and preventive measures to minimize the problem of severe erosion in unlined emergency spillway channels.

e. To maintain and continually up-date an observational data base which documents important erosive spillway overflow events at CE projects.

f. To provide timely technology transfer in this problem area to CE personnel and other interested parties in Federal, state, and local agencies.

Scope

3. This report, the fourth in a series, provides further documentation of the causes-and-effects of bedrock erosion in emergency spillway channels, the relationship between spillway channel erosion and erosion in natural stream channels, provides detailed analyses, and attempts to quantify the phenomena and processes identified and discussed in earlier reports, (see Cameron et al. 1986, 1988a, and 1988b). These phenomena and processes encompass the geotechnical and hydraulic factors which control spillway channel response to overflow events.

4. These reports are intended to serve as a mechanism for communicating research results, ideas, and concepts to interested CE personnel and their counterparts in other Federal, state, and local agencies. CE District experience, case histories, and site visits, as well as technical input from other concerned agencies, continue to provide vital elements of the working observational data base and serve as the foundation for development and refining of research tasks.

Objectives of Laboratory Research

5. The primary objective of this research is to determine the significance of geologic and hydrodynamic controls on the mechanics of headward or knickpoint erosion. This was accomplished by:

a. Viewing the spillway erosion problem as a "continuum" from tractive force scour of individual grains to turbulent dynamic block scour and contending that block failure mechanisms are most critical in determining the rate of headward erosion.

b. Showing that knickpoints cannot develop very easily in a homogeneous media, but ideally need a harder more resistant layer overlying a softer more erodible layer.

c. Breaking the complex headward erosion phenomenon into a basic two-layered system for analyses.

d. Designing mixes to simulate rock of various strengths for physical modeling tests.

e. Modifying a hydraulic, tilting, recirculating flume to accommodate layered samples.

f. Laboratory testing of a simulated two-layer rock system in the hydraulic flume under controlled flow conditions.

g. Using a designed hydraulic drop structure as an analog for determining the influence of venting on knickpoint migration.

h. Comparing laboratory results with observations made in the field.

i. Documenting block failure mechanisms in laboratory tests by use of video recorder.

j. Calculating critical turbulent flow particle velocities.

PART II: KNICKPOINT EROSION

6. Knickpoint migration or headcutting is the most severe form of structure-threatening erosion in emergency spillway channels. The term "knickpoint" refers to a point along the longitudinal profile of a stream channel at which there is an abrupt change in gradient. It is also the most unpredictable form of erosion because it is controlled mainly by the geology at a particular site. Ongoing complimentary erosion studies, carried out at WES, analyzed geometric and hydraulic parameters in respect to severity of erosion (Cameron et al. 1988a). The absence of a statistical correlation among the variable parameters is ascribed to different geological conditions at the data base sites. Structural and stratigraphic discontinuities were not included in the regression analyses.

Review of Related Research

7. Numerous research efforts have dealt with the subject of erosion, but only a few of these can be applied directly to the problem of violent, turbulent knickpoint erosion which is associated with short-lived emergency spillway flow events. Spillway erosion is controlled by a variety of complex geological and hydraulic factors including:

- a. Flood frequency, magnitude, and duration.
- b. Channel design.
- c. Channel gradient.
- d. Rock discontinuity.
- e. Rock erodibility.

8. The preceding factors are interrelated and often act in concert (Cameron et al. 1986, 1988a, and 1988b). The processes associated with turbulent block scour are not as well understood as those dealing with tractive force scour. Guy, Simons, and Richardson (1966) used flumes to determine the effects of the size of the bed material, temperature, and fine sediment on the hydraulic and transport variables in alluvial channels.

9. Schumm (1985) states that an understanding of the geomorphic controls on erosion processes in fluvial systems is critical. The natural erosion susceptibility of a stream system can be increased by human-related

activities such as channelization, overgrazing, blasting, and road construction (Smith 1979; Whitten and Patrick 1981).

10. The US Department of Agriculture is conducting hydraulic model testing for the design of vegetated channels at its Stillwater, Oklahoma, laboratory (Figure 1). Methods have been derived for applying tractive force

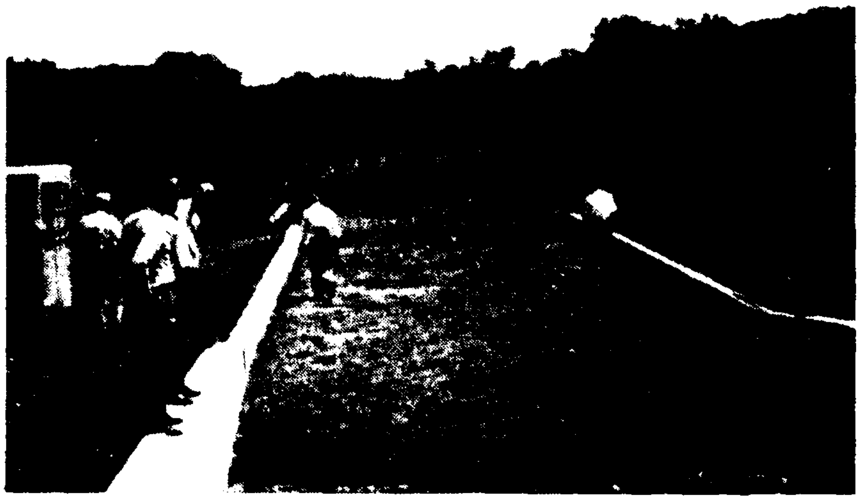

Figure 1. One of the grass-lined hydraulic models used for erosion studies at the USDA Research Laboratory at Stillwater, Oklahoma (WES photo file)

concepts to the design of grass-lined spillways (Temple 1980, 1982, 1983, 1984, 1986). Studies at the US Department of Agriculture Sedimentation Laboratory at Oxford, Mississippi, have related local channel instability to an early-Holocene silt unit with well developed polygonal structures that cause near-vertical bank angles which result in bank instability (Grissinger and Bowie 1984). The hydraulic parameters associated with an overfall were studied by Robinson at the Soil Conservation Service (SCS) Laboratory at Stillwater, Oklahoma (Robinson 1987). The US Department of Agriculture has an ongoing study that is designed to determine the critical factors causing erosion in emergency spillway channels (Soil Conservation Service 1973, 1984a, 1985b). WES has been working closely with the US Department of Agriculture Emergency Spillway Flow Study Task Group which has published four spillway performance reports documenting emergency spillway flows which took place in Mississippi, Kentucky, and Arkansas in 1982, 1983, and 1984 (Soil Conservation

Service 1984b, 1985c, 1986). The major factors influencing spillway erosion according to these reports are:

a. Major channel slope changes.

b. A road or trail in the spillway paralleling the flow.

c. A thin layer of soil over hard rock that may be "rafted" away.

d. Overshooting during construction blasting.

11. The Bureau of Reclamation used fuse-plug embankment models to study the erosion process. A fuse plug is an embankment designed to wash out in a controlled and predictable manner when the flow capacity exceeds the normal capacity of the service spillway. The fuse plug flow is primarily determined by gravity and inertia forces (Pugh and Gray 1984).

12. The ratio between the model and the prototype is determined from the Froude Law. The Froude Number is the velocity divided by the square root of the acceleration due to gravity times the depth of flow. Bureau of Reclamation studies obtained a high degree of both geometric and kinematic similarity. Geometric similarity occurs when the ratios of all homologus dimensions, between the model and the prototype, are the same. Kinematic similarity, or similarity of motion, means that the ratios of velocities and accelerations between the model and the prototype are equal (Pugh and Gray 1984).

13. A series of tests for relative erodibility of undisturbed sedimentary rock samples was conducted by Perry (1982) at the Waterways Experiment Station Geotechnical Laboratory. Perry used a self-contained, recirculating, tilting flume. Water was accelerated across a rock sample mounted flush in the floor of the flume and the rate of erosion was measured.

14. Numerous hydraulic modeling studies have been conducted at the Hydraulics Laboratory at the Waterways Experiment Station. An example is an investigation conducted on the Los Esteros Spillway in Guadalupe County, New Mexico, to investigate the feasibility of increasing the capacity of the spillway from 175,000 to 430,000 cu ft/sec* (Fletcher 1982). The model was constructed to a linear scale ratio of 1:80. Hydraulic similitude was achieved by using Froudian criteria to express the mathematical relations between the dimensions and hydraulic quantities of the model and prototype. The modeling proved that flows as high as 430,000 cu ft/sec would not

---

* A table of factors for converting non-SI to SI (metric) units of measurement is presented on page 5.

jeopardize the dam. The Grapevine Spillway was also modeled by the Hydraulics Laboratory (Figure 2). Useful hydraulics data were obtained from the Grapevine modeling; however, a noncohesive sand was used in the modeling effort and many geotechnical questions were not addressed.

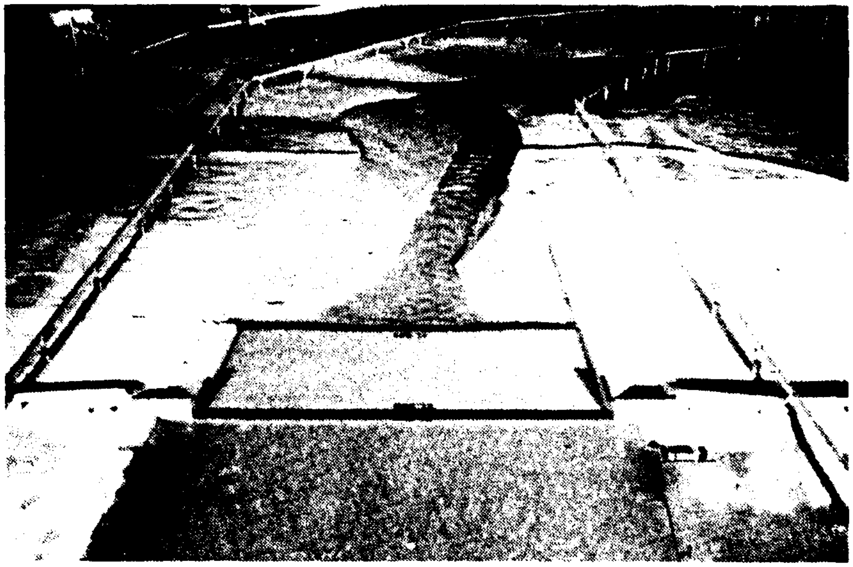

Figure 2. Hydraulic model of the Grapevine Spillway and emergency spillway. The unlined portion of the spillway was modeled with noncohesive sand (WES photo file)

15. Studies dealing with erosion caused by free falling trajectory jets may be more realistic to describe the turbulent and dynamic end of the "erosion continuum" (Figure 3). Vieux (1986) of the Soil Conservation Service studied plunge pool erosion in cohesive soils at two dams in Kansas, where scouring at horizontal pipe outlets has occurred. A formula based on unconfined compressive strength was used to predict the equilibrium scour pool length to within 5 percent of the measured length. The maximum depth of scour (D_m) for granular beds can be computed from the following empirical equation used by Mason (1984):

$$D_m = K \frac{(q^x)(H^y)(h^w)}{(g^v)(d^z)} \tag{1}$$

where

K = coefficient

q = discharge per unit width of the jet at the impact point

H = head drop from reservoir level to tail-water level

h = tailwater depth downstream of the scour hole

g = acceleration due to gravity

d = mean particle size of the eroded bed material

v,w,x,y,z = exxpotentials for g , h , q , H , and d , respectively

Figure 3. Turbulent overfall at the Delta, Melville, Abraham, and Deseret Irrigation (DMAD) spillway in Utah (WES photo file)

16. Mason (1984) reviewed the case histories of scour development on selected prototypes including: the Tarbela Dam in Pakistan; Alder Dam and Nacimiento Dam in the United States; Picote Dam in Portugal; Grand Rapids Dam in Canada; and Kariba Dam in Zimbabwe. Mason pointed out the difficulties in quantitatively predicting the erosive characteristics of free-trajectory jets. Unacceptable scour is by no means limited to soft rocks such as shales, sandstones, and limestones but occurred in competent igneous and metamorphic rocks such as andesite, granite, and gneiss. He also discussed hydraulic model testing and said that in every case he had studied the Froude law was used as the scaling law.

17. Mason developed formulae for calculating the depths of erosion under free jets for both models and prototypes. He noted that the most common problem in modeling scour is representing the geology of the site at a model

scale. A common approach is to examine the rock onsite and to estimate the size of the blocks that will result from the joint and fissure patterns. The rock in the model is then represented by an equivalent size of gravel. The gravel can be left as noncohesive for a worst case condition or mixed with various percentages of clay, cement, chalk powder, and water to add cohesion.

18. A rational approach was presented by Spurr (1985) for estimating the scour downstream of large dams by taking into account the mean surplus jet energy in relation to the geology and estimated flow durations. According to Spurr, the scour depth D_t, at any time t, resulting from a submerged jet eroding bedrock is a function of the jet energy E_a, available at the surface of the bedrock and the rock's capacity E_b, to absorb or deflect the erosive forces, such that:

$$D_t = f(E_a - E_b - E_x) \tag{2}$$

where E_x is the jet energy deflected by the bedrock at time t (Figure 4). Spurr presented the most important geological considerations as:

a. The rock mass's resistance to hydrofracture, as governed by its tensile properties, its degree of fracturing, faulting, and bedding plane spacings.

b. The bedrock's resistance to the erosive shear forces exerted on its surface by the action of the jet, as governed by its cohesive strength.

Spurr applied the empirical formula for scour depth (Equation 1) developed by Mason (1984). This formula reproduced the known scour depth at the prototype reference sites and effectively calibrated Spurr's model.

19. Blaisdell (1983) and Blaisdell and Anderson (1984) also studied ways to predict scour at cantilevered pipe outlets. Analyses of laboratory and field data indicated that the maximum depth of scour Z, in terms of the pipe diameter D, occurs when the ratio Z/D, approximately equals 5.

20. Reinius (1986) measured the water pressures around simulated rock blocks in a hydraulic flume. His study was based on the assumption that the rock has cracks in several directions and that water can enter the cracks causing pressure to build within them. The pressure forces act on the sides and bottom of the rock block and the pressure from the flowing water acts on the top surface of the block. If the uplift force is not offset by the weight of the block, and no other forces in the joints stop movement, the block will

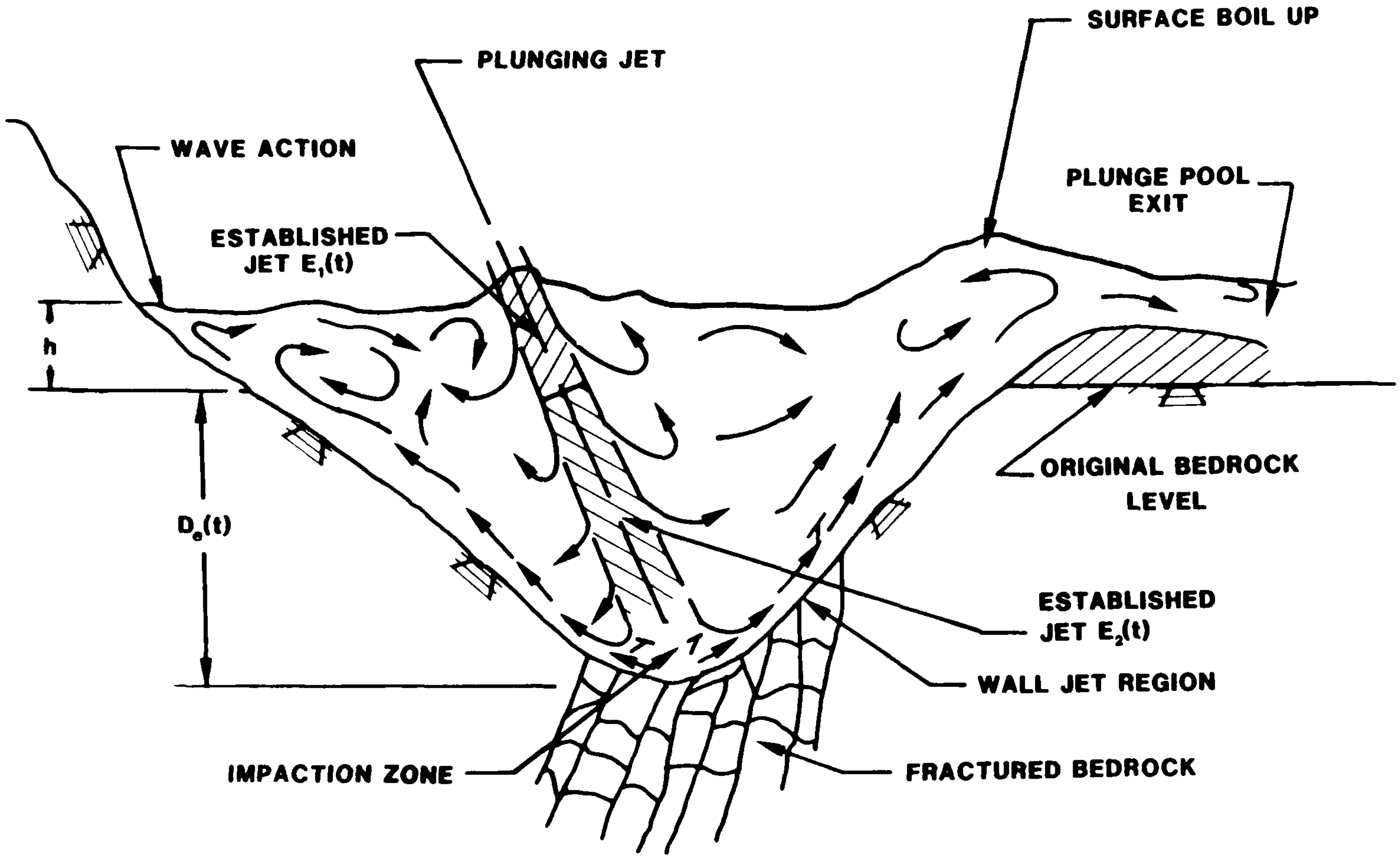

Figure 4. Conceptual diagram of a jet in a developing plunge pool (after Spurr 1985)

be lifted and carried away. He also discusses remedial measures, such as dental concrete to seal and waterproof fractures, and the use of rock bolts and pressure relief holes.

21. Clemence (1987) used an air flume to determine the influence of stratigraphy and structure on knickpoint erosion. She hypothesized that the mechanisms of knickpoint retreat involved not only cantilever toppling but also horizontal fluid boundary shear and pore pressure (Figure 5). The air flume studies showed that a caprock failing by cantilever toppling remains stable as long as the caprock's undercut length is less than one-half the fracture length and the caprock is strong enough to resist cantilever failure. The thickness and angle of the erodible unit to the overlying caprock control the amount of undercut. The development of significant fluid pressures in a permeable erodible unit decreases resistance to shear. An impermeable erodible unit may also concentrate the force of the water on the undercut slab and cause tension fractures in the caprock. Thin discontinuous caprock units were rapidly eroded by fluid boundary shear. As bedding thickness increases, the knickpoint erosion is controlled by fracture spacing and cantilever toppling. The flume study by Clemence indicates that fracture spacing and rock tensile strength are the most significant factors in knickpoint erosion at sites where unerodible caprock overlies an erodible unit.

22. An analysis was made of spillway erosion at a private lake near Waco, Texas (Pettigrew 1986). A knickpoint was migrating up the spillway of Badger Ranch Lake at a rate which would threaten the spillway in a few years. An estimated 100,000 cu ft of material was removed by the erosion process. The investigation indicated two possible causes for the structure-threatening erosion:

- a. Excessive velocities at the end of the exit channel may have initiated the gully.
- b. A knickpoint migrating from downstream could have been the cause.

23. One of the main areas of the investigation was the analyses of the erosion occurring at the knickpoint. A model was presented which showed a cycle of headwall collapse and debris removal controlling the headward migration of the gully. The headward migration was accelerated by erosion of the fissile shale underlying a resistant clay. The mechanics of the collapse were worked out and described as a wedge failure occurring at a critical height of

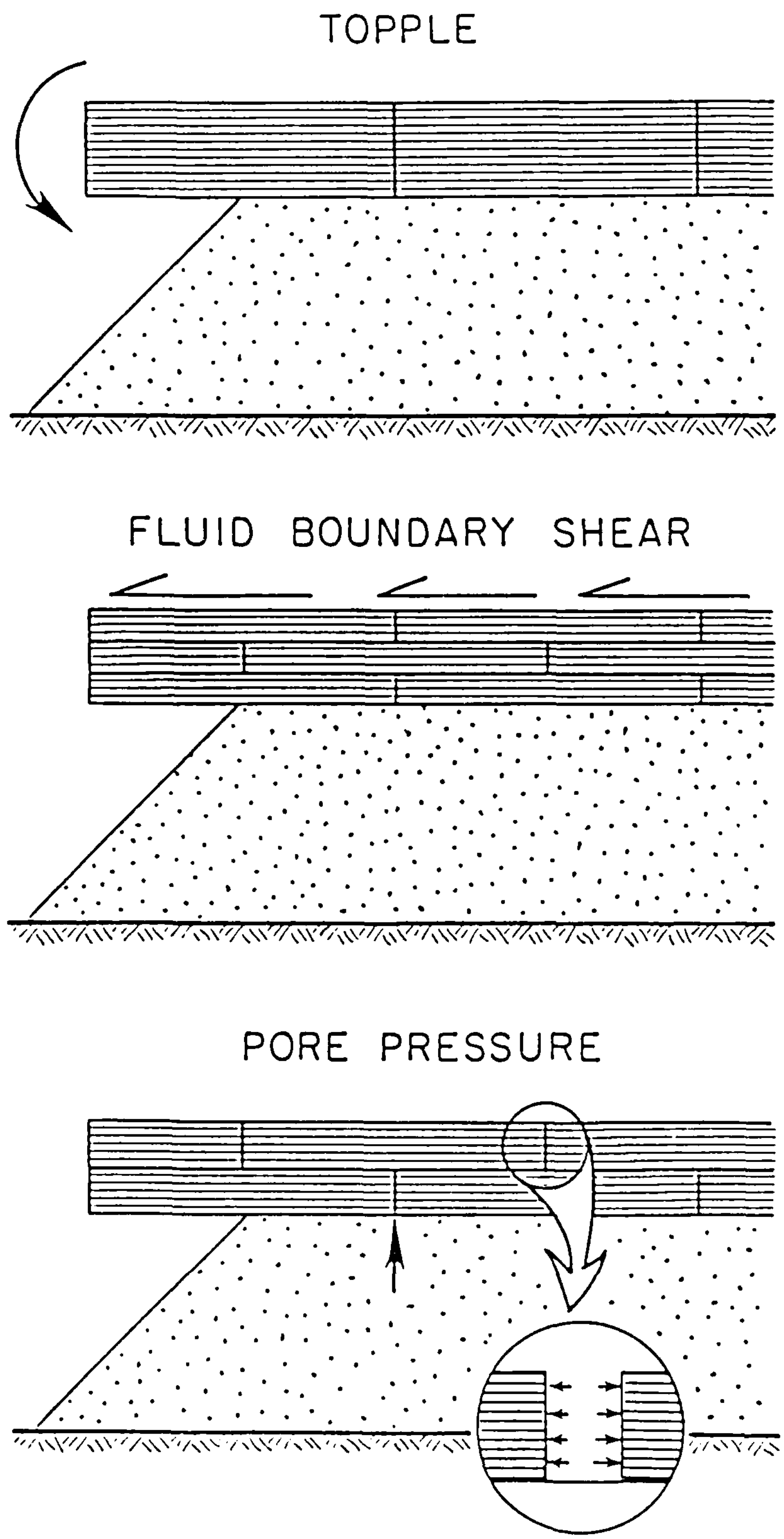

Figure 5. Mechanisms of knickpoint retreat determined from air flume studies; mechanisms include cantilever toppling, fluid boundary shear, and pore pressures (after Clemence 1987)

11.6 ft (Figure 6). The equation used to calculate the critical height (H_c) is:

$$H_c = \frac{(N_s)(C)}{(\gamma)} \quad (3)$$

where

H_c = the height of the face at failure

N_s = a stability factor based on the angle of the face

C = cohesion

γ = unit weight

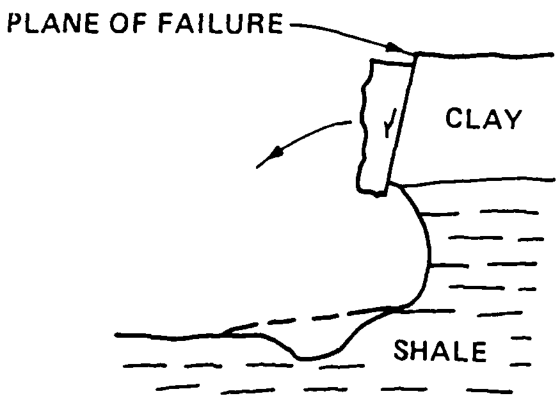

Figure 6. Mass failure mechanisms at Badger Ranch Lake spillway near Waco, Texas (after Pettigrew 1986)

24. A comparison of rainfall and knickpoint retreat at the Badger Ranch Lake spillway correlated better than the comparison of peak discharge and knickpoint retreat. The sediment transport from the gully appears to be a more important controlling factor in the migration process than the peak flow. This phenomenon was also seen in data from gully studies in the loess-covered glacial till of Iowa where it is suggested that lowering flood peaks, but not flood volume, might actually increase erosion (Piest, Bradford, and Wyatt 1975).

25. A model study of knickpoint migration and associated slope changes in noncohesive homogeneous material suggests that bed-load movement is a prerequisite for migration of a knickpoint once it has formed (Brush and Wolman 1960). An oversteepened slope in homogeneous material bounded by less steep slopes upstream and downstream tends to become less steep with time. A stream has a natural tendency to flatten out any oversteepened reach in homogeneous material; therefore, a knickpoint migrates upstream for only a short distance before becoming too faint to recognize. At a particular flow, the rate of

migration is controlled by the size of the material, and the total migration will depend on the difference in fall between the average and oversteepened reach. Five hypothetical examples of different geologic environments where knickpoints occur are presented by Brush and Wolman (1960) and shown in Figure 7. Type A is similar to the flume experiment conducted by Brush and Wolman and should apply to all knickpoints in homogeneous material as in many alluvial valleys. Type B has a resistant layer intersecting the stream profile at some arbitrary angle. The knickpoint will remain indefinitely or until the resistant layer is removed. If the resistant layer is completely removed B becomes identical with A. Type C occurs where a resistant layer

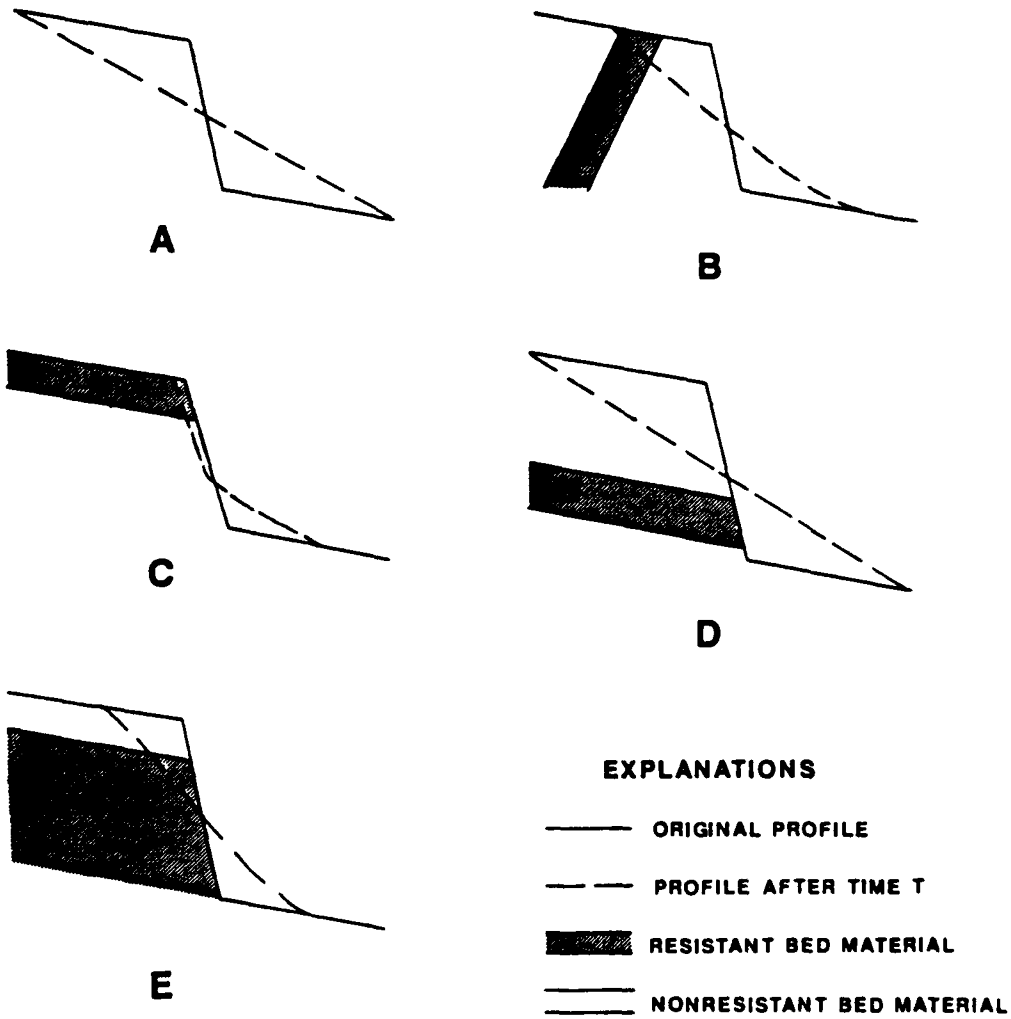

Figure 7. Five hypothetical examples of different geologic environments where knickpoints occur. Only Type C allows significant lateral migration of a knickpoint (after Brush and Wolman 1960)

caps an underlying nonresistant bed. In the case of Type C, the slope below the knickpoint may be vertical depending on the relative differences in resistance to erosion of the two kinds of material. Types D and E are special cases of the preceding types.

26. Falls are a special case of Type C where the vertical slope is caused by undermining. A knickpoint cannot easily bypass a resistant layer and in some cases a series of knickpoints caused by various base level or climatic changes will merge at one point along a stream profile. Headcut development and migration in alluvium or colluvium may involve seepage or underflow as well as differential resistance.

27. The maximum distance a knickpoint may travel given unlimited time is controlled by the ratio of the slope of the oversteepened reach to the average slope of the channel. The greater the ratio, the farther the knickpoint will migrate given unlimited time.

Theoretical Considerations

General statement

28. Studies by Schumm (1973) point out that the concepts of complex response and geomorphic thresholds in stream systems are related to erosion phenomena such as rapid mass movement and tributary rejuvenation. These geomorphic thresholds imply that morphogenetic processes are episodic in nature. The triggering mechanisms for these episodic events can be external forces such as rainstorms or seismic activity or internal forces such as oversteepening of reaches. Aggradation and degradation at different loci within a stream system cause episodic sediment yields which move downstream and result in major changes in channel morphology with time.

29. For the purpose of this research effort, the emergency spillway is considered to be a small portion of a stream system. The erosion in emergency spillways is controlled by phenomena that occur upstream and downstream of their immediate vicinity. The unlined portion of the emergency spillway is subject to vertical degradation and headcutting, as shown in Figure 8.

30. In order for an emergency spillway to flow, the upstream lake or reservoir must receive a large volume of water in a relatively short period of time. Emergency spillways are therefore subject to violent, turbulent, short-lived flow events. The downstream end of most emergency spillways abruptly

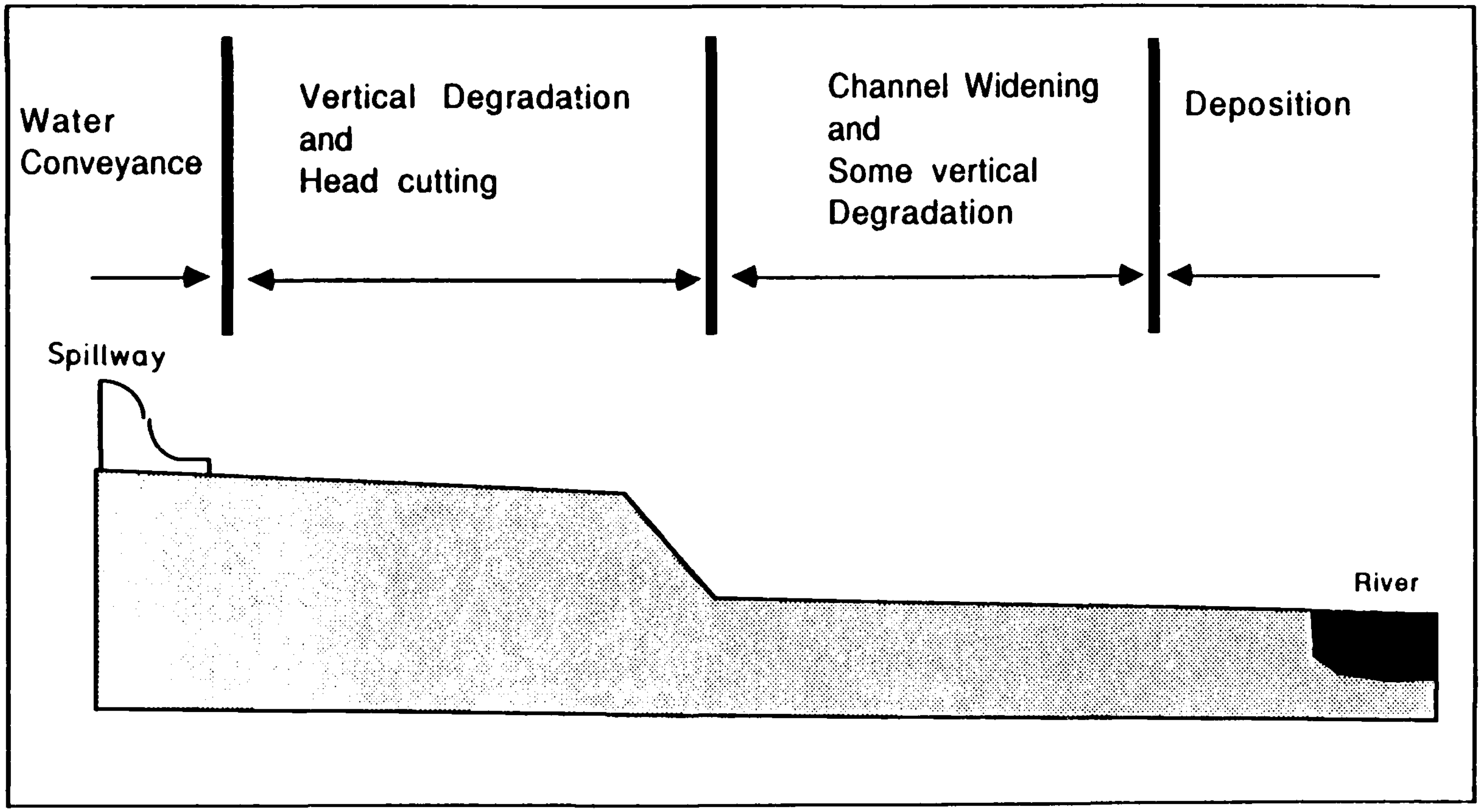

Figure 8. Diagrammatic cross section of spillway and excavated channel showing the major processes acting along the longitudinal section (Cameron et al. 1988a)

drops into a natural stream valley, thus producing a severe oversteepened reach or knickpoint.

31. The hypothesis of this research is that during these violent flow events severe erosion is governed by certain erosion thresholds, which are in turn primarily controlled by the flow velocities and the site geology. The site geology is important because it is responsible for the geometry of the knickpoint. The erosion thresholds pertaining to emergency spillways are also present in certain reaches of natural streams and could explain, in part, the episodic erosion phenomena that have been reported so often by other researchers such as Piest, Bradford, and Wyatt (1975).

Spillway erosion as a continuum

32. Because of the numerous complex factors which contribute to the spillway erosion problem, it was viewed as a "continuum" with tractive force scour of individual grains on one end and turbulent flow dynamic block scour on the other end. During the study of numerous case histories, it was noted that various types of erosion could occur at the same location within a given spillway during a single flood event. Tractive force scour is usually taken into consideration in the design of emergency spillways. The SCS has developed excellent criteria for the design of grass-lined spillways (Temple 1980, 1982, 1983, 1984, 1986). However, the significant erosion problems which occurred at most of the sites visited during this research were not caused by the scour of individual grains (Figure 9) but by the mass wasting of large blocks of material (Figure 10). Tractive force scour is often the first phase in the emergency spillway erosion "continuum" and may lead to the more severe block erosion.

33. Figure 11 shows large blocks of in situ sandstone which have been exposed by the force of running water in an SCS emergency spillway in Virginia. The thin layer of soil and grass has been stripped away exposing the highly jointed and fractured bedrock underneath. Once the veneer of soil and grass has been removed, high velocity turbulent flow conditions are generated which can start to move large blocks of material.

34. These large blocks of bedrock are moved out of place and downstream primarily by two mechanisms--plucking or floating out individual blocks and undercutting, which causes the bedrock to fail in tension or shear or to topple because of the fracture or joint spacing.

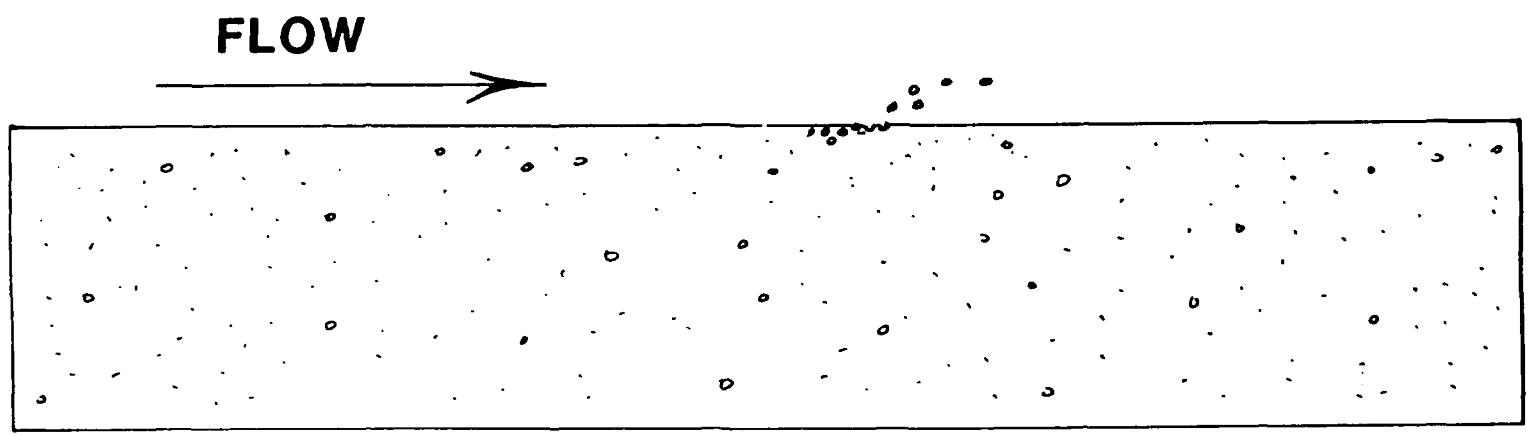

Figure 9. Schematic diagram showing scour of individual grains

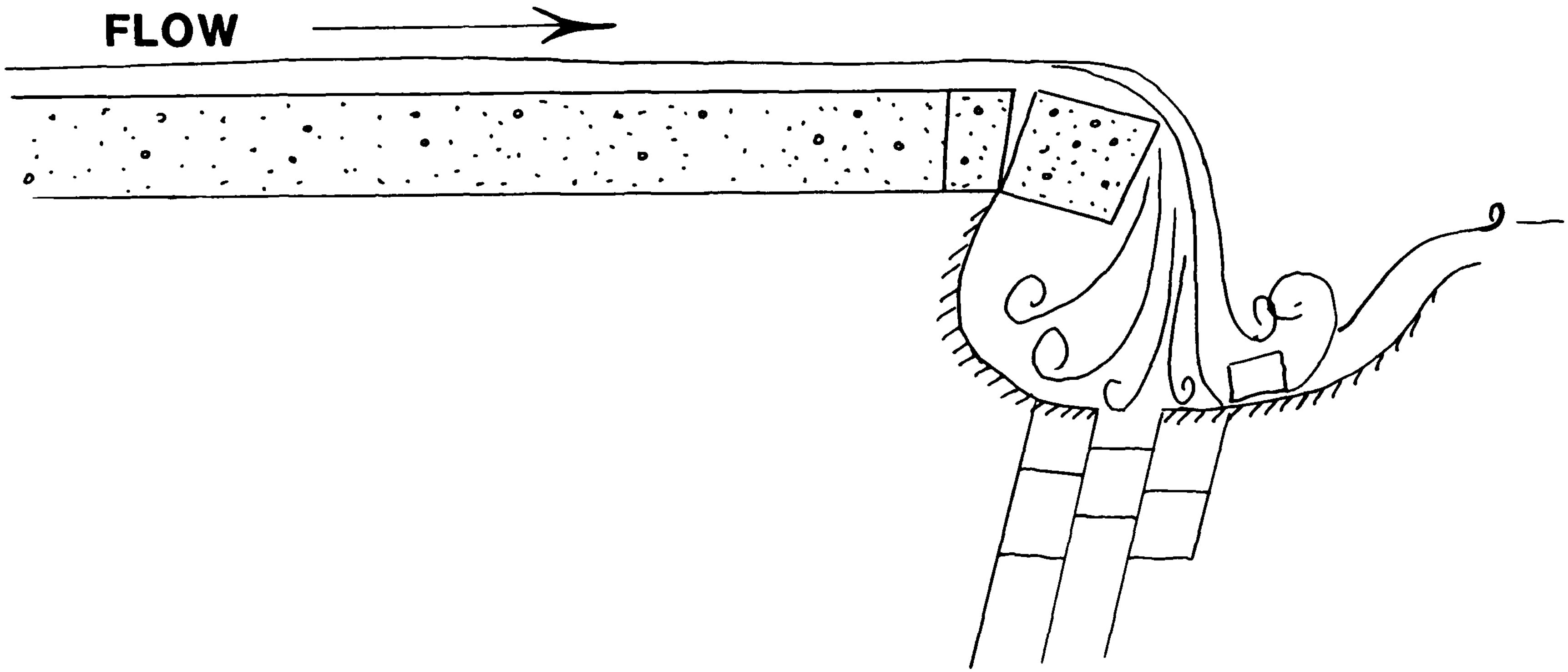

Figure 10. Schematic diagram of block erosion mechanisms; blocks are scoured from the plunge pool and the caprock

Figure 11. Tractive force scour has removed the veneer of soil and grass in the bottom of this SCS spillway and exposed the underlying jointed bedrock (WES photo file)

Rock mass versus
particle or grain erosion

35. The concept of rock mass properties versus grain-to-grain properties in relation to erosion has to be kept in proper perspective. The erosion and transport of granular noncohesive material has been studied in detail by many prominent researchers. Very little of this data, however, can be applied to the problem of spillway erosion in unlined spillway channels. In the same light, many of the standard engineering properties such as compressive strength and cohesiveness are very misleading when it comes to predicting erosion. In the grain-to-grain context a rock can appear to be very resistant, yet be susceptible to severe erosion because of its mass properties.

36. It was determined during tests using a water jet to cut various types of rock, that the most important factor in making a rock erodible is rock permeability (Rehbinder 1980). Rock mass permeability is very important in determining its erodibility.

37. Tractive force scour. Tractive force scour of grains and particles must be discussed as an end member in the erosion "continuum" concept. Berg (1986) discussed the complex processes that influence the erosion, transport, and deposition of material by considering the forces that act on individual particles. He found that grain size and shape along with adhesion tension are important variables in calculating erosion velocities for sediments. If the orientation of the grains relative to the water flow is known, the drag force needed to cause movement can be expressed by the equation:

$$F_d = F_g(\tan\phi) \tag{4}$$

where

F_d = drag force

F_g = the gravitational force

ϕ = the angle of repose

38. It is also important to consider the orientation of the grains in relation to the flow of water. Berg (1986) estimated erosion velocities for differing grain orientations. For example, using the angle of repose ϕ, the surface area exposed to drag, and grain size, he determined the threshold velocity for material with a grain diameter of 1 mm would be approximately 19 cm/sec. Sediments that have been partially dried may contain small amounts of water at points of grain contact. The adhesion of water gives the material more erosion resistance. Berg's velocities agreed closely with those presented by Hjulstrom (1939) and shown in Figure 12.

39. If grains or particles are cemented they become even more resistant to the forces of moving water. Regardless of how cemented the grains of a material may be, if the velocity of the water is high enough, scour will take place. According to CE guidance on the design of channels, even competent igneous and metamorphic rocks will be scoured at a mean channel velocity of 20 ft/sec (US Army Corps of Engineers 1970). The velocities needed to scour various materials are presented in Table 1.

40. Simonson (1979) indicates that material with compressive strengths of 14,000 psi can be scoured by velocities of 29 ft/sec. Tractive force scour of grains or particles was not dealt with in this study except as an end member in the erosion "continuum" concept.

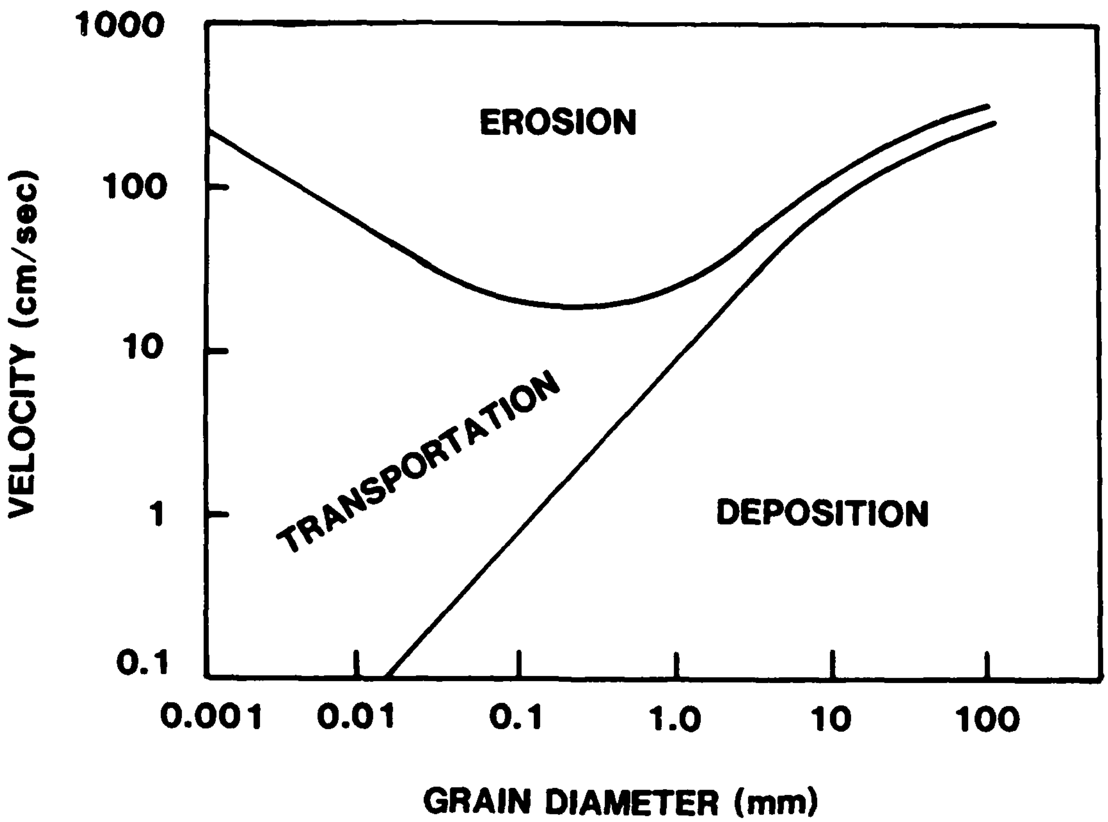

Figure 12. Hjulstrom's (1935) diagram shows the velocities needed to erode, transport, and deposit grains of varying sizes

41. Dynamic block scour. The failure of large blocks of material can occur in several ways including plucking or lifting of fractured blocks, cantilever toppling based on fracture spacing, tensional failure of the capping layer, and shear failure of large homogeneous masses of material. In fractured rocks, water can propagate into the cracks causing pressure to build up within them. The pressure acts on the sides and bottom of a block, while the pressure from the water flowing across the top of the block causes an uplift force (Reinius 1986). The plucking of large blocks of material can result in very large volumetric erosion and removal of material from a site.

42. The research concerning the dynamic block erosion caused by free-falling trajectory jets gives insight into the knickpoint migration problem, but cannot be applied directly to the problem of block scour at knickpoints (Vieux 1986; Mason 1984; Spurr 1985). The trajectory jet studies are concerned with depth of scour; whereas, the knickpoint migration problem concerns rapid lateral erosion. The geological considerations presented by Spurr (1985) as being important in predicting erosion, such as resistance to

Table 1

Maximum Permissible Mean Channel Velocities

(US Army Corps of Engineers 1970)

Channel Material	Mean Channel Velocity, ft/sec
Fine sand	2.0
Coarse sand	4.0
Fine gravel	6.0
Sandy silt	2.0
Silty clay	3.5
Clay	6.0
Grass-Lined Earth (Slopes less than 5 percent)	
Bermuda grass--sandy silt	6.0
Bermuda grass--silty clay	8.0
Kentucky Blue Grass--sandy silt	5.0
Kentucky Blue Grass--silty sand	7.0
Poor Rock (Usually Sedimentary)	
Soft sandstone	8.0
Soft shale	3.5
Good Rock	
Igneous or metamorphic	20.0

hydrofracture and resistance to erosive shear, are also critical factors in block scour at knickpoints. The maximum depth of scour values is often based on the assumption that the erosion has progressed to some stage of equilibrium. In the case of emergency spillway erosion equilibrium is seldom reached during a single flood event.

Geologic Controls

Structural discontinuities

43. A discontinuity is an interruption in lithologic and physical properties in a rock mass (American Geological Institute 1980). Structural discontinuities are caused by natural compressive and tensional forces which alter rock mass properties. Discontinuities such as fractures, faults, joints, igneous dikes, and veins are common causes of knickpoint formation.

Fractures are due to mechanical failure by stress and include erosion in general and knickpoint initiation in particular. The shearing and brecciation associated with faulting can also result in enhanced chemical and physical weathering of affected rock.

44. Joints, which usually occur in sets, are planar surfaces along which no displacement has occurred. Joint fissures, which are the fractures which separate the rock, may be filled with clay, calcite, gypsum, crushed rock fragments, or other material at depth, or they may be open near the surface. The tendency of joint sets to divide rock into blocks is important in predicting erosion potential. Reinius (1986) demonstrated that blocks of rock can be easily plucked by the forces of moving water and transported downstream. For example, open-joint fissures segmented the hard sandstone ledges, forming the floor of the Saylorville spillway, and contributed to the severe erosion.

Stratigraphic discontinuities

45. The majority of the erosion case histories studied for this research was associated with stratigraphic discontinuities. Stratigraphic discontinuities include stratified sedimentary rock sequences including those interbedded with volcanic and volcano-clastic rocks. These discontinuities include bedding planes, bed contacts, stratigraphic contacts, unconformities, pinchouts, facies changes, and sedimentary structures and textures (Cameron et al. 1988b).

46. Bedding planes are surfaces of deposition that visibly separate successive layers of stratified material (American Geological Institute 1980). These bedding planes separate lamina (less than 1 cm thick), stratum (greater than 1 cm thick), and beds (thicker units composed of several strata or lamina). Bedding planes often mark distinct boundaries between materials deposited in various environments of deposition. Coarse grained basal alluvial sand and gravel can have an abrupt contact with an underlying shallow marine clay. Bedding planes play an important role in erosion, especially in the propagation of a head cut where a resistant layer overlies a more erodible unit. Bedding planes are also important in conjunction with joints because at the intersections the strata are divided into blocks which are susceptible to plucking during flood events. Thinly bedded shales are easily weathered and subsequently eroded by tractive force shear.

47. Sedimentary structures are described by Berg (1986) as being the most characteristic features of sedimentary rocks and resulting from either primary stratification caused by sedimentary processes or secondary stratification produced by biological or physical changes shortly after deposition. Critically located sedimentary structures can initiate and influence the rate of erosion.

48. Unconformities represent erosional or nondepositional surfaces in the geologic record that can bring rocks of vastly different ages and compositions into abrupt contact. An unconformity which places a nonerodible material over an erodible one forms the same stratigraphic discontinuity as bedding contacts between materials of different erodibilities. Pinch-outs and facies changes can cause abrupt lateral lithologic changes which are important factors in initiating a headcut. The rate of migration is often dependent on lateral facies changes and can increase or decrease dramatically as a result of these changes. Lithostratigraphic control is the "key" factor which controls the initiation and rate of erosion in stratified rock sequences. Sudden changes in stratigraphy, both vertically and laterally, control the geometry of the knickpoint, which in turn controls the severity of erosion.

49. The occurrence of a knickpoint is dependent on stratigraphic or other types of inhomogeneities in underlying materials. The location of the knickpoint is controlled by the occurrence of erosion-resistant materials in the channel which temporarily prevent downcutting. An example of a knickpoint in a natural stream is shown in Figure 13. Erosion studies by the Soil Conservation Service in northern Mississippi showed that erosion-resistant paleosols caused knickpoints to form. The knickpoints migrated upstream as the paleosol failed in large blocks which were bounded by ancient desiccation cracks (Grissinger 1984).

50. Knickpoints are caused by a combination of conditions which cause channel degradation. According to Schumm (1973), the parameters that describe the geometric and discharge characteristics of stream channels which control degradation are:

W, stream width (L)

D, stream depth, water depth (L)

s, stream gradient (L/L)

Mw, meander wavelength (L)

Figure 13. Knickpoint in Hotopha Creek in Lafayette County, Mississippi (Whitten and Patrick 1981)

S, sinuosity units (a measure of actual channel length relative to straightline distances between two points along the channel)

Q_w, water discharge (L × L × L/T)

Q_s, sediment discharge (L × L × L/T)

51. On the basis of field and flume studies the following empirical relationships were described by Schumm (1973):

$$Q_w \approx \frac{(WDMw)}{s} \quad (5)$$

$$Q_s \approx \frac{(WsMw)}{(DS)} \quad (6)$$

It can be observed from the above proportionalities that channel degradation and the formation of knickpoints may be caused by increased water discharges without a coincident increase in sediment discharges. Proportionality 6 shows that an increase in channel gradient will also produce an increase in channel depth and eventually a knickpoint. Channel gradient increases are caused by changes in base level resulting from phenomena such as man-made channels or channel straightening and natural cut-offs of meander loops.

52. A spillway channel can be considered as a modified portion of a natural stream. Major differences between a spillway channel and a natural

stream are that flow in the spillway channel is usually sporadic and the knickpoint is usually located where the constructed portion of the spillway intersects the natural topography. A significant drop in elevation also usually occurs at this intersection which initiates headward migration of the knickpoint.

53. Very subtle variations in erosion resistance can cause the development of a knickpoint such as one at an SCS emergency spillway on Mistequay Creek in Michigan observed by the author. At first glance the material at this site seemed to be composed of fairly uniform glacial till, but closer examination revealed a buried paleosol which was slightly more resistant to erosion than the material just below it. The inhomogeneity provided by the paleosol helped to initiate a large knickpoint which migrated headward toward the dam. It cannot be overemphasized that discontinuities and inhomogeneities are critical factors influencing the initiation and rate of migration of knickpoints. The knickpoint phenomenon apparently played a key role in erosion which led to structural failure at the DMAD reservoir in Utah and at Black Creek No. 53, an SCS project in Holmes County, Mississippi (Cameron et al. 1986). Knickpoint migration was also apparent at CE emergency spillways at Grapevine and Saylorville Reservoirs (Cameron et al. 1986).

Stair-step phenomena

54. Field observations have shown that knickpoints often occur in groups that have a classic stair-step configuration as shown in Figure 14.

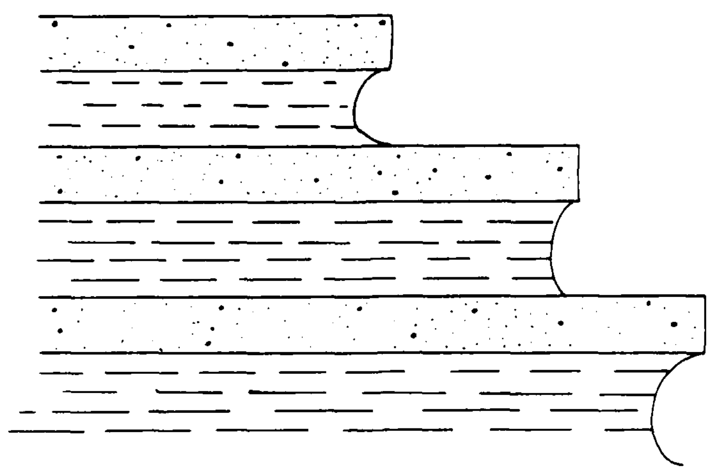

Figure 14. The knickpoint phenomenon producing a stair-step configuration in layered materials which have varying degrees of erodibility

The stair-step configuration is caused by repetition of the knickpoint phenomenon as it acts on layered materials with varying degrees of erodibility. Given enough time that stair-step configuration would evolve to an overfall that would be controlled by the most erosion resistant layer. However, the short duration flows in emergency spillways commonly cause a stair-step pattern to develop.

Mass failure mechanisms at the knickpoint

55. Although mass failure mechanisms associated with knickpoint migration are often complex, they generally fall under one of the following categories which are illustrated in Figure 15:

a. Undercutting of caprock resulting in cantilever toppling of jointed or fractured caprock.

b. Undercutting of caprock resulting in tensile failure and toppling of caprock.

c. Rafting of large blocks of jointed material as a result of water entering joints or fractures.

d. Undercutting of a thick erosion resistant top layer resulting in shear failure of large block of material.

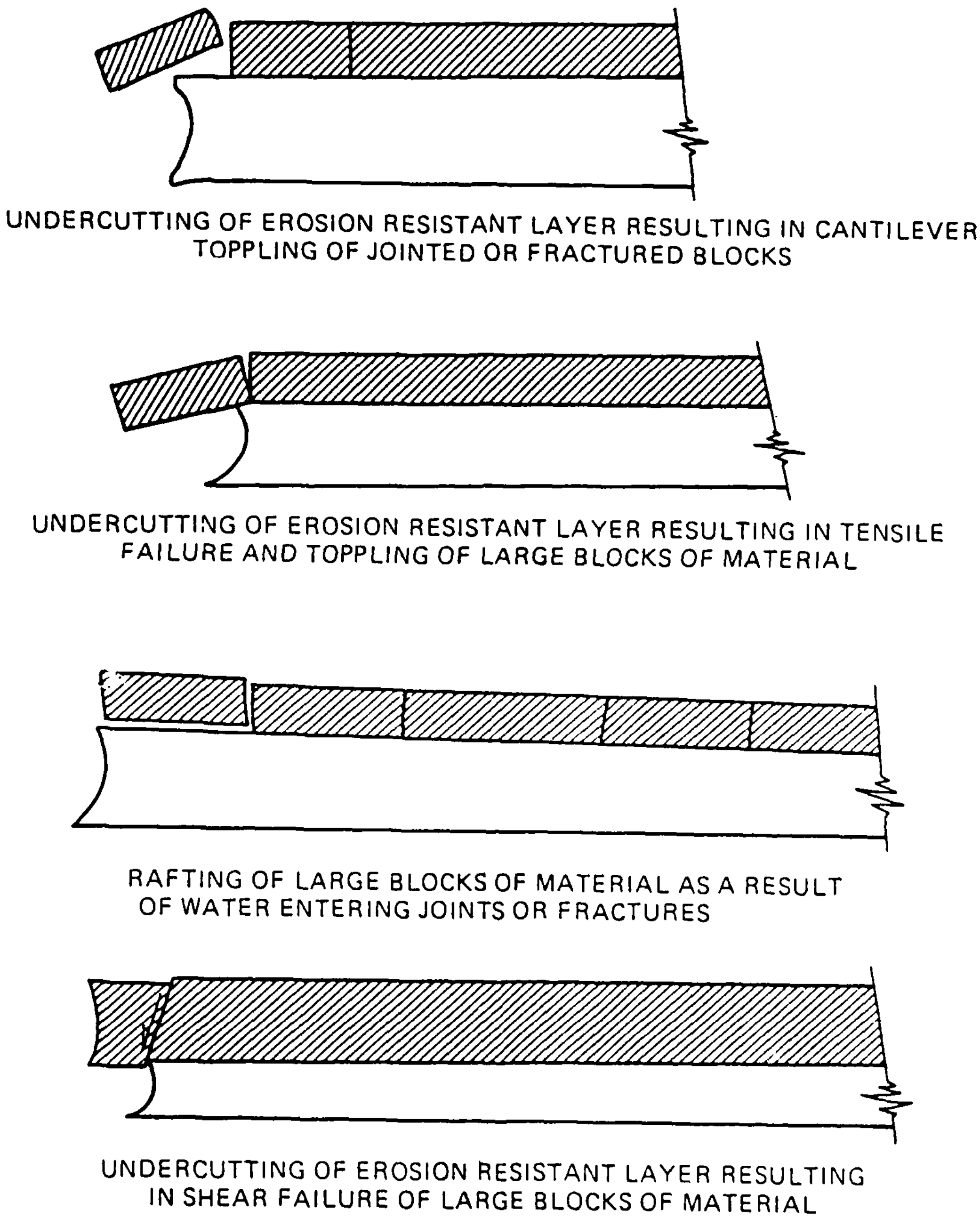

Figure 15. Generalized examples of mass failure mechanisms

PART III: EXPERIMENTAL DESIGN AND PROCEDURES

Flume Design

Principles of operation

56. A tilting recirculating hydraulic flume was used for the laboratory testing of the simulated rock material (Figure 16). The flume was capable of producing flows in excess of 20 ft/sec. The flume channel was 1 ft wide by 16 ft long and could be tilted as much as 5 deg. To modify the flume for testing simulated layered rock samples, a false bottom was constructed as shown in Figure 17. A removable sample holder was designed to hold the two-layered sample (Figure 18). The downstream end of the in-place sample formed the knickpoint and was analogous to the point at which a constructed emergency spillway intersects the natural topography.

Velocity measurements

57. The flow velocity in the area just upstream of the knickpoint was measured with a Pitot tube to determine the difference between the static and

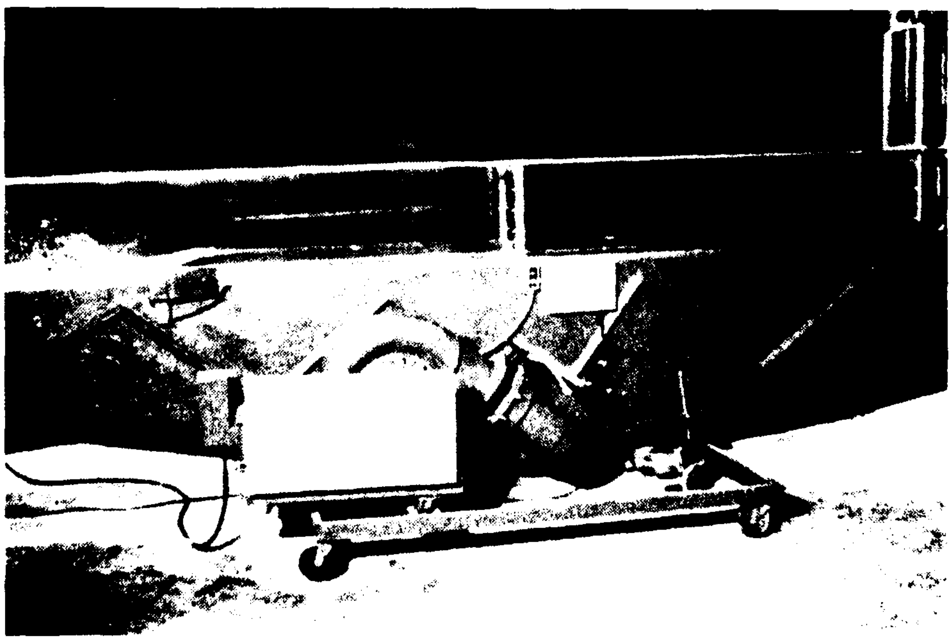

Figure 16. Photograph of tilting, recirculating, hydraulic flume used in erosion test

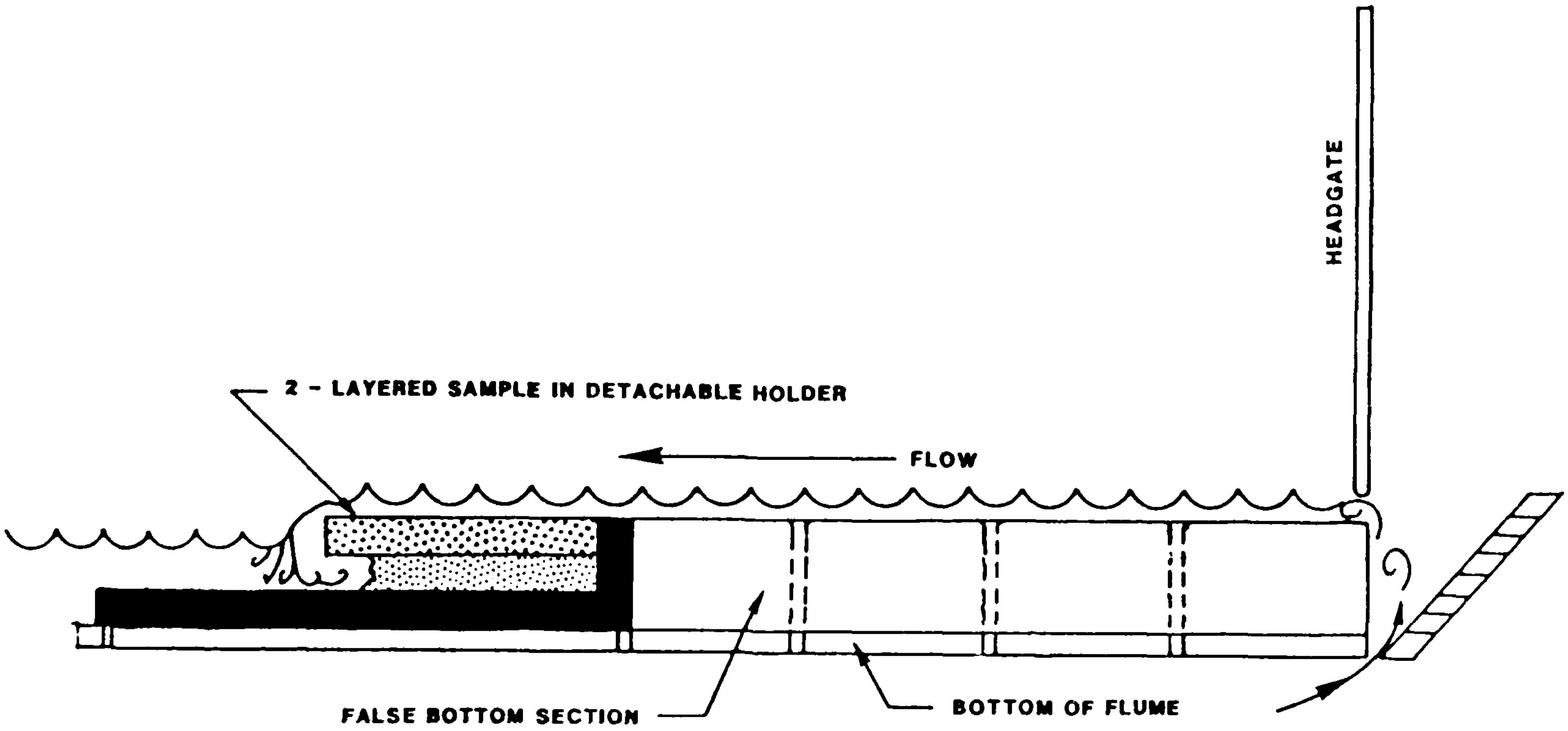

Figure 17. Drawing showing how the flume was modified for studying knickpoint retreat in layered material

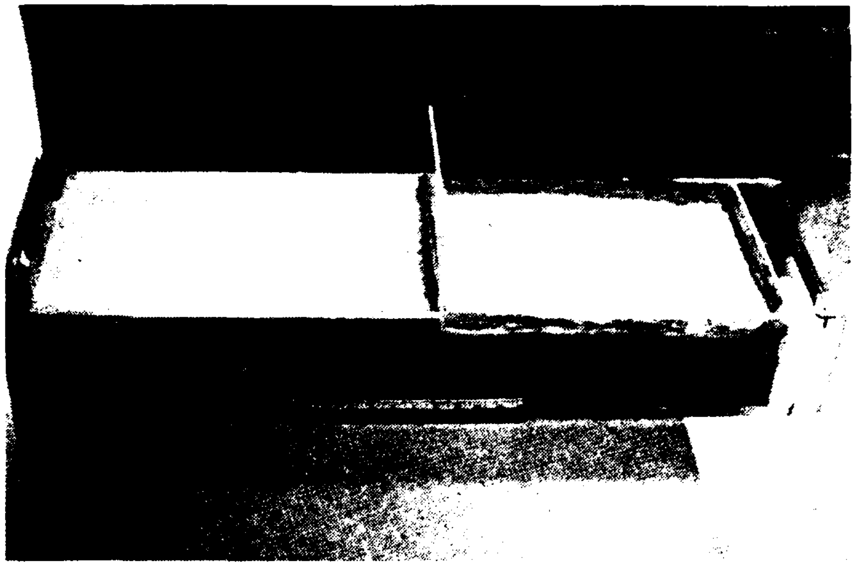

Figure 18. Photograph of removable sample holder

dynamic pressures. Once the pressure difference had been determined, flow velocity V was calculated by use of the following equation:

$$\frac{(V^2)}{2g} = \frac{(P - P_o)}{\rho g} \tag{7}$$

Solving for V yields:

$$V = \left[\frac{2(P - P_0)}{\rho}\right]^{1/2} \tag{8}$$

where

V = flow velocity (ft/sec)

P = dynamic pressure at the tip of the Pitot tube (lb/sq ft)

P_o = static pressure near the tip of Pitot tube (lb/sq ft)

g = acceleration of gravity (ft/sec^2)

ρ = mass density of the eroding fluid (lb sec^2/ft^4)

The velocity distribution (Perry 1982) near a smooth surface is:

$$\frac{V}{V_s} = \left[\frac{8.74(V_s)(y)}{\mu}\right]^{1/7} \tag{9}$$

where

V = flow velocity at a distance y from the boundary (ft/sec)

V_s = shear velocity (ft/sec)

y = distance from the boundary (ft)

μ = kinematic viscosity of the eroding water (sq ft/sec)

The shear velocity is:

$$V_s = \left(\frac{T}{\rho}\right)^{1/2} \tag{10}$$

where

T = hydraulic or tractive shear stress (lb/sq ft)

ρ = mass density of the eroding fluid (lb sec^2/ft^4)

58. By placing the Pitot tube on the bed of the flume, the distance y from the boundary at which the flow velocity can be measured is:

$$y = \frac{d_t}{2} \tag{11}$$

where d_t is the outside diameter of the Pitot tube (ft). In order to calculate the tractive shear stress, Equations 10 and 11 were combined with Equations 8 and 9 to yield:

$$T = (p - p_o) \left[\frac{\rho^{1/7}}{38.2} \left(\frac{2M}{d_t}\right)^{2/7}\right]^{7/8} \tag{12}$$

For a 0.125-in. outside diameter Pitot tube and water at 70° F the tractive shear stress is:

$$T = 9.62 \times 10^{-3} \left(P - P_o\right)^{7/8} \tag{13}$$

59. For the knickpoint erosion studies the Pitot tube system had to be modified. A three-way in-line valve was installed so that the tubes could be filled with water and the air allowed to bleed out. The Pitot tube apparatus and transducer were separated from the flume by constructing a wooden frame which held the apparatus and buffered vibrations during erosion tests (Figure 19).

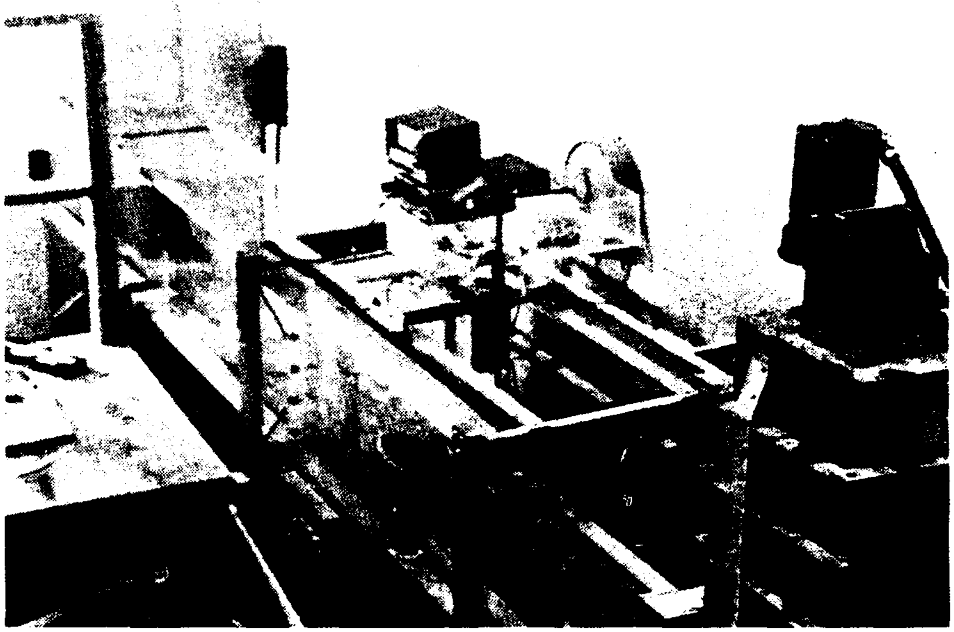

Figure 19. Pitot tube and instrumentation for measuring pressure differentials used to calculate flow velocity

Sample configuration

60. A simple two-layered model was used to study the knickpoint phenomena. The top layer was always the more resistant layer and allowed the undercutting of the less resistant bottom layer (Figure 20). The two-layered system was similar to the Type C case of Brush and Wolman (1960) which allows rapid parallel retreat of a knickpoint. In the WES flume studies the bottom of the flume served as a nonerodible lower layer.

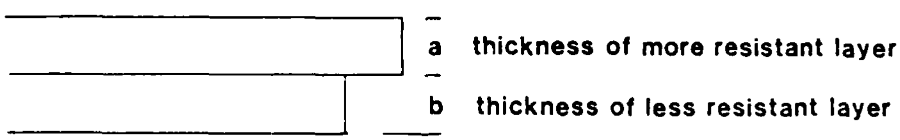

Figure 20. Conceptual two-layered system with the capping layer more resistant than the lower layer

61. A Plexiglas sample holder was designed so that a two-layered sample could be prepared, stored in the laboratory, and then transported and installed in the flume prior to testing. Several sample holders were constructed so that one sample could be tested while another was being prepared. The sample holder is 3 ft long and 11 in. wide, but the length of the sample

could be adjusted by inserting dividers at the desired length. When the sample holder was completely filled with material it weighed as much as 90 lb. As testing progressed, it was learned that all the area in the holder was not needed to produce the desired test results; therefore, smaller samples were constructed which were more easily handled. Also, for some of the latter tests Plexiglas layers were used to simulate nonerodible upper rock layers. A typical two-layered sample is shown in Figure 21.

Figure 21. Two-layered sample ready for testing in the flume

62. The height of the knickpoint was fixed at 6 in. for all the flume experiments. This allowed for several variations in thickness ratio between the erodible and nonerodible layers. Test specimens having stratigraphic ratios (erodible layer thickness)/(noneroding layer thickness) of 1:5 to 5:1 were tested.

Data Acquisition and Documentation

63. Data from each test were recorded on a formatted work sheet. These work sheets contain pertinent information such as the configuration of the flume during the tests and detailed data on the sample composition and configuration. Other data provided include: flow characteristics of water, headwater and tailwater depths, pressure differentials (for calculating velocity), temperature of the eroding water, test duration, and any other important observations. The flume test data sheets are presented in Appendix A.

64. Many of the flume tests were recorded with a video camera. The video camera proved to be an invaluable tool for studying and documenting the erosion process. The ability to stop the turbulent action was critical in understanding the failure mechanisms that were observed. Velocities of particles in the turbulent flow were calculated by using stop action and a measured grid. Photographs were also taken as appropriate to document specific aspects of the tests.

Procedures

Sample runs

65. Due to the iterative nature of erosion research and the lack of precedence for the kinds of tests which were conducted, several types of sample runs were made. The first type of test was designed to provide information needed to produce a rock simulant which would erode in a realistic manner. The ideal material had to not only erode within a reasonable time but also maintain enough strength to reproduce the failure mechanisms observed in the field. Tests SACON 1-I (shock absorbing concrete mixes) thru SIGEL 1-5 (sodium silicate mixes) were used to determine the erosive properties of weak concrete mixes, shock absorbing concrete, sodium silicate mixes, and Knox gelatin mixes. The second type of test, SILGEL 4-1, was conducted to reproduce a worst case scenario for rapid headward erosion. A third type of test, PLEXIGEL 2-2 thru PLEXIGEL 3-12, was for the purpose of determining the effect on headward erosion caused by varying the thickness of the capping layer while keeping all of the other variables constant.

66. A fourth type of test investigated pressure differentials associated with the establishment and maintenance of the knickpoint. The fifth type

of test determined the effects of the shape of the lip of the overfall on the formation and maintenance of the knickpoint.

Control of flow

67. Flow control during the tests was maintained by controlling the pump valve and the tilt of the flume. Flow conditions were reproduced for various geologic conditions by maintaining identical headwater heights and flow velocities for similar tests. The velocities were measured by the Pitot tube method described previously. Because the cross sectional area of the flume was known, the volume of flow per unit time could easily be calculated.

Test duration

68. Duration of each test run was highly variable depending on the type of test being conducted. The tests were designed to be completed in a reasonable amount of time, usually 30 min to 1 hr. Since most of the tests were simulating relatively short-lived, dynamic flow events, as opposed to long-term, equilibrium-producing flows, the shorter tests times appeared reasonable. The length of the tests ranged from 9 to 125 min.

Volume of eroded material

69. The volume of eroded material was determined by replacing the end plate on the sample holder after the end of each test, sealing the end plate to prevent leakage, and filling the eroded space with water. The volume of water required to fill the void is equal to the volume of the eroded material for a given test.

Velocity of particles in turbulent flow

70. By using a grid on the side of the flume in conjunction with the video recorder and stopwatch, the velocity of particles in the turbulent flow was calculated. The detailed procedures are given in Appendix B.

PART IV: DESIGN OF SIMULATED ROCK FOR FLUME TESTS

71. Because of the lack of detailed guidance in the literature, a great deal of research had to be performed to design a material which would satisfactorily simulate natural rock under knickpoint erosion conditions. The original logic was that, because the flume that was used for the tests had extremely high velocity capability, the rock simulant should be relatively high in strength. It turned out that high velocities were not as critical as originally thought and much weaker materials could be used. The details of the mixes which were used are presented in Appendix C. A general discussion of the various mixes which were tested is presented below, along with the reasons why each one was chosen or rejected.

72. Perry (1982) used the flume to test cores of shale and sandstone from the Woodbine and Eagle Ford Formations. He used very high velocities to erode the materials. The natural materials which he tested were as hard as weak concrete; therefore, the decision was made to start the knickpoint erosion studies using a weak concrete mix to simulate soft to moderately hard rock. The weak concrete mixes did not erode at low velocities and at higher velocities the knickpoint erosion and migration could not be reproduced. The concrete mixes had several other disadvantages. They had to be tested at the exact same time after mixing in order to obtain comparative results and at very low strengths the results of strength tests could not be repeated.

73. Several types of concrete mixes were used in preliminary tests. First, a portland cement, crushed limestone, and water mixture were used, but proved to be too erosion resistant for modeling.

74. A light-weight cellular concrete consisting of foam, cement, and water was designed by Bob Denson of the Structures Laboratory at WES. The cellular concrete looked very promising in early tests because during erosion the water remained perfectly clear and the details of the failure mechanisms could be observed. Another advantage of using the cellular concrete was that realistic fracture patterns could be carved into the upper surface of the sample. However, the shock absorbing properties of the cellular concrete made it erosion resistant.

75. Erosion along the traces of the fractures in the cellular concrete looked very realistic; although, the knickpoint or headward erosion could not

be reproduced. The cellular concrete may be so erosion resistant that it could be used as a remedial measure to prevent erosion in special cases.

76. Knickpoint migration was accomplished by using a mixture of gravel, chalk powder, cement, and water. However, the water became so cloudy that the failure mechanisms could not be seen during the test.

77. Clay mixtures had been used by other researchers in previous hydraulic modeling tests with some success, but, because of the need to keep the water clear so that the details of erosion could be observed, the clay mixtures were eliminated from further consideration.

78. Sodium silicate grout was the next material tested. Sodium silicate has several advantages over the portland cement-based mixes. A distinct advantage was that gravel could be placed into the holder and the sodium silicate poured into the gravel until all the voids were filled. The sodium silicate would then harden in place and the sample would be ready for testing. This greatly simplified the sample preparation because only the sodium silicate components had to be mixed and not the aggregate and the grout. Another advantage of using the sodium silicate was that it kept the eroding water clean. Mixing procedures, however, had to be very strict because factors such as mixing time, temperature, and size of the sample being prepared all had to be carefully controlled.

79. Although the sodium silicate mixes provided the most realistic rock simulants under erosive conditions observed up to that point, the knickpoint phenomena could not be reproduced consistently with two layers of sodium silicate alone. A two-layered sample, with the capping layer composed of sodium silicate cemented gravel and the underlying layer composed of gelatin cemented gravel provided the most realistic results.

80. Knox gelatin has proved to be a valuable engineering tool in studies involving dynamically loaded foundations, ground motion propagation, and seismic exploration phenomena. Cratering tests conducted by WES used a gelatin model (Paek and Heller 1968). Gelatin mixed with gravel eroded very well in preliminary flume tests. The gelatin mixes kept the water clear so that failure mechanisms and the development of the air pocket under the overfall could be studied in detail. The recommended simulated rock for reproducing the knickpoint migration phenomena for the velocities and geometry which were used in this research is sodium silicate and gravel for the top layer and gelatin and gravel for the bottom layer.

PART V: HYDRODYNAMIC MECHANISMS

81. The phenomenon of undercutting has been documented for years, but the actual mechanics involved were largely unknown. During the flume studies conducted in this research the actual sequence of events, geologic conditions, geometries, and velocities necessary to cause undercutting were actually reproduced and understood. The flume studies have demonstrated that the mechanics of knickpoint migration or headcutting are controlled by the geometry of the knickpoint and the velocity of the flow. The geometry of the knickpoint is in turn governed by the geology at the specific site. Therefore, geology, in conjunction with topography, plays a key role in the initial location of a knickpoint.

Drop Structure as a Knickpoint Analog

82. Because the knickpoint plays such an important role in emergency spillway erosion, it is necessary to understand what is taking place at the knickpoint from a hydraulics perspective. The review of literature directly relevant to knickpoint formation and growth showed that the actual mechanics which controlled the process were largely unknown. However, it was noted that a hydraulic "drop structure" is geometrically very similar to a knickpoint. Drop structures are installed at various intervals in steep channels to dissipate energy and prevent scouring of the channel floor (Figure 22).

83. There is a great deal of energy loss in the area where the free falling jet strikes the floor of the channel. The amount of energy loss has been determined experimentally by Moore (1943). The energy dissipated at the base of a free overfall is shown in Figure 23.

84. Based on the concept that drop structures are designed to prevent scour and headward erosion, it seemed appropriate to assume that knickpoints which happen to meet the same geometric and hydraulic standards would be much less likely to have severe erosion potential. Conceptually, the overall research effort was geared toward creating a model for a worst case scenario for headward migration of a knickpoint and determining the role of stratigraphic variation on erosion.

85. In order for the calculations for the jet impact angle θ to be valid, the area underneath the waterfall must be vented to the atmosphere. If

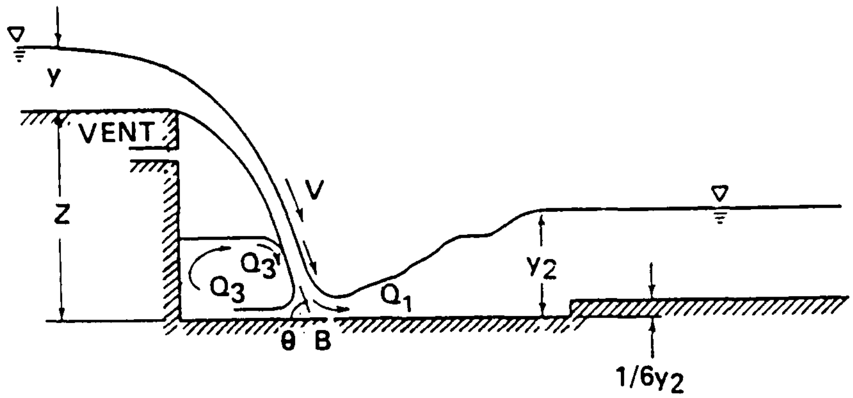

Figure 22. The hydraulic drop structure is geometrically very similar to knickpoints and was used as an analog to study the knickpoint migration phenomena (after Henderson 1966). An explanation of the symbols in the above figure is as follows:

Y = critical depth of flow above knickpoint
Z = height of knickpoint above datum
Y_2 = depth of tailwater below knickpoint
Q_1 = that portion of the initial discharge that flows downstream
Q_3 = that portion of the initial discharge that flows back toward the overfall
B = the point where the jet impacts
θ = the angle at which the jet impacts
V = velocity of the jet

this area is not vented a pressure differential will occur which will draw the waterfall inward against the vertical face and cause severe erosion. The unvented condition was used to study the worst case condition for undercutting. In unvented conditions the waterfall can be drawn underneath a less erodible layer at an angle greater than 90 deg.

86. The tailwater depth is critical in controlling the stresses that are acting on the area underneath an overfall. For a particular set of knickpoint or drop structure conditions, stresses will be transmitted to the channel floor in proportion to the depth of the tailwater. Figure 24 (Robinson 1987) shows a plot of observed stresses and backwater depths from tests using a 3-ft wide flume with a 2.5-ft overfall drop and a flow rate of 3.2 cu ft/sec. When the tailwater depth was greater than 2.5 ft the stresses underneath the waterfall were negligible, but increased to a maximum of 0.36 lb/sq ft as the tailwater was lowered. The tailwater was lowered as much as possible during the current modeling efforts so that the energy was at a maximum.

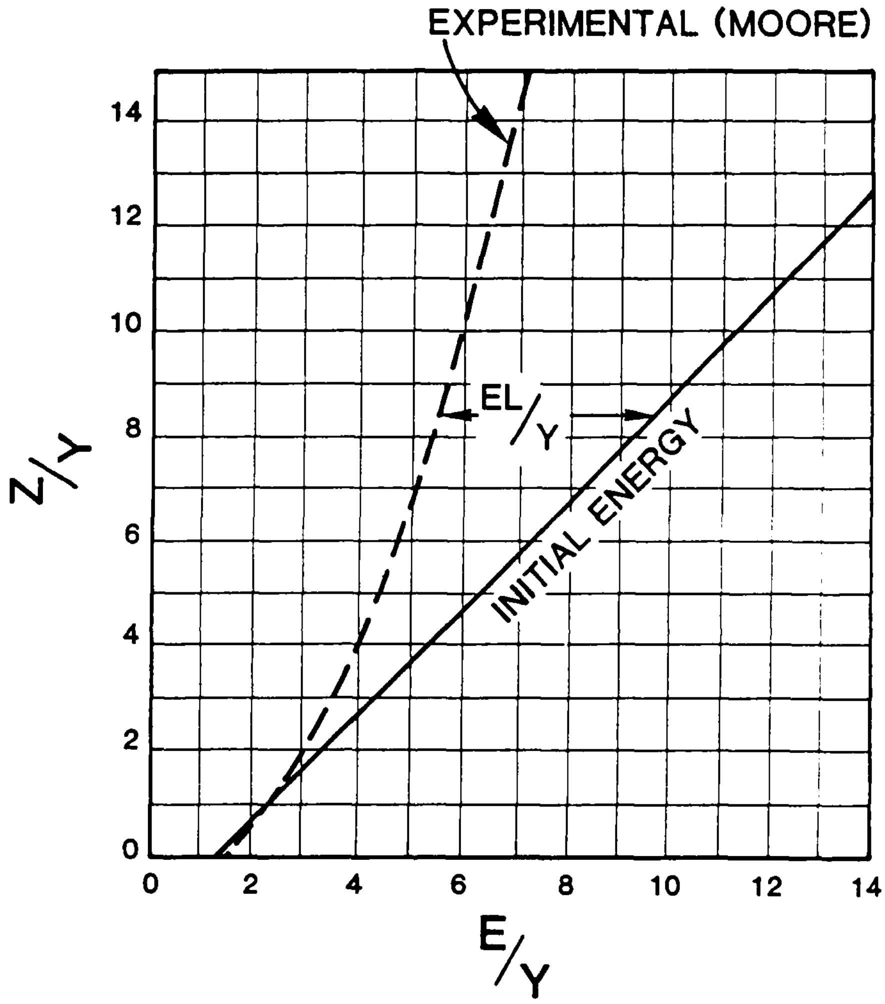

Figure 23. The energy (E) dissipated at the base of a free overfall is dependent on the critical depth of the water (Y) and the height of the fall (Z) (after Henderson 1966). E_L is energy dissipated

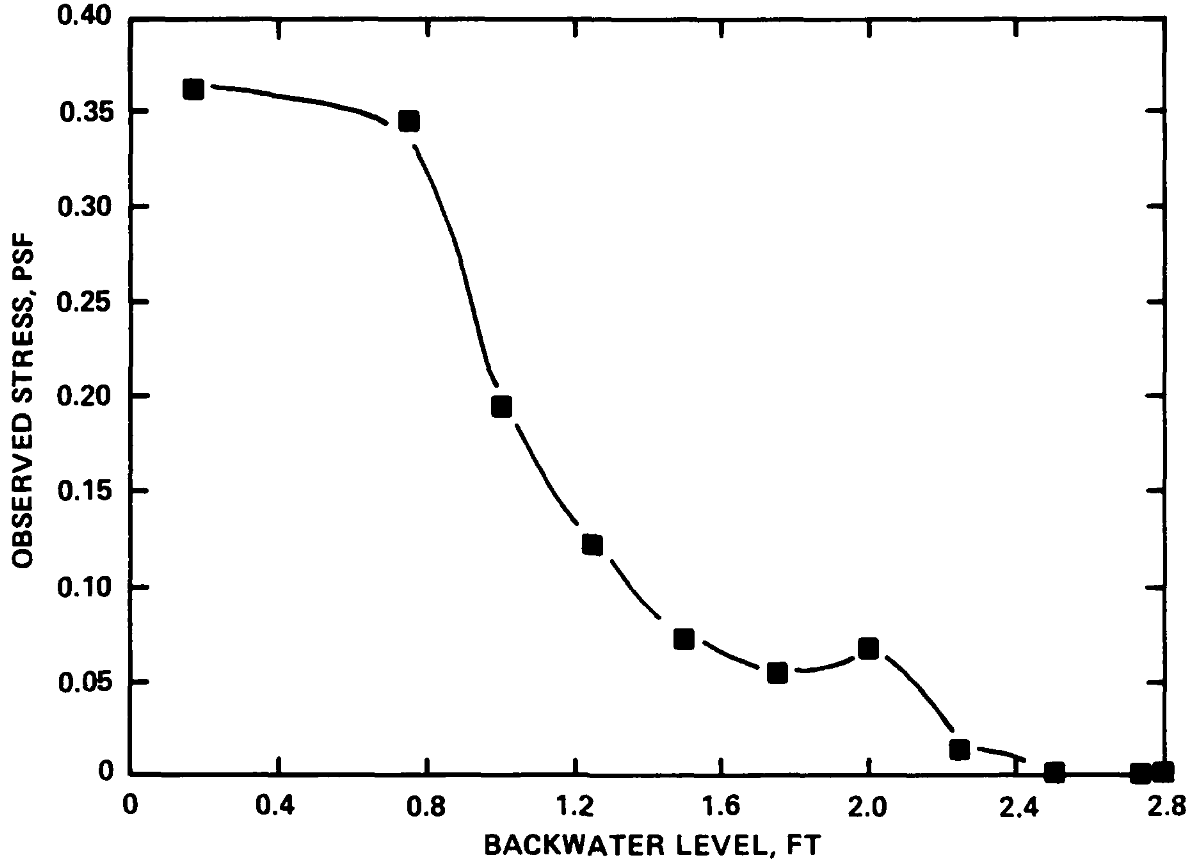

Figure 24. Plot showing the relationship between backwater depth and transmission of stresses to the channel floor (after Robinson 1987)

87. For headcutting to occur the reverse roller portion of the overfall must be in close proximity to the vertical face of the knickpoint. The reverse roller can come in contact with the vertical face in one of several ways:

a. A vented knickpoint in which the ratio of height of fall Z to depth of flow Y is greater than 8/1.

b. An unvented knickpoint in which negative pressures hold the flow against the vertical face (Figure 25).

In the vented case, erosion is controlled by the flow conditions and the knickpoint geometry.

Geometric Control

88. Calculations show that erosion is greater when the ratio of the height of fall Z to critical water depth Y is greater than 8 to 1 for

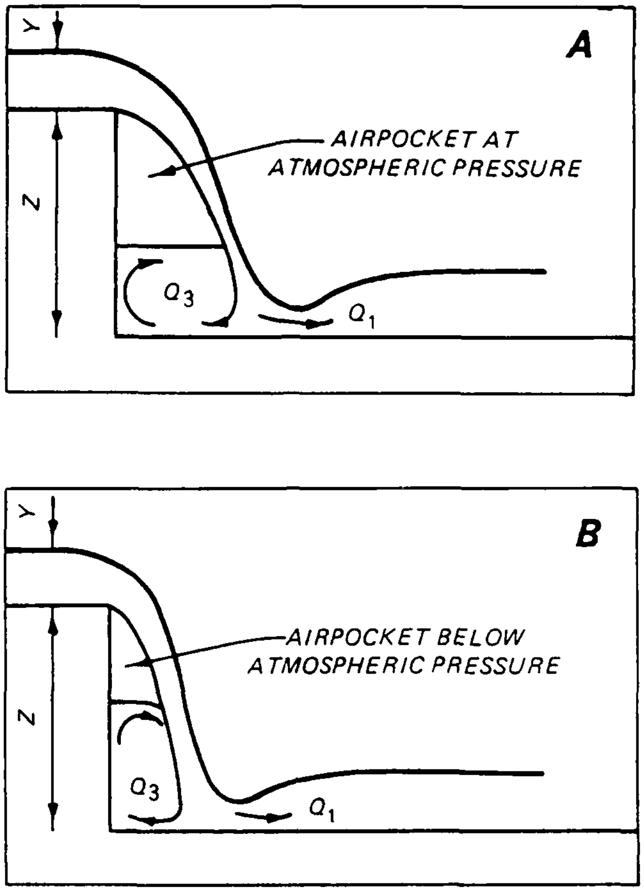

Figure 25. Schematic diagram showing vented (A) and unvented (B) conditions at a knickpoint

a minimum tailwater depth. Figure 26 shows the significance of the Z:Y ratio in controlling the impact angle θ . As the ratio of Z:Y becomes larger the angle of impact approaches 90 deg and a higher percent of the original discharge is entrained in the reverse roller portion of the jet. The point of impact is controlled by the velocity of the flow going over the knickpoint for a given height of fall.

89. The $Q_3:Q_1$ curve in Figure 26 shows that as the impact angle approaches 90 deg a higher percentage of the total discharge volume is entrained in Q_3 and directed toward the vertical knickpoint face. The velocities of rock particles in the reverse roller were measured using a video recorder and stopwatch. The velocities averaged 0.71 ft/sec with a maximum velocity of 1.4 ft/sec.

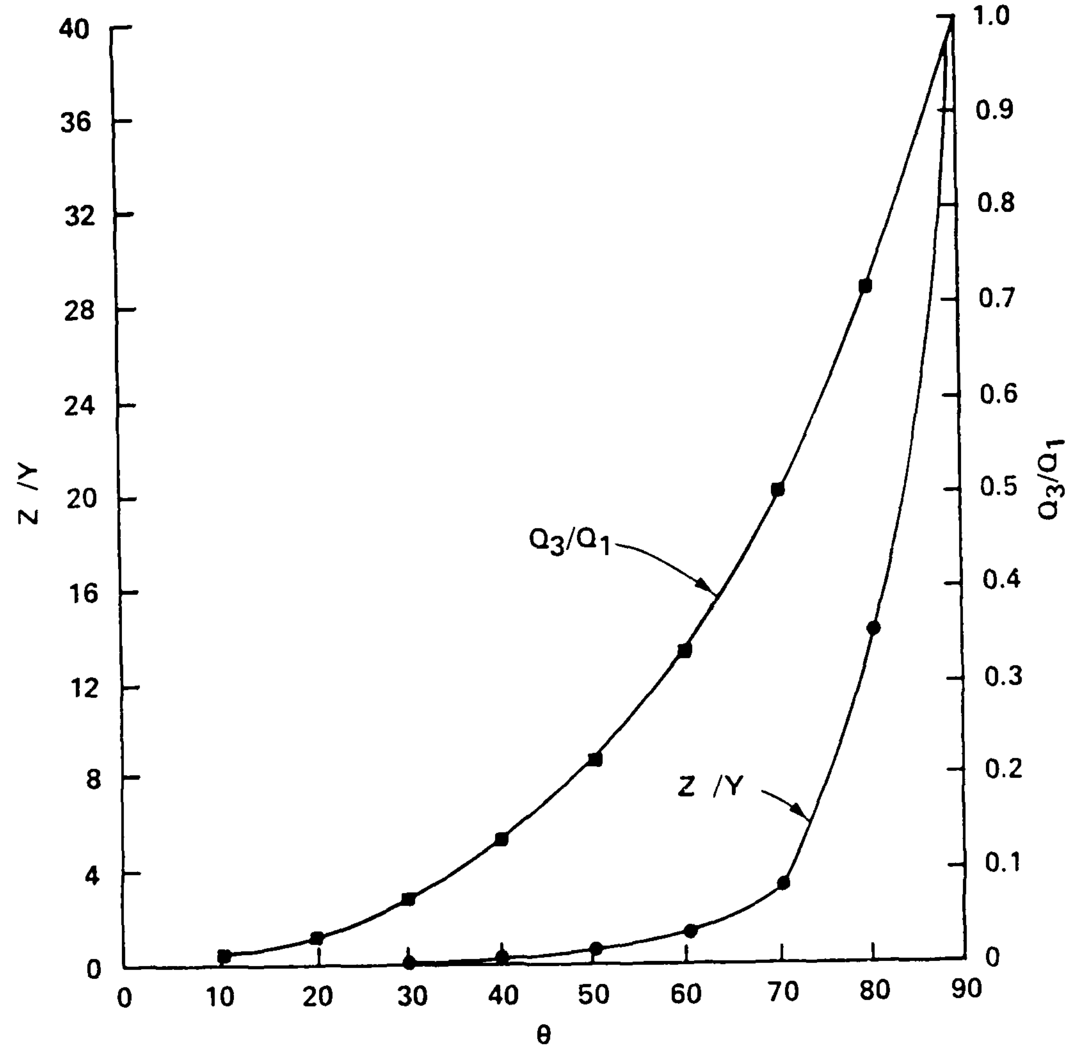

Figure 26. Relationship between the Q_3/Q_1 and Z:Y ratios to the impact angle θ . The plots are based on the relationships $\cos\theta = (1.06)(Z/Y + 3/2)^{1/2}$ and $Q_1/Q_3 = 1 + [(\cos\theta)/1 - \cos\theta)]$

90. Higher flow velocities move the point of impact further away from the vertical portion of the knickpoint and reduce the potential for undercutting. This is not intuitively apparent because in tractive force scour the higher the velocity the more severe the erosion. For the modeling effort it was decided to use the geometry and velocity that would bring the jet as close to the vertical face of the knickpoint as possible.

91. Geology plays a critical role in determining the height of the overfall. In areas where the spillway or natural stream is underlain by

layered sedimentary units, the height of the overfall is controlled by the distance between one erosion resistant layer and the next underlying resistant layer. For example, in an area where the flow depth is typically 2 ft, a 16-ft section of resistant material overlying erodible material would yield a Z:Y ratio of 8:1. These conditions would bring the overfall near the vertical face.

Unvented Control

92. The above scenario is for the vented natural knickpoint. In the unvented case the pressure differential can cause the water to be drawn against the vertical face regardless of the Z:Y ratio. For any given set of geometric and velocity conditions, the position of the trajectory jet and the reverse roller associated with it could be reproduced in the flume. The flume was modified to vent the area below the jet or nappe when desired and to measure the pressure in this region during unvented conditions (Figure 27). Starting from a v nted condition (Figure 28), the unvented condition associated with accelerated erosion was reproduced by first increasing the discharge and then decreasing the discharge (Figure 29).

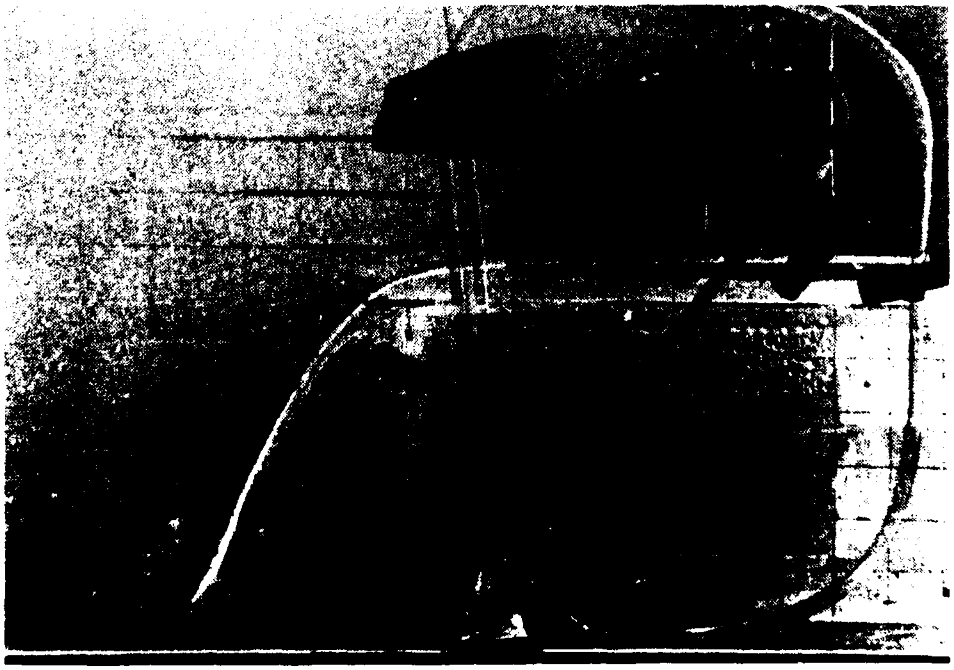

Figure 27. Venting port installed in the side of the flume to measure pressure differentials underneath the nappe

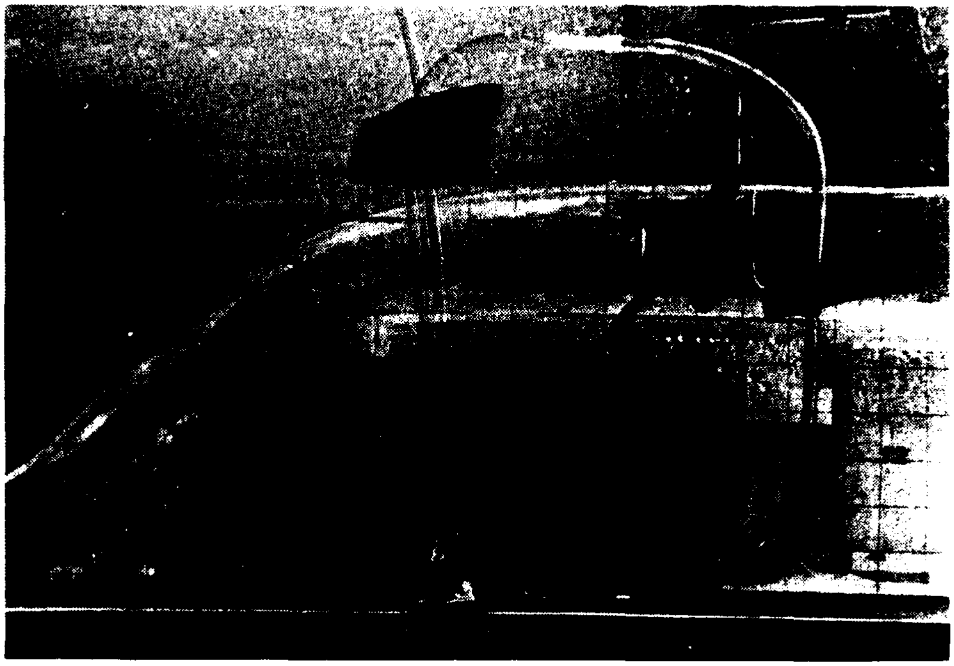

Figure 28. Initial condition produced in the flume. Note that the impact angle θ is small

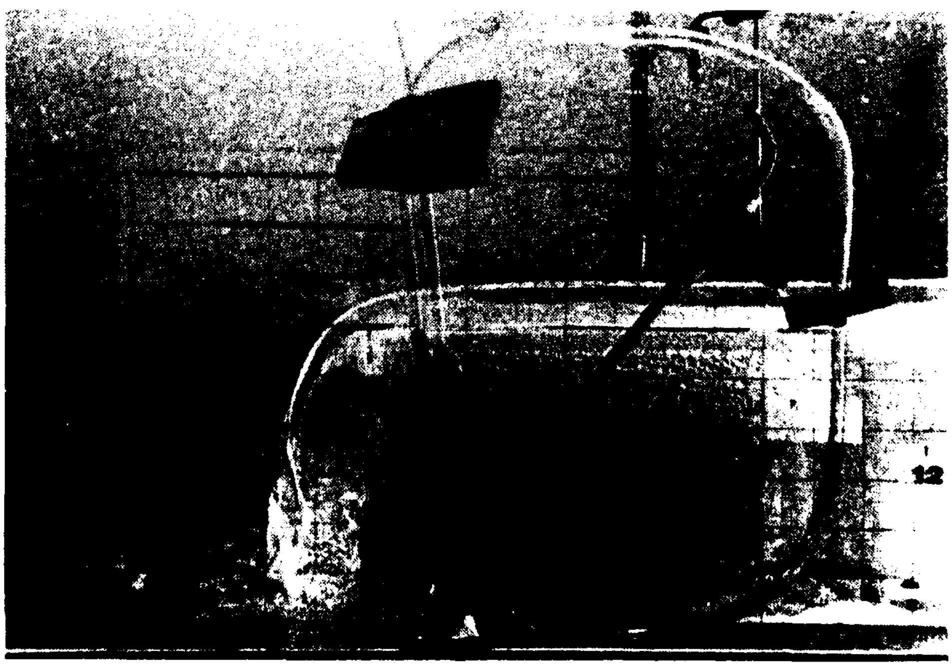

Figure 29. Unvented condition produced in the flume. Note that the impact angle θ is near vertical

The unvented condition was also established by raising the tailgate and flooding the knickpoint and then lowering the tailgate (Figures 30 and 31). The unvented highly turbulent condition was reproduced either by fluctuating the discharge or by fluctuating the tailwater elevation.

93. By venting and unventing the area under the nappe, the position of impact and the corresponding reverse roller can be positioned in a predictable and repeatable manner. The pressures measured in the area under the nappe ranged from 0.02 to 0.04 psi below atmospheric pressure to 0.03 psi above atmospheric pressure. The positive pressures were noted during periods of accelerated flow. These small negative pressures move the trajectory jet from a position where no significant headcutting can take place to a position very close to the vertical face of the knickpoint where the erosion potential is extremely high.

94. The position of the tailwater also influences the location of potential undercutting because, as the position of the tailwater moves up and down, the jet creates turbulence on the vertical face of the knickpoint at an adjacent position.

Hydraulic Similitude

95. The Froude numbers for flume Tests 3-1 through 3-12 averaged 1.35. The Froude numbers for ten SCS spillway flows in Kentucky and six SCS spillway flows in Mississippi were 1.2 and 1.03, respectively (Cameron et al. 1988a). Because the Froude number is used to formulate the equations for similitude in hydraulic scale modeling, portions of the results of the flume tests may be used for studying larger knickpoints.

Effect of Key Geological Variables

Erodible layer thickness

96. A series of tests were designed to study the effect of varying the thickness of the eroding layer on the unvented undercutting phenomena. It was decided to use Plexiglas as the capping layer and gelatin cemented gravel as the underlying erodible material. The variables such as velocity and duration of flow were kept as low as possible during each test. Because of the

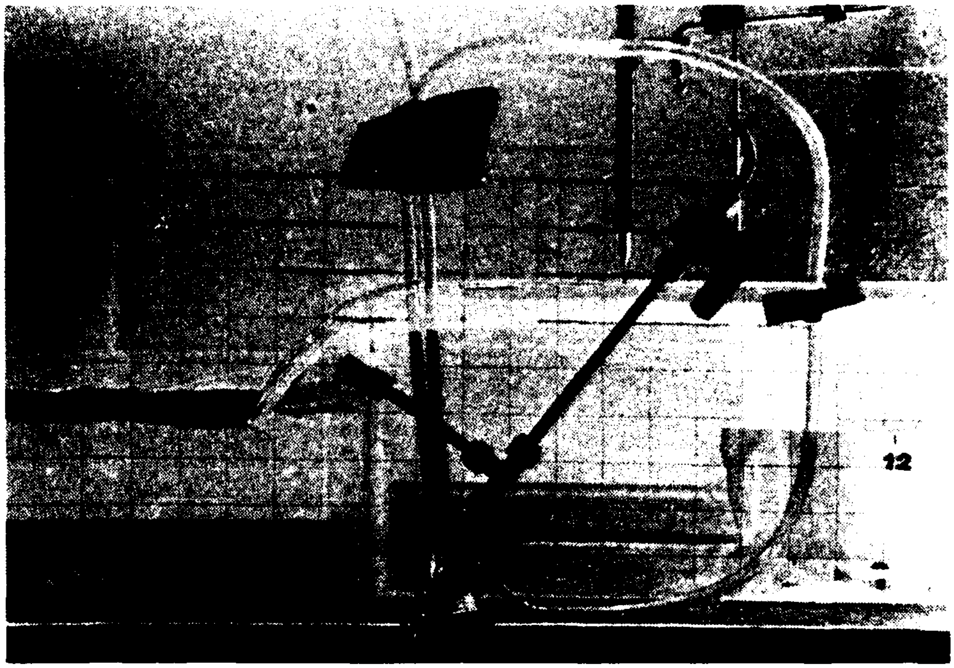

Figure 30. Unvented condition being generated by flooding the knickpoint and slowly lowering the tailwater level

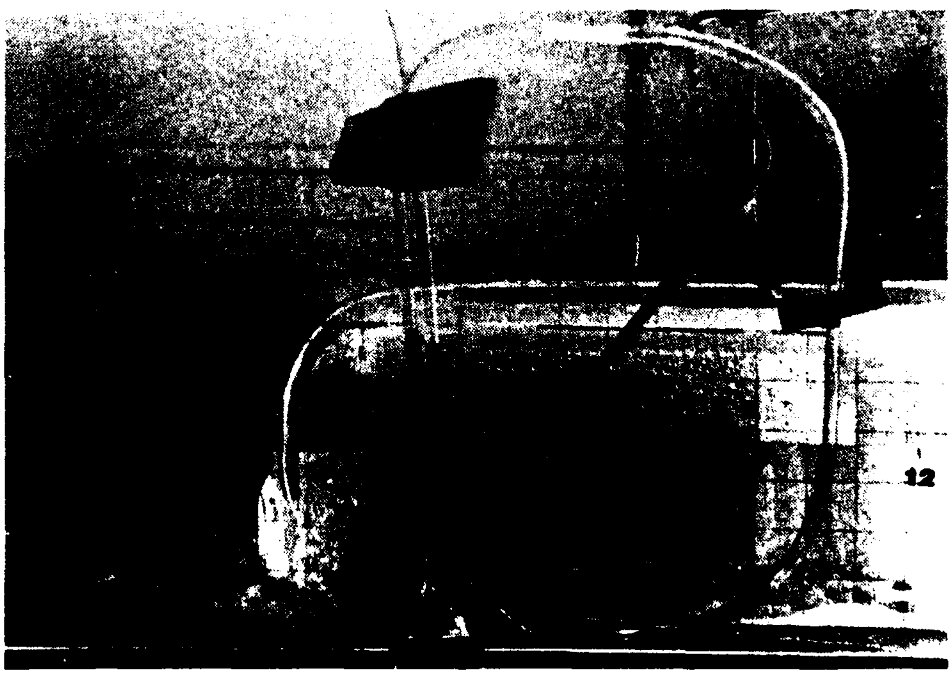

Figure 31. Unvented condition as a result of lowering the tailwater

nonerodible nature of the capping layer, the sample could not fail incrementally as would be the case under natural conditions. Instead, the reverse roller worked its way headward only as far as the eroding layer thickness and geometry of the turbulent flow would allow. When the volume of material eroded was plotted against the ratio of the thickness of the eroding layer to the diameter of the reverse roller it was apparent that the data fell into two regimes as shown in Figure 32. The test results are tabulated in Appendix D.

97. For the geometry and velocity used in this series of tests the size of the reverse roller was approximately 2 in. When the eroding layer was less than 3 in. thick the reverse roller could not easily undercut and erode the lower layer. As the thickness of the eroding layer was increased to more than 3 in., the erosion pattern drastically changed from that of removing a particle at a time to a pattern which involved mass failures of the gelatin-gravel mix. This pattern of erosion indicates that if the thickness of the erodible layer, in a two-layer system, is greater than about 1.5 times the diameter of the reverse roller created at a particular knickpoint, shear strength of the material being eroded becomes a significant factor and the migration rate of the knickpoint increases.

<u>Shape of the overfall lip</u>

98. Hydraulic engineers have designed the best shapes for various weirs and drop structures to take advantage of the negative pressures generated by running water. A few simple tests were conducted to investigate the effects of altering the shape of the overfall lip. The previous tests were conducted with an abrupt 90-deg angle for the overfall lip. Of particular interest was the rounded lip, because in nature many knickpoints become rounded relatively soon. It was found that for the geometries that were used during this research, rounded overfall lips enhanced the negative pressure conditions below the nappe. The effect of a lip that extends beyond the face of the knickpoint, as would be the case with a very resistant unfractured capping layer such as the limestone ledges at Brownwood, was also investigated. It was found that the air pocket beneath the nappe remained at lower than atmospheric pressure and a large volume of water accumulated behind the nappe (Figures 33 and 34).

<u>Open fractures</u>

99. The effect of open fractures at a knickpoint was demonstrated by placing a 90-lb sample into the flume without securing it in place or sealing

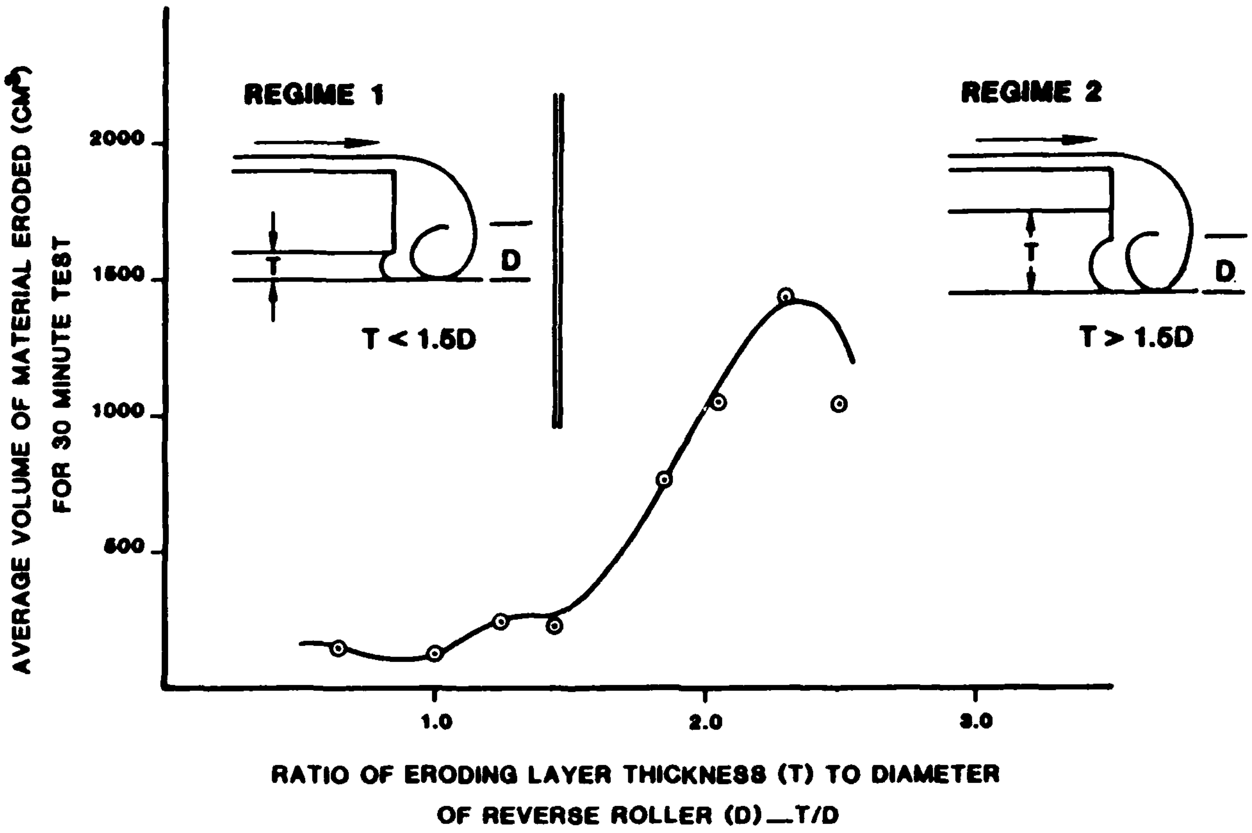

Figure 32. Plot of the eroding layer thickness versus the volume of material eroded during a given time

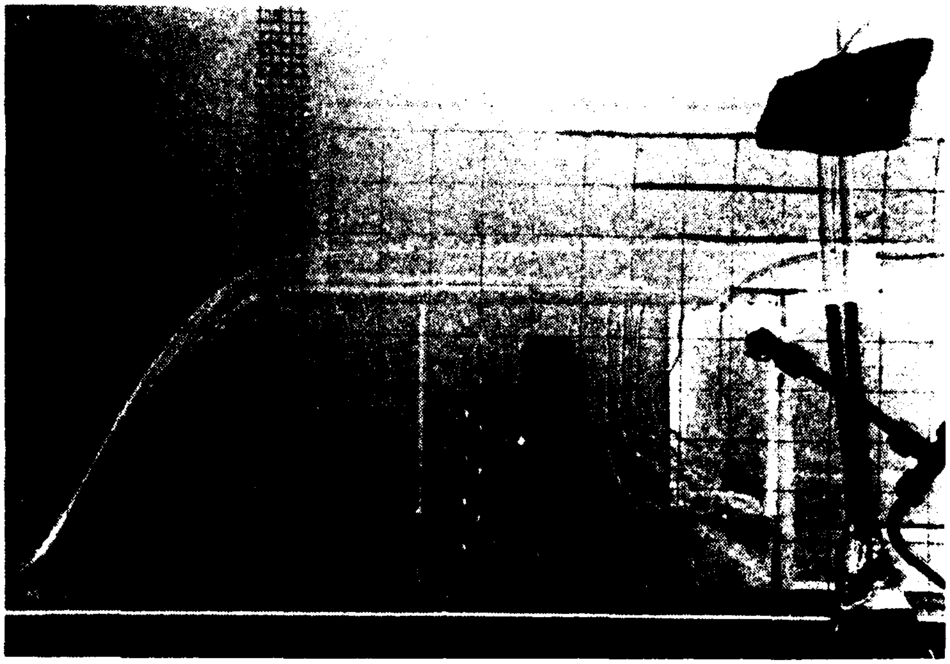

Figure 33. The extended overfall lip under vented conditions

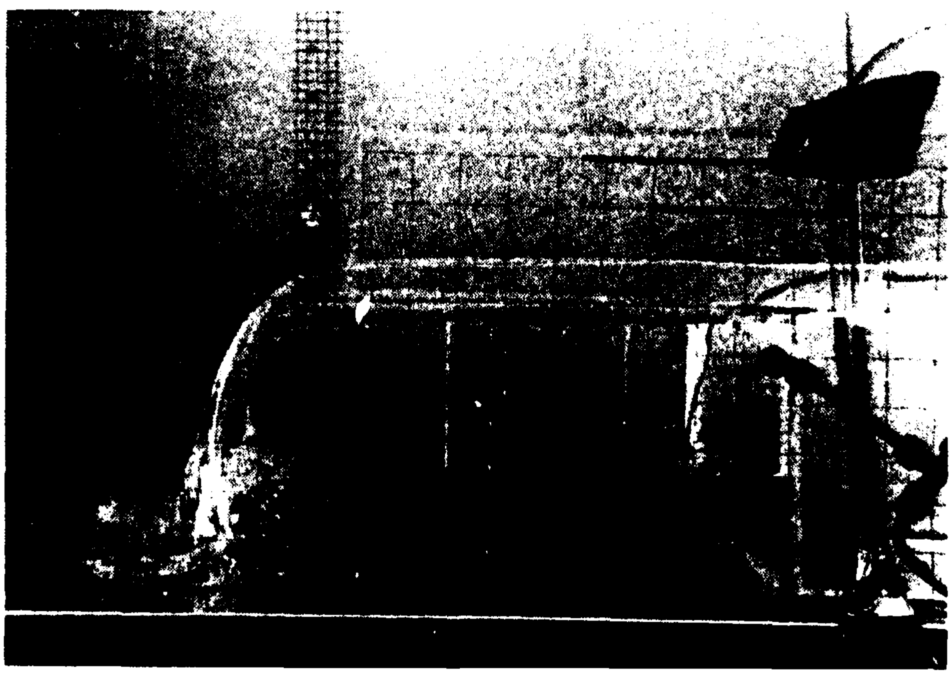

Figure 34. The extended overfall lip under unvented conditions

the space between the inner flume walls and the outer sampler holder walls. When the flow in the flume started, the heavy sample was rafted downstream within seconds. At a natural occurring knickpoint the same phenomena would also be enhanced by the negative pressure underneath the nappe.

Maximum erosion rate

100. To put the headward erosion phenomena in proper perspective it was necessary to demonstrate a worst case scenario. In this case situation the failure mechanism had to be of a repetitive nature so that once the erosion was initiated it would proceed headward until the entire simulated spillway reach was eroded. The sample was designed to simulate an erodible layer emplaced between a capping layer and a nonerodible lower layer. If the bottom layer had been erodible a plunge pool could have developed which would have dissipated energy and actually slowed headward movement. The tailwater was kept as low as possible to maximize erosion and keep the reverse roller positioned at the bottom of the erodible layer. By keeping the reverse roller at the bottom of the softer material, the resulting undercutting also triggered mass slumping and tension failure of the capping material. This test dramatically demonstrated past peak erosion at its worst.

PART VI: CONTROLS AND MECHANISMS IN THE FIELD

101. Four basic types of mass failure mechanisms are associated with rapid headward migration of knickpoints:

- a. Undercutting of a capping layer resulting in cantilever toppling of jointed or fractured caprock.
- b. Undercutting of caprock resulting in tensile failure and toppling of caprock.
- c. Undercutting or erosion resistant layer resulting in shear failure of large blocks of material (slumping of water saturated material would be included in this category).
- d. Rafting of large blocks of jointed material as a result of water entering joints or fractures.

The geology, coupled with the severity of the unvented condition, controls which of these mass failure mechanisms will dominate at a specific site. Case histories for the following sites are given in Cameron et al. 1986.

Undercutting and Toppling of Fractured Caprock: Saylorville Spillway

102. The Saylorville spillway exhibits several types of mass failure mechanisms. The knickpoint in the vicinity of center line sta 22+00 was chosen to illustrate a classic example of the undercutting and toppling of fractured or jointed caprock (Figure 35). The caprock was described by the US Army Engineer District, Rock Island (1984) as "an argillaceous limestone which separated along joints trending N70°E with a 2 to 3 ft spacing." The underlying erodible shale was described as "soft, gray, mottled, maroon shale with joints trending N10°W and N75°E." The shape of the knickpoint indicates that undercutting occurred in an unvented condition. The height of the knickpoint, approximately 3 ft, in relation to the depth of flow, 3 to 4 ft, would not provide the necessary geometry for vented undercutting conditions to occur. The sequence of failure is shown in Figure 36. It is postulated that as the water impacted the vertical portion of the knickpoint, unvented undercutting occurred in the friable shale causing the blocks of limestone to become unstable and topple (Figure 37). The toppling failure was aided by the low pressure zone beneath the nappe which allowed the eroding water access to any weak points such as fractures and weathered zones in both the limestone

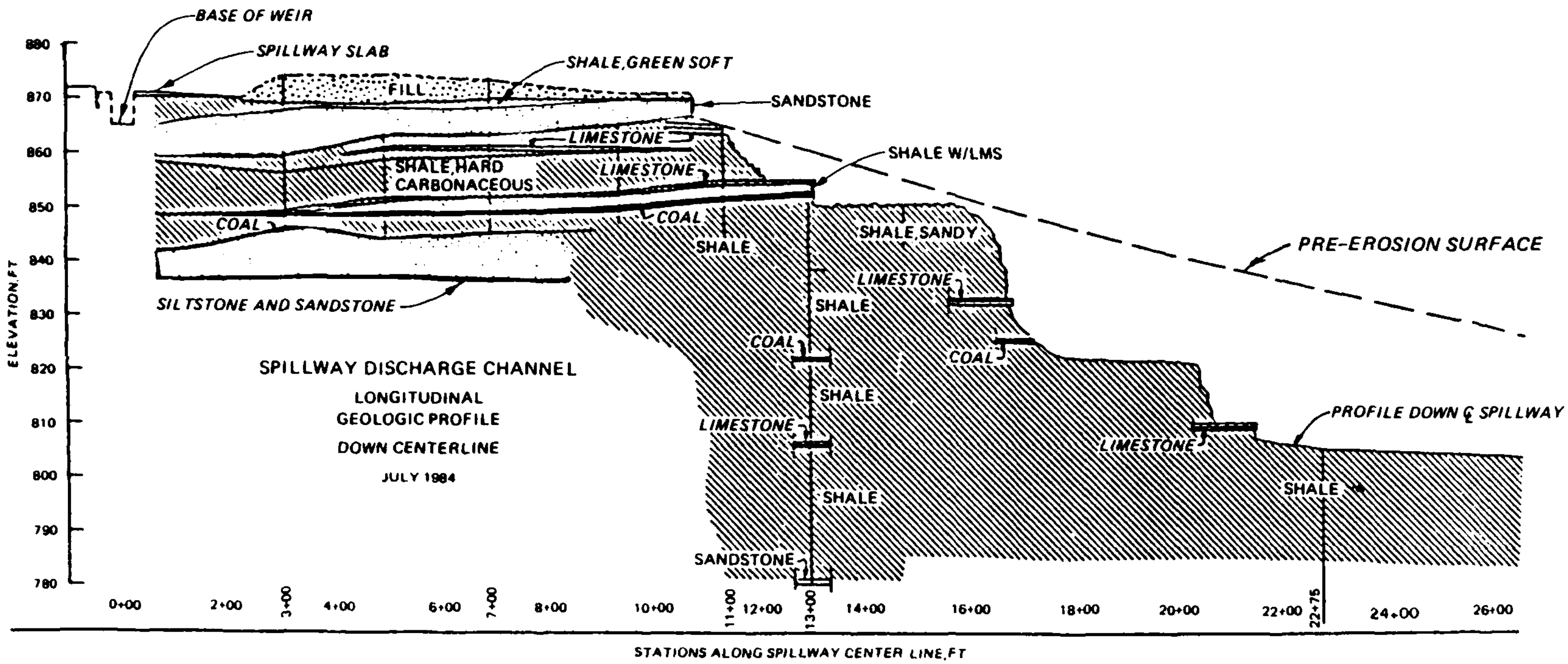

Figure 35. Geologic cross section along the center line of the Saylorville emergency spillway (US Army Engineer District, Rock Island 1962)

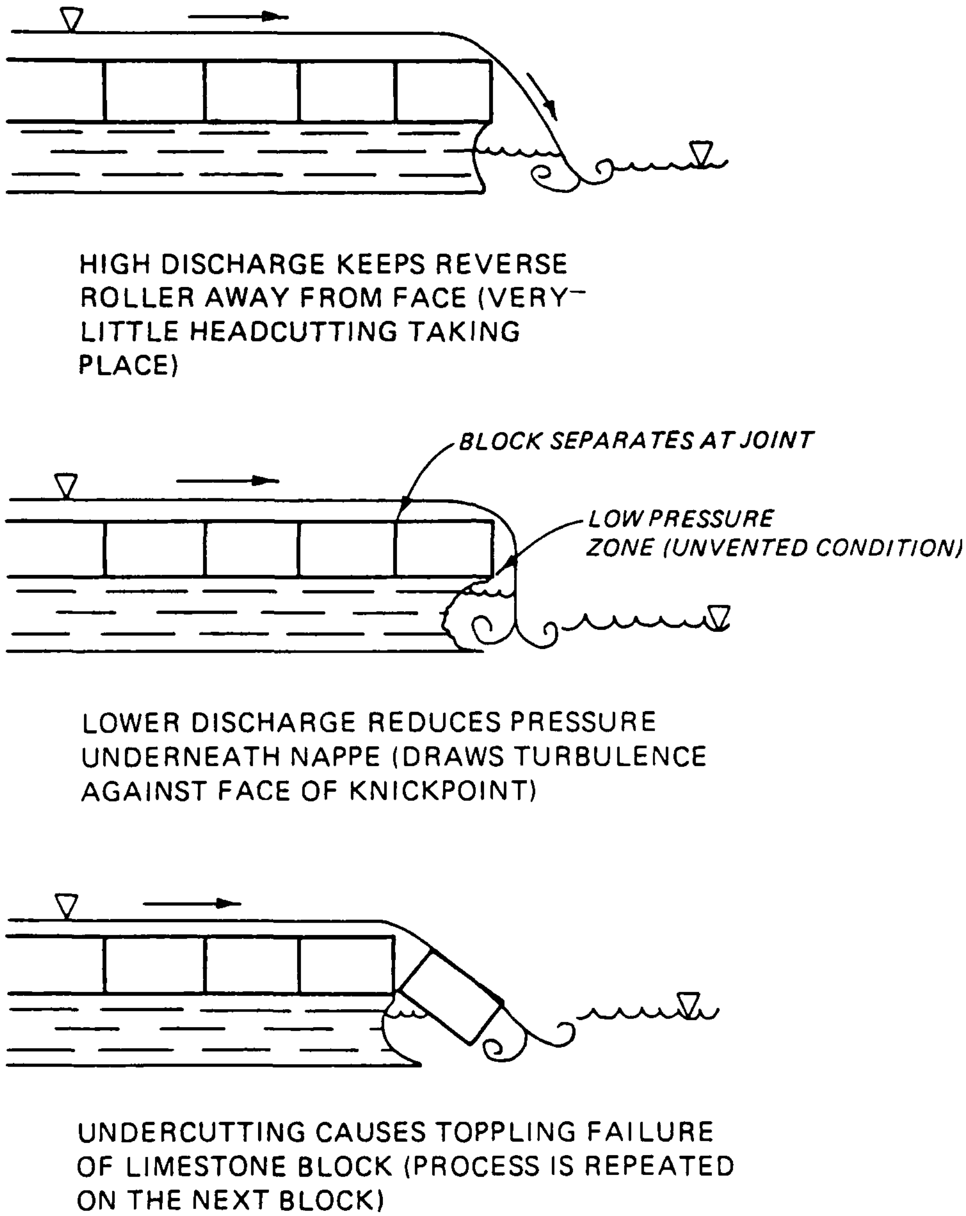

Figure 36. Combined effect of venting and geologic controls on mass wasting at one knickpoint in the Saylorville spillway channel

Figure 37. Large displaced blocks of rock in the Saylorville emergency spillway channel (Waterways Experiment Station photo file)

and the shale. As joints were opened up in the limestone, water could enter the fractures and raft out blocks in combination with the toppling failures.

Undercutting and Tensile Failure of Caprock: Lake Brownwood Spillway

103. The Lake Brownwood spillway is a dramatic example of a knickpoint which is controlled by a resistant unfractured continuous layer of limestone (Figure 38). Despite numerous flow events, the rate of headward migration is relatively slow (Figure 39). The two resistant limestone sequences at the site are separated by 30 ft of shale that contains thin sandstone interbeds. The uppermost knickpoint, located near center line sta 4+00, was selected to demonstrate an important failure mechanism involving undercutting and tensional block failure. The sequence of failure mechanisms is shown in Figure 40.

104. In the upper knickpoint the thick layer of more easily erodible shale could have led to vented conditions in some flood events where the channel may not have been bankfull. If venting occurred, this would have minimized the erosion potential during those events. In most flood events, however, it appears that mass failure occurred in the following manner:

- a. The flow peaked and the discharge began to decrease (Figure 40).
- b. As the discharge decreased, pressure underneath the nappe was reduced and the jet moved closer to the face of the knickpoint.
- c. As the softer shale was removed, the space underneath the limestone ledge became larger (Figure 40).
- d. During low flow conditions on the declining side of the hydrograph, the low pressure zone below the nappe draws the reverse roller under the overhang and flushes out much of the eroded material.
- e. Finally, as the overhanging limestone became more and more unsupported, large blocks would fail in tension as shown in Figure 40, topple and be transported downstream (Figure 41).

Influence of Rounded Lip at Knickpoint: Saylorville Spillway

105. Saylorville spillway has an excellent example of a knickpoint with a rounded lip. The knickpoint is located at center line sta 16+00. A resistant siltstone overlies soft maroon easily erodible shale at this location.

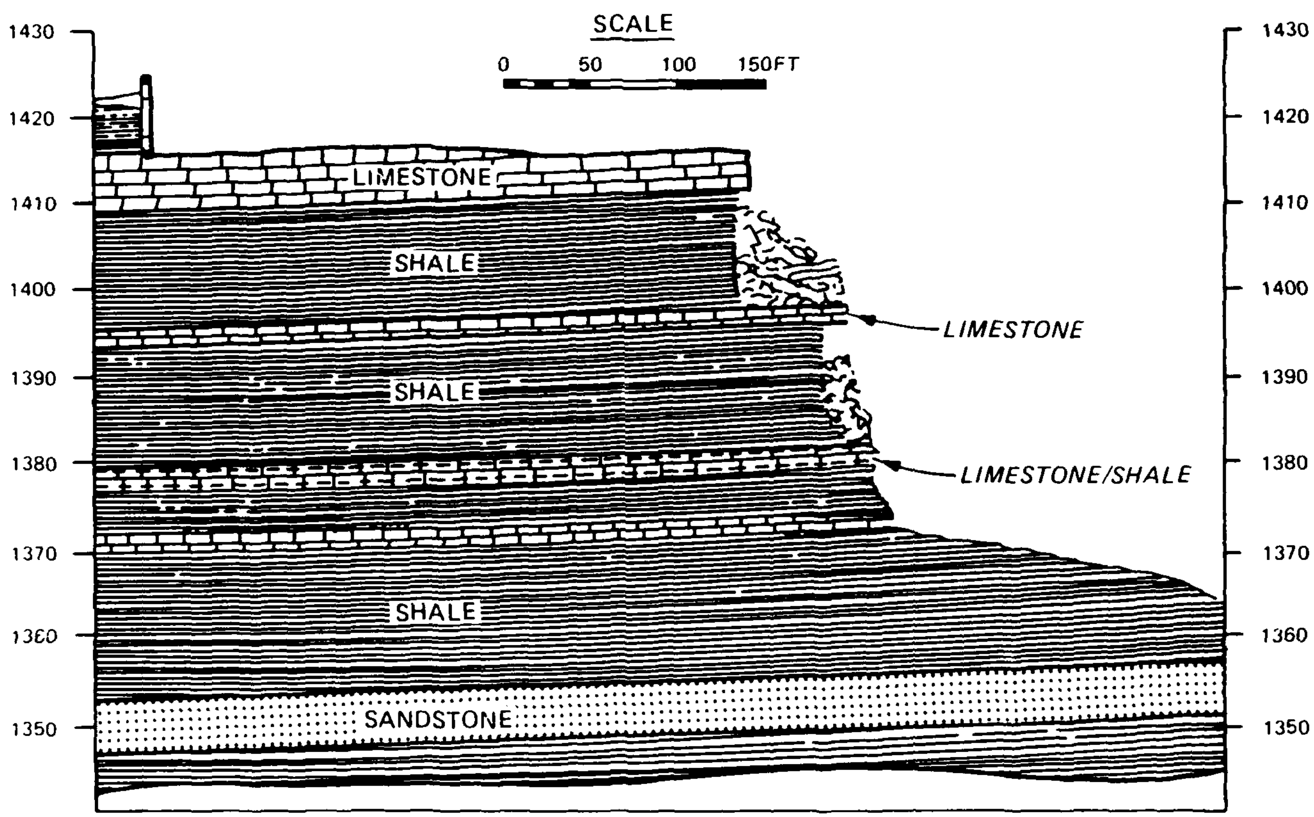

Figure 38. Geologic cross section along the center line of the Lake Brownwood emergency spillway (US Army Engineer District, Fort Worth 1971)

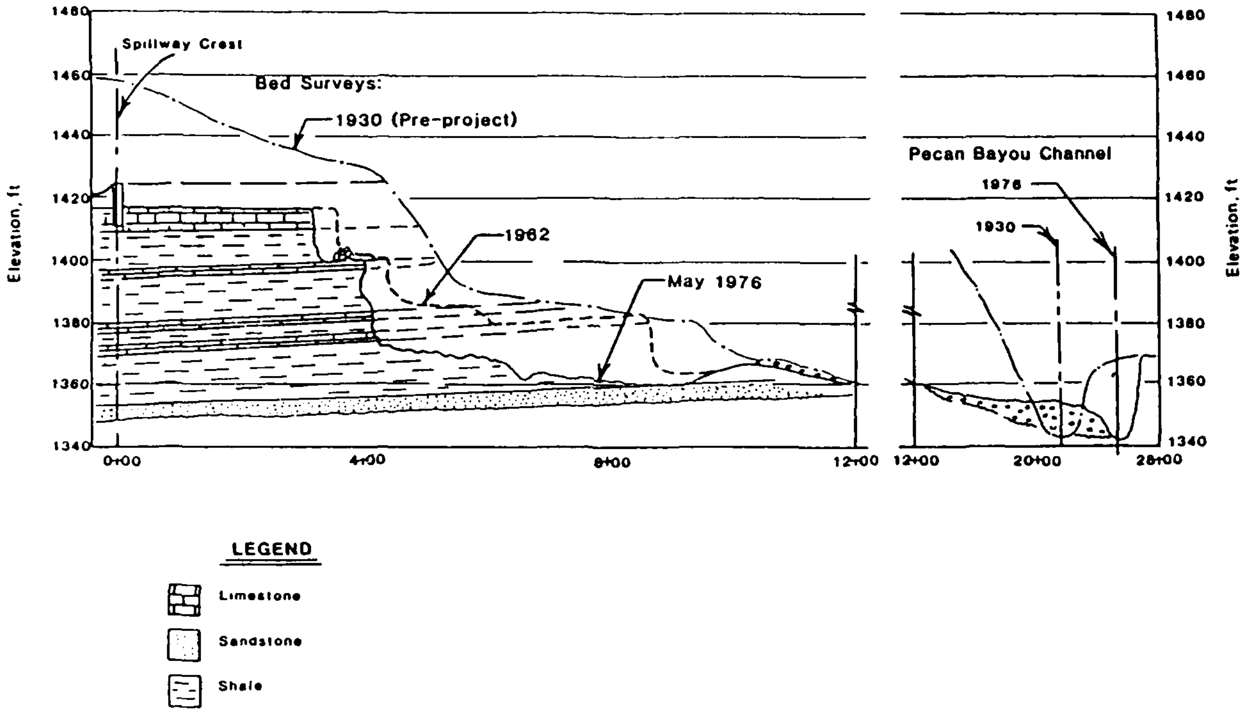

Figure 39. Topographic and geologic profiles of the Lake Brownwood emergency spillway channel (US Army Engineer District, Fort Worth 1971)

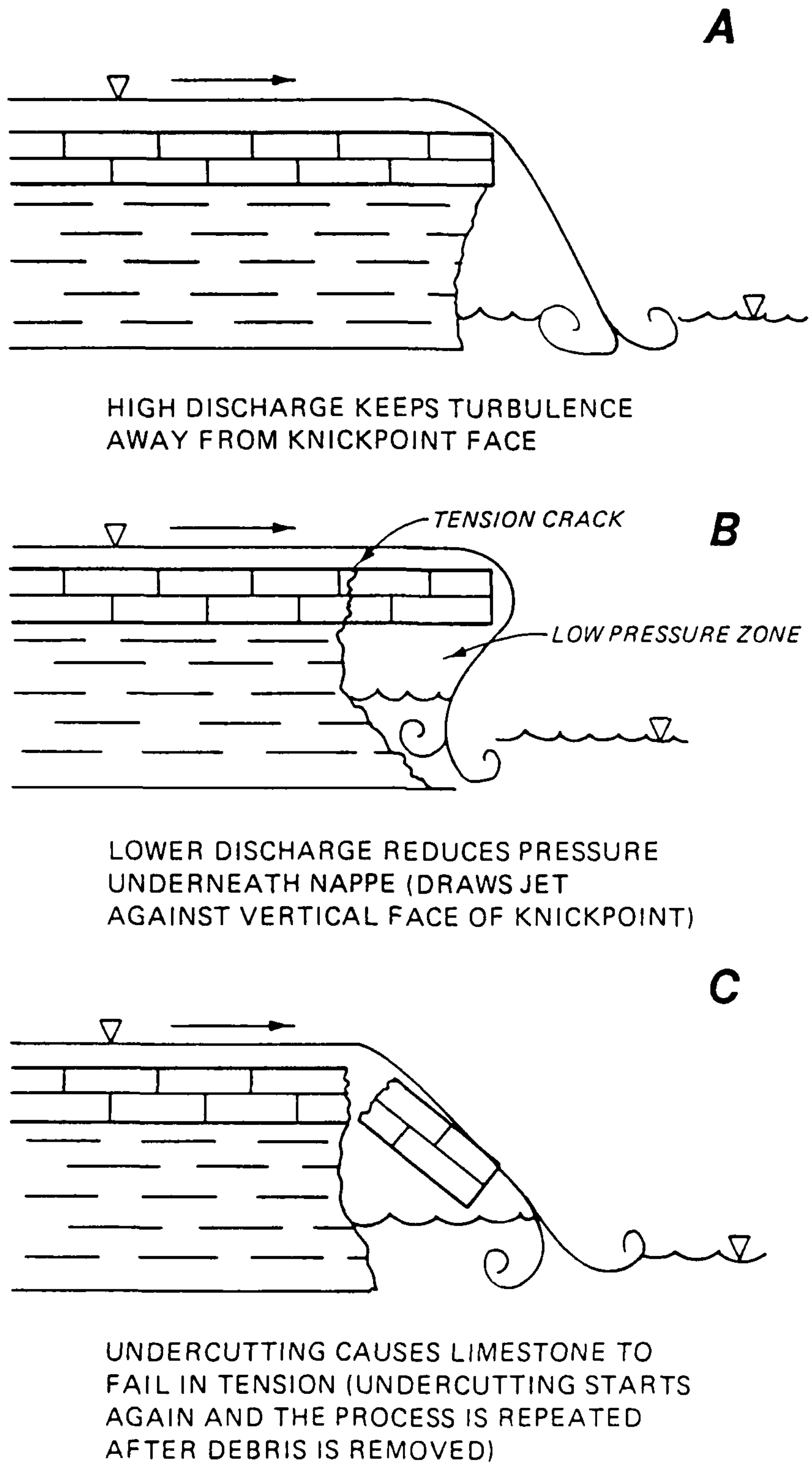

Figure 40. Schematic diagram of the mass failure mechanism at Lake Brownwood, Texas

Figure 41. Knickpoint in the Lake Brownwood emergency spillway (US Army Engineer District, Fort Worth 1971)

Rounded lips of this configuration were found to enhance the development of unvented conditions in the flume tests. The degree to which undercutting has occurred at this knickpoint seems to be more pronounced than the undercutting shown at the knickpoints where the lip is more angular.

Undercutting of Resistant Material Resulting in Shear Failure of Large Blocks of Material: Black Creek Spillway

106. Black Creek spillway in Holmes County, Mississippi, represents an ideal condition to investigate the undercutting and shear failure of large blocks of material. The knickpoint formed at Black Creek differs from the knickpoints described at Saylorville and Brownwood in that the capping layer is not as resistant nor is the contact between the capping layer and the more erodible layer as well defined (Figure 42). The capping layer at Black Creek spillway was composed of loess and the underlying layer was composed of sand, silt, and gravel. The erodible sand and gravel layer extended completely underneath the spillway to the lake. A man-made knickpoint in the form of a roadbed was located where the sand and gravel cropped out. A probable sequence of failure is proposed:

- a. As flow increased, the embankment formed by the road caused an unvented knickpoint to develop. The turbulence caused the

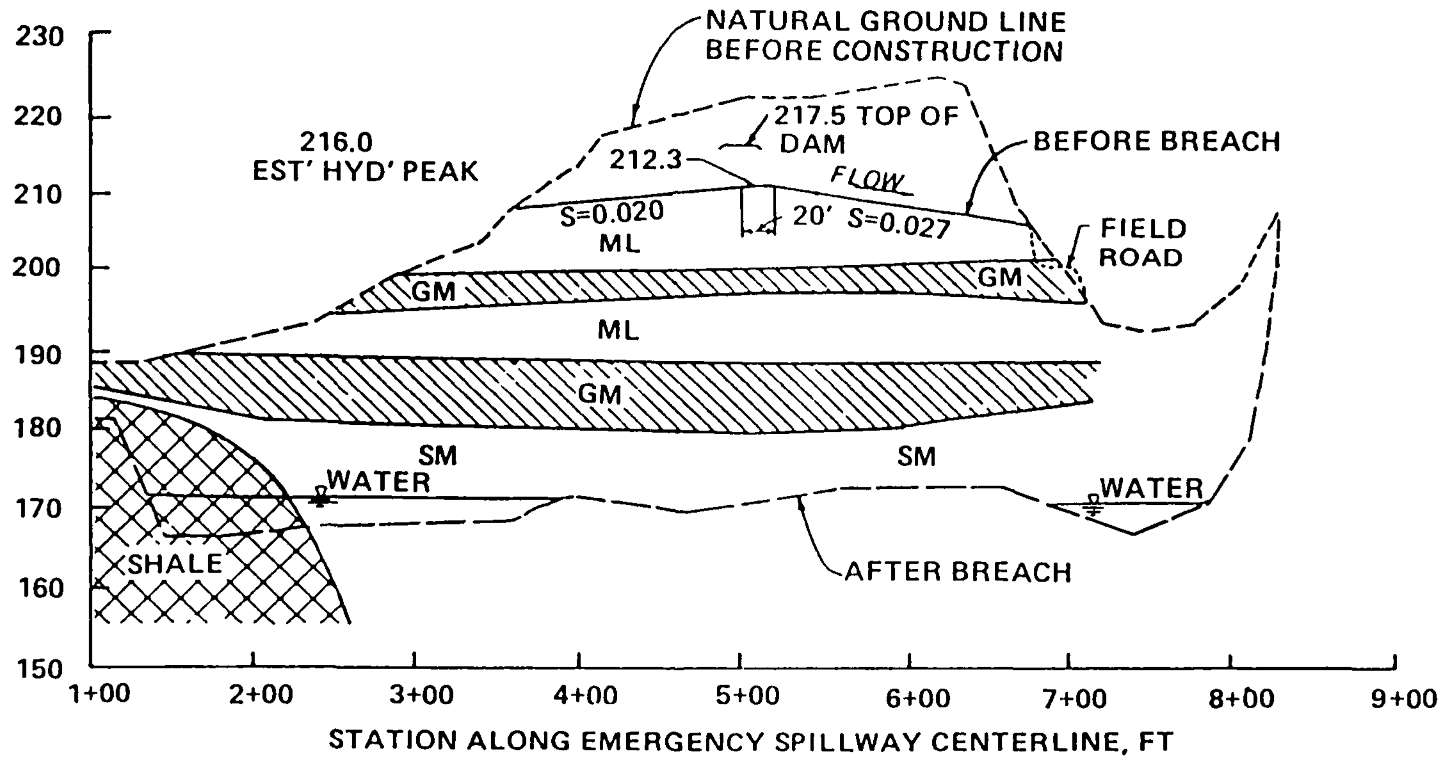

Figure 42. Geologic profile along the center line of SCS Black Creek No. 53 emergency spillway in Mississippi (Soil Conservation Service 1985c)

undercutting of the overlaying loess as the erosive force of the water removed the easily eroded silt, sand, and gravel (Figure 43).

b. As the peak of the flow passed the negative pressure below, the nappe increased and the reverse roller was able to undercut the loess even further (Figure 43).

c. The loess failed in shear and large 2- to 3-cu ft blocks were transported downstream (Figure 43).

107. The flume studies of the effect of varying the thickness of the eroding layer showed that not only does the capping material fail in shear but also the material underlying an erosion resistant layer can fail in shear if the thickness is greater than the diameter of the reverse roller.

108. A variation of this failure mechanism develops when a lower permeable unit is saturated and in a quick condition prior to the flood event and flows from beneath the capping layer. Undercutting can extend for a considerable distance regardless of the position of the reverse roller. Either of these mechanisms could have occurred at Black Creek.

Uplift and Rafting of Large Jointed Blocks: SCS Virginia Site 81

109. The SCS Virginia Site 81 was chosen to demonstrate another important mass failure mechanism which causes the erosion of large volumes of material, but is not usually as dangerous or structure-threatening as the aforementioned undercutting mechanism (Soil Conservation Service 1985a). This type of failure mechanism is important where the capping layer is thick in relation to the more erodible underlying unit. If the underlying erodible unit is thin the amount of undercutting will be relatively small. In some jointed rocks, hard layers are present which have no soft interbeds between them. In this case the classic stairstep erosion pattern can evolve by rafting and uplift without undercutting taking place (Figure 44).

110. Even though there is not an erodible underlying unit, the unvented nappe still plays a critical role in the headcutting process. If the unvented condition dominates at the knickpoint, the jet of water will be drawn to the vertical face and attack whatever weak points exist, such as a thin erodible sedimentary unit or weathered or secondary material within fractures (Figure 44). The resistance of a block to uplift is controlled by its shape, weight, and the shear forces between adjoining blocks. As the material

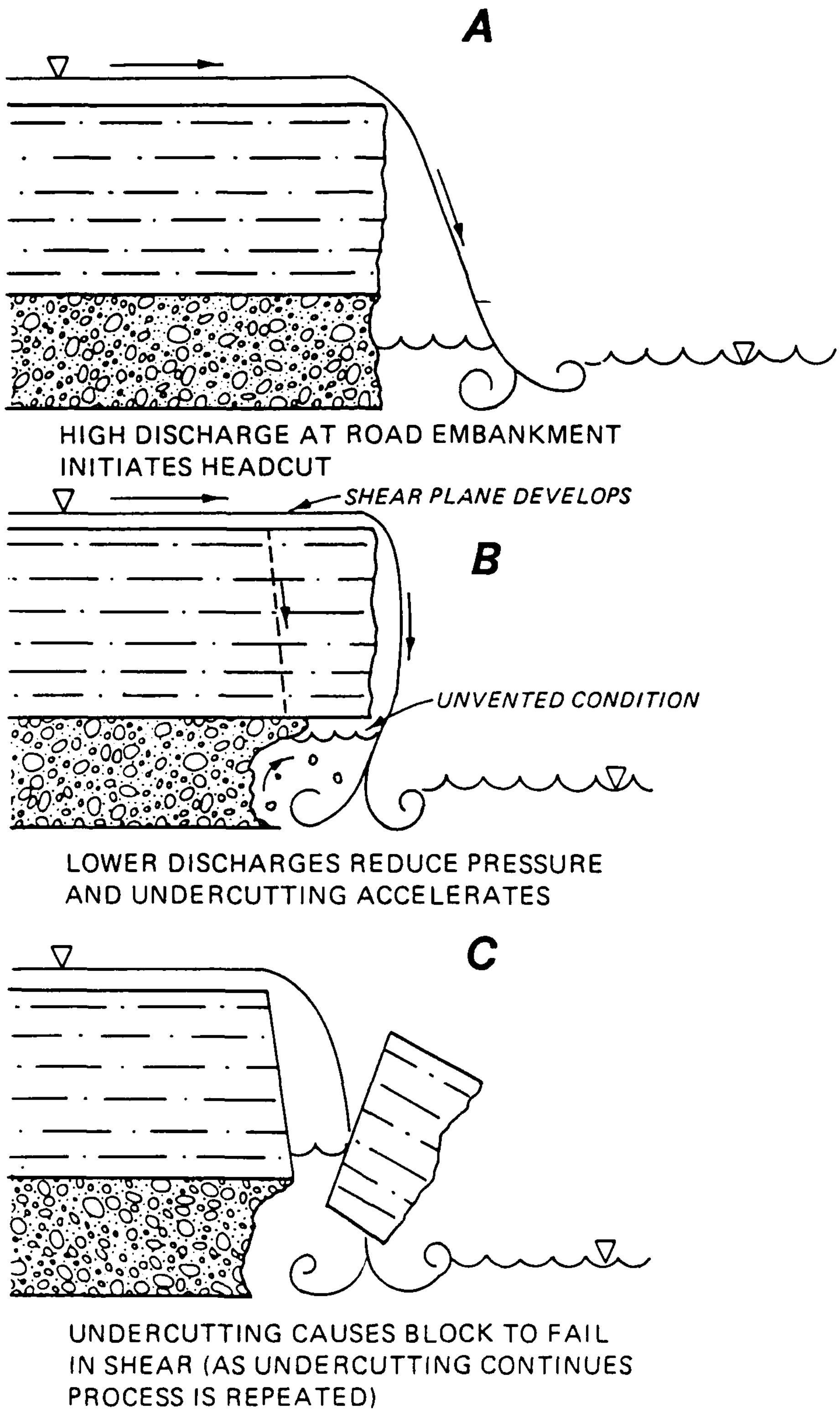

Figure 43. Schematic diagram of the mass failure mechanism at Black Creek spillway

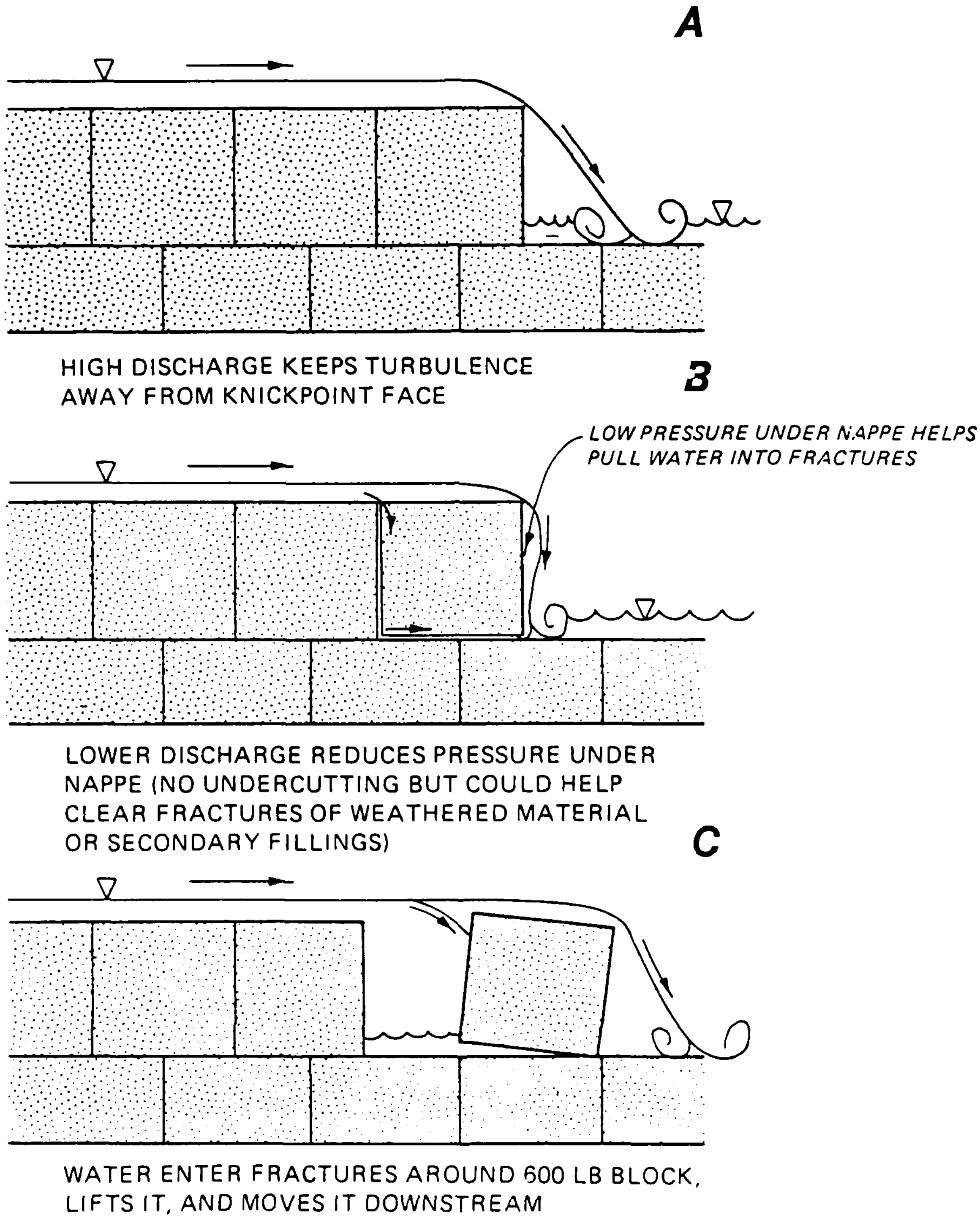

Figure 44. Schematic diagram of the mass failure mechanism at SCS Virginia Site 81

surrounding a block is eroded the water has access to the fractures. The negative pressure in the unvented knickpoint aids in drawing water into the fractures from above the knickpoint. Elevated pore pressures within the bounding fractures combined with removal of any downstream restraining blocks can lead to erosion of the block (Figure 44). As each particular block is displaced and moved downstream, the knickpoint moves upstream and the process is repeated.

PART VII: KNICKPOINT MIGRATION

Geometric Factors

111. The mechanisms defined by this research offer an explanation as to why severe knickpoint migration occurs sporadically and at relatively low flows as opposed to at peak flows. By evaluating the knickpoint as a vented or unvented drop structure, the conditions necessary to position the reverse roller for maximum undercutting can be predicted. Erosion thresholds are controlled by various combinations of knickpoint geometry and flow velocity. The geometry in turn is controlled by the site geology.

112. The point of impact of the water jet must be near the vertical face of the knickpoint for maximum undercutting. Under these conditions the angle θ at which the water jet strikes at the base of the knickpoint is approximately 90 deg (Figure 45). In a vented condition, when the ratio of

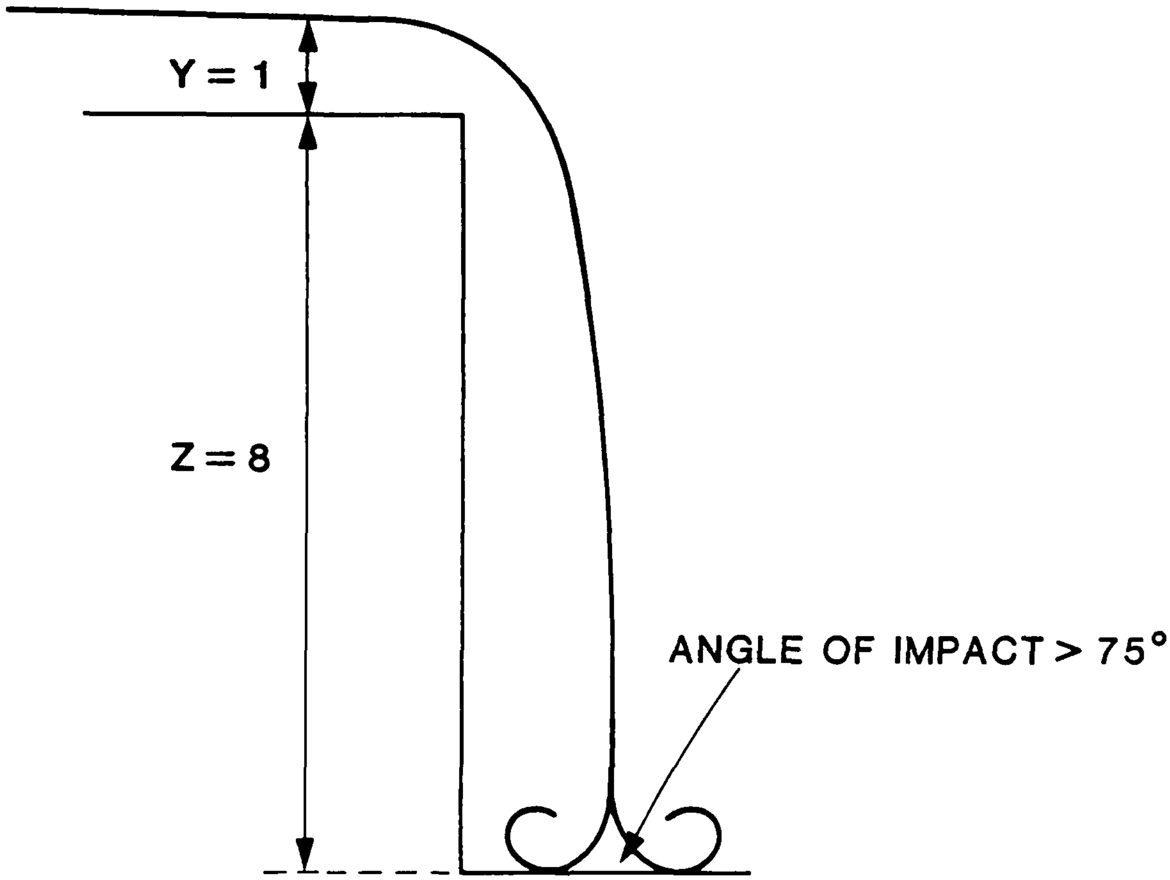

Figure 45. Position of the water jet in a geometrically controlled knickpoint at the lower limit of maximum undercutting (Z/Y > 8/1) in a vented condition

Z:Y is 8:1 or greater and the tail water is low, the angle of incidence approaches 90 deg, and geometrically controlled erosion is enhanced (Figure 46).

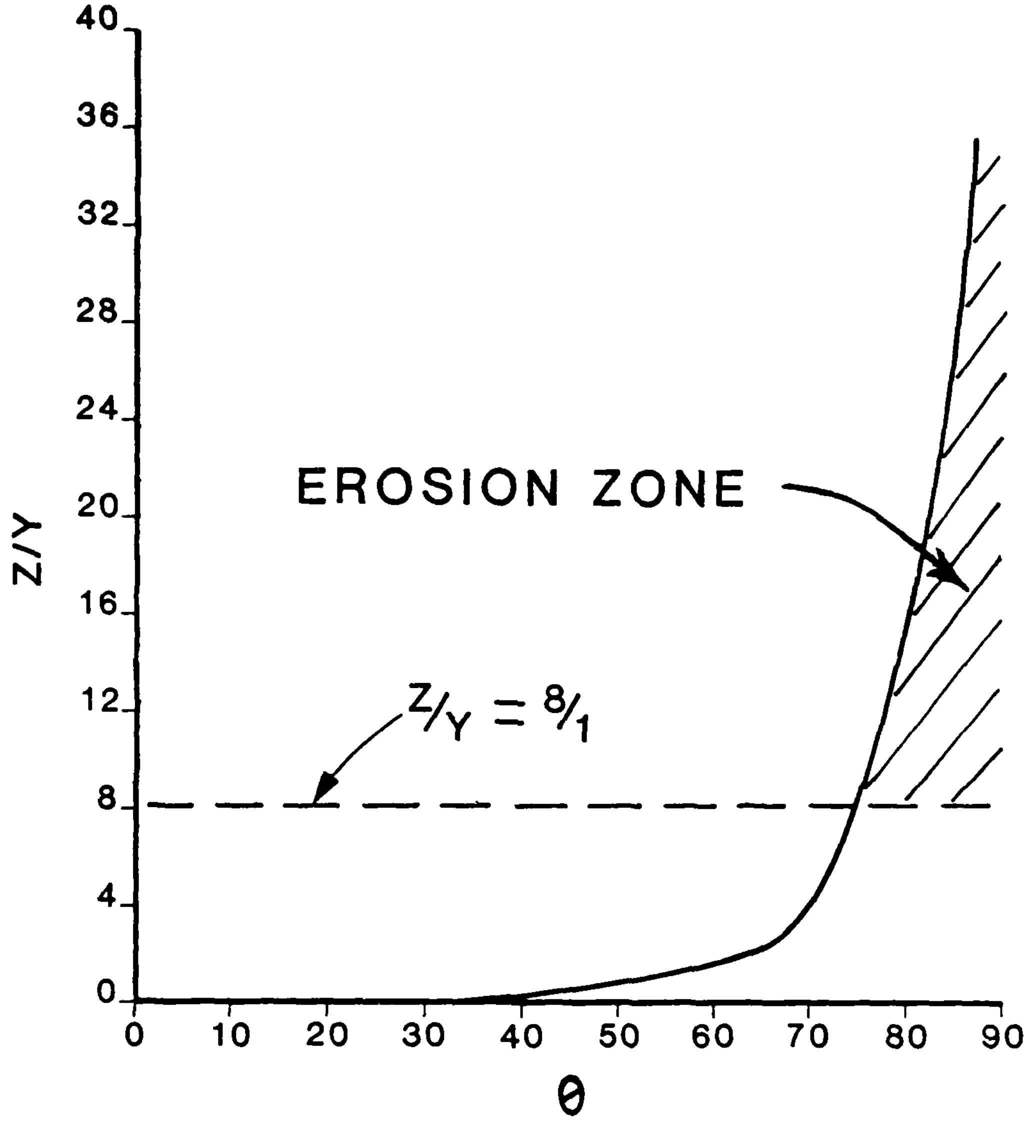

Figure 46. Plot of Z/Y and θ to show critical ratios needed for maximum headcutting in the vented condition

113. In the unvented condition, the low pressure zone below the nappe draws the water jet into the face of the knickpoint and maximizes the erosive effort of the reverse roller. These negative pressures below the nappe also have a significant impact on knickpoints developed in fractured competent rock units. Water is drawn through fractures or pores toward the low pressure areas resulting in increased pore pressures and reduced shearing resistance (Figure 47). Figure 48 shows how the pressure can vary at different points in the knickpoint environment.

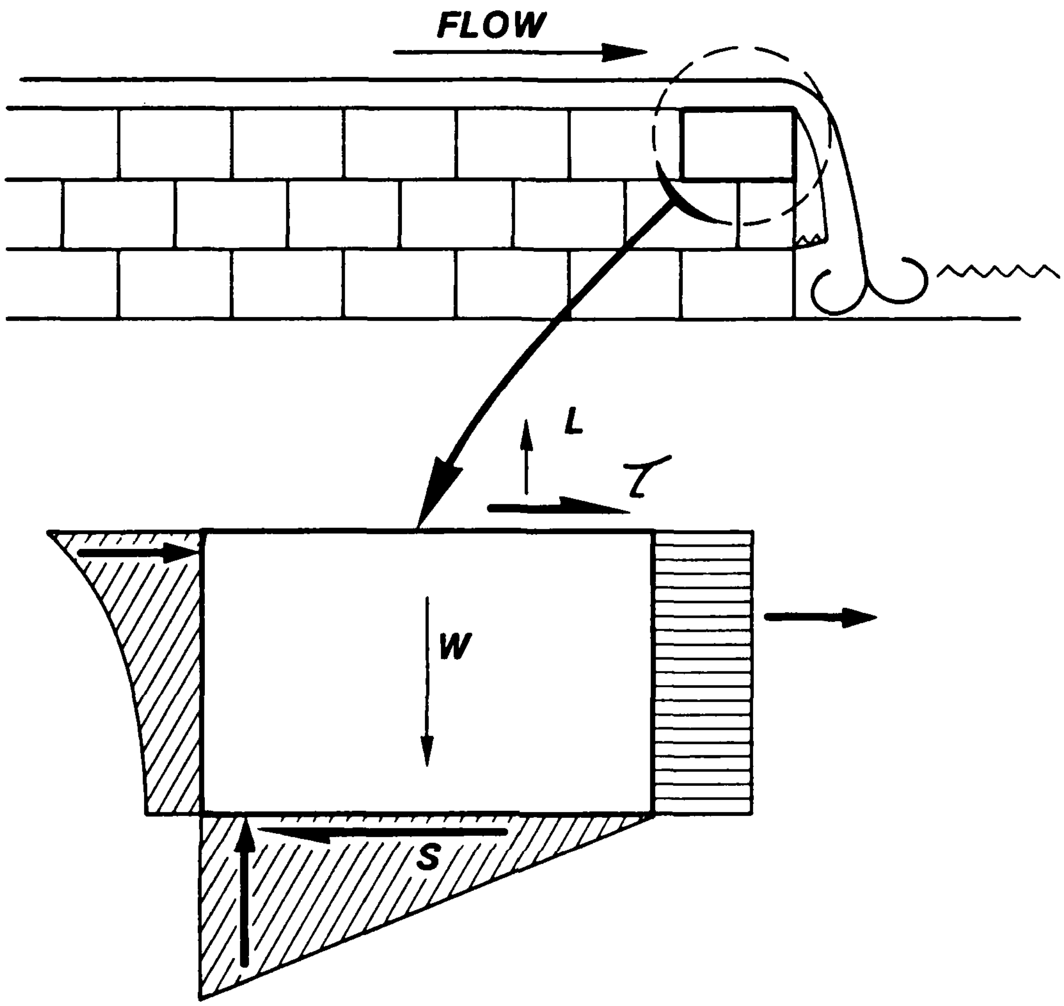

(hatched)	INFERRED EXCESS FRACTURE PRESSURE DISTRIBUTION DUE TO DYNAMIC FLUID IMPACT PRESSURE, ASSUMING DRAINAGE TO FACE
S	SLIDING RESISTANCE: (ONLY RESISTING COMPONENT)
W	SUBMERGED WEIGHT OF THE BLOCK
(horizontal lines)	INFERRED NEGATIVE PRESSURE IN UNVENTED CASE
τ	FLUID BOUNDARY STRESS
L	INDUCED LIFT DUE TO FLOWING FLUID

Figure 47. Inferred pressure differentials at a knickpoint characterized by widely spaced fractures in the capping rock

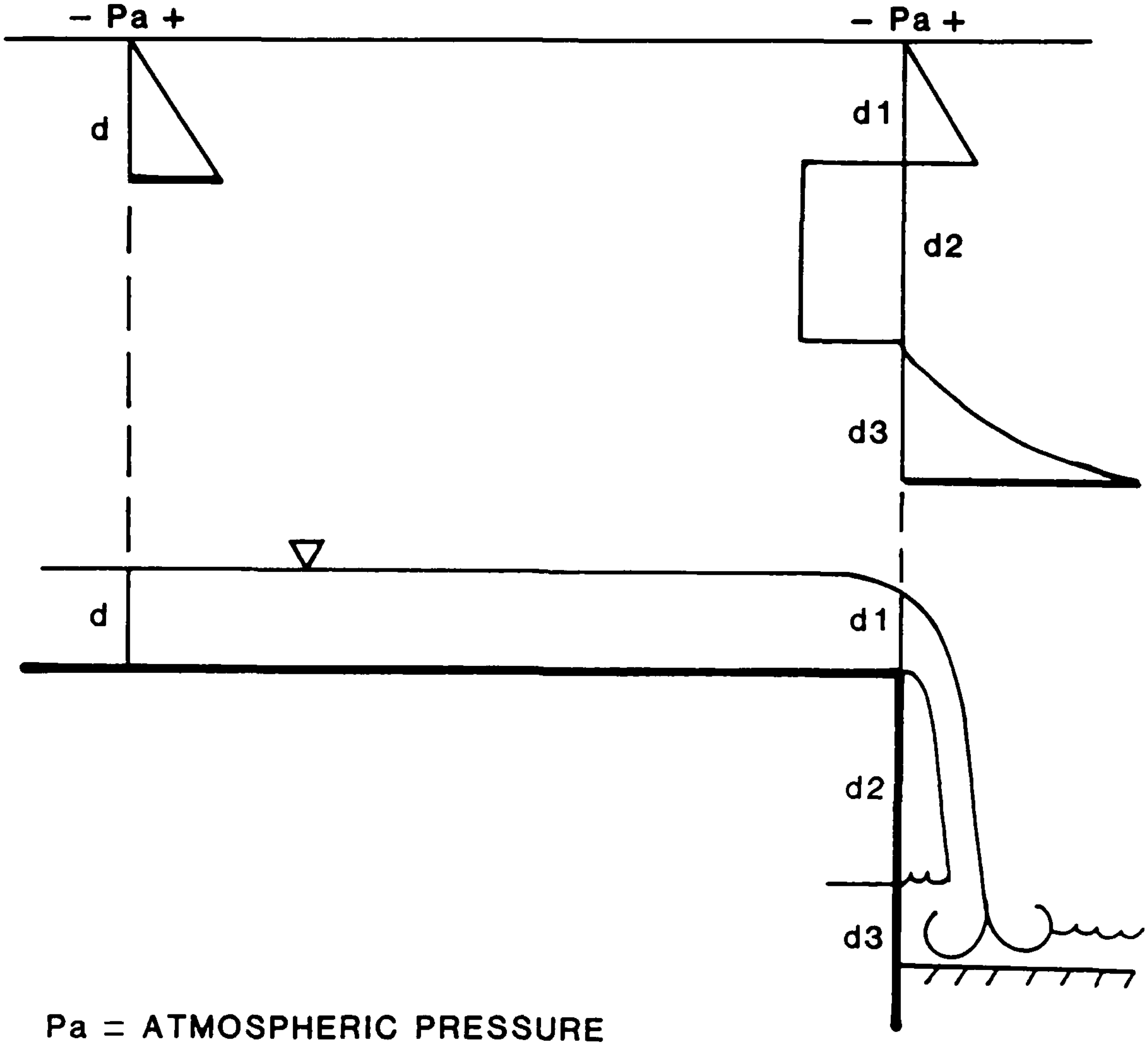

Pa = ATMOSPHERIC PRESSURE

d = DEPTH OF WATER UPSTREAM OF OVERFALL

d1 = DEPTH OF WATER AT KNICKPOINT

d2 = LENGTH OF FACE EXPOSED TO NEGATIVE PRESSURE

d3 = LENGTH OF FACE SUBJECTED TO REVERSE ROLLER IMPACT PRESSURE

Figure 48. Schematic diagram showing inferred complex variations in pressure which can enhance erosion potential at a knickpoint

Geological Factors

114. Knickpoint failure mechanisms described in this research are for two-layered geologic systems. One, or more, of these mechanisms probably occur during each flood event. The most dangerous erosive condition appears to occur when one dominant failure mechanism can act unimpeded along the spillway channel length.

115. Of the four major types of mass failure mechanisms associated with knickpoint migration, the worst case is where a laterally extensive low strength material is undercut, such as at a knickpoint in a fining-upward alluvial sequence where the reverse roller erodes the sand and gravel layer and the upper silt and clay capping layer fails. The next severe case is where a continuous resistant, but open, jointed layer is being undercut. In situations where large blocks are lifted and moved without undercutting a large volume of material can be eroded. However, this situation is not believed to be structure-threatening during short-term flow events characteristic of emergency spillways. The most stable knickpoint occurs where an unfractured, very resistant capping layer is being undercut and is failing in tension.

Hydrologic Factors

116. This research indicates that certain erosion thresholds are reached at a given knickpoint as the discharge changes. Figure 49 shows the relative amount of undercutting that takes place as the discharge is increased from zero to peak flow and then decreased back to zero flow. This discharge pattern is very similar to hydrographs of actual emergency spillway flow events. It is possible that maximum unvented undercutting could take place throughout the entire hydrograph if the peak flow does not exceed the upper flow threshold. As the discharge increases, changes in water depth and turbulence cause the nappe to move further from the vertical face and erosion to decrease. For the assumed knickpoint conditions in Figure 49 no headcutting takes place above the upper threshold. For the unvented condition the amount of erosion due to undercutting is much more severe and continues during a greater portion of the hydrograph. Frequently, the falling limb of the hydrograph has a flatter slope than the rising limb which causes a greater period of erosion.

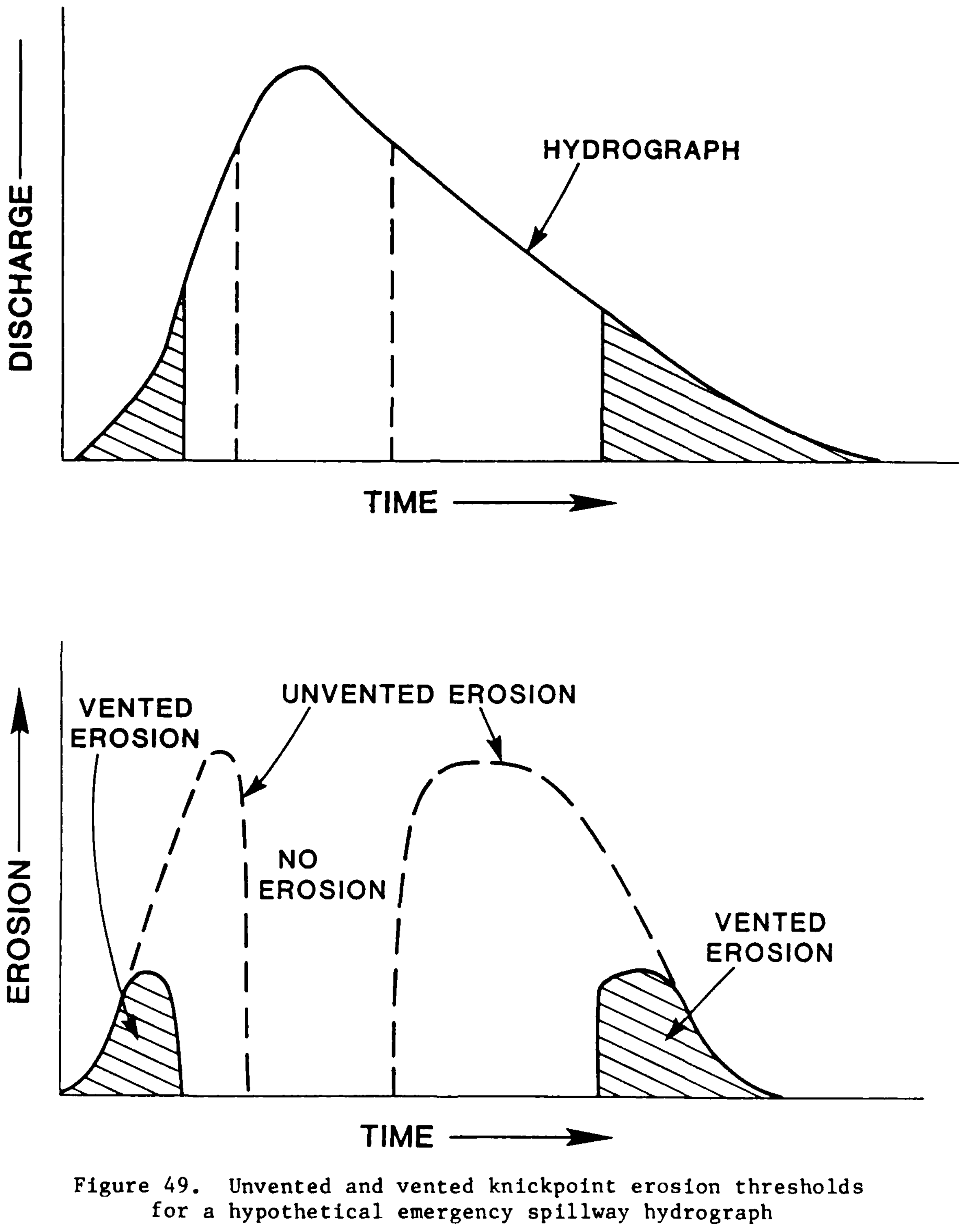

Figure 49. Unvented and vented knickpoint erosion thresholds for a hypothetical emergency spillway hydrograph

117. A qualitative summary of the conditions important in predicting undercutting and mass failure mechanisms at knickpoints in terms of the Z:Y ratio, venting, and position on the hydrograph is shown in Table 2. Knickpoint erosion is given in relative terms in Table 2 because geologic conditions and the character of the flood hydrograph are site specific.

Table 2

Knickpoint Erosion as a Function of Z/Y, Venting, and Hydrograph Position

Vented	Z/Y Ratio	Position on Hydrograph	
		Rising Limb	Falling Limb
Yes	>8/1	Erosion	Erosion
Yes	<8/1	None	None
No	Not critical	Erosion	Erosion

Remedial Considerations

118. Accelerated knickpoint migration represents a significant risk to the stability of the spillway channel and reservoir and a life safety hazard to the public downstream. The results of this and other related research studies suggest that remedial and/or operational concepts can be applied to reduce the severity of knickpoint migration. Remedial measures fall into two general categories; modify the channel conditions or control the flow conditions (Cameron et al. 1988b).

119. Channel modifications to ensure vented conditions provide the greatest reduction in knickpoint migration. Modification of the capping rock to increase shearing resistance or reduce toppling through the installation of rock bolts or soil nails will reduce migration by stabilizing the resistant layer. Installation of drain holes in fractured, competent rock units to drain the fractures will reduce pore pressures and increase stability. The use of "dental" concrete to remove abrupt channel floor irregularities will reduce impact pressures at fractures and reduce pore pressures within fractures. Dental concrete should be considered whenever the structural discontinuities are oriented into the flow such that dynamic impact pressures can be directed below the blocks. In cases where a knickpoint may develop within a

stratigraphic sequence, such as the fluvial section of Black Creek, a complete cutoff wall to below the erodible layer may be necessary. Such walls should always be considered at the downstream end of the concrete spillway apron because the apron can act as the capping layer and concentrate undercutting below the structure.

120. Knickpoint migration can also be reduced by controlling the flow in the spillway channel. Dams equipped with gated emergency spillway structures should be operated such that the flow is either below or above the threshold flows for knickpoint erosion. At uncontrolled spillway structures, some flow control may be possible if the outlet works and/or power plant conduits are managed to control spillway discharges.

121. Because this research dealt primarily with emergency spillways, the summary was given in terms of a theoretical hydrograph. It should be remembered, however, that the unvented condition with resulting erosion potential can be generated by falling tailwater levels as well as increasing discharge. Thus, it is as important to properly manage the tailwater levels as it is to manage the channel discharge if knickpoint migration risks are to be reduced.

PART VIII: CONCLUSIONS AND RECOMMENDATIONS

Conclusions

122. Based on the literature review, laboratory test results, and analyses of field data, the following conclusions can be drawn from this research:

- a. Techniques developed in this research can be used to hydraulically model certain aspects of headcut erosion using rock simulants. Rock simulants consisted of various combinations of sodium silicate cemented gravel, gelatin cemented gravel, and Plexiglas. These materials eroded in a very realistic manner and kept the eroding water clear.
- b. The major types of mass failure mechanisms observed in the field at sites where severe headward erosion had occurred can be reproduced in the laboratory by the techniques developed during this study.
- c. Knickpoint migration occurs where a relatively continuous resistant capping layer overlies a less resistant layer.
- d. The headcutting or knickpoint migration phenomenon is dependent on the geometry of the knickpoint and the velocity of the water. The geometry of the knickpoint is dependent on the geology at a specific site. The geometry of an undeveloped knickpoint can be predicted if enough geologic information is available.
- e. The highest rate of headcutting does not necessarily correspond to the highest velocity or discharge. Laboratory results have shown that headcutting can be negligible at higher velocities and accelerate greatly as the velocity is reduced.
- f. In order for maximum headcutting to take place, the falling jet of water must impact near the vertical face of the knickpoint. At very high velocities the impact area of the jet is far enough away from the vertical face that very little force is acting directly on the face. The angle of impact must also be steep enough so that a high percentage of the discharge in the falling jet is directed back and underneath the overfall as a reverse roller.
- g. The angle of impact and the point of impact can be calculated for a "vented" knickpoint. If "unvented" conditions prevail standard calculation methods are invalid. Unvented conditions can occur when the nappe is confined within parallel walls downstream of the knickpoint.
- h. Unvented knickpoints in laboratory tests accelerated headcutting by orders of magnitude other than at vented knickpoints. The low pressure underneath the nappe drew the jet closer to the vertical face of the knickpoint causing severe undercutting. Not only was the position of the jet moved to where it would do more damage, the discharge for a given head was

increased because of the reduced pressure. Because of the rectangular shape of many spillways and natural channels, unvented conditions are probably common.

i. In laboratory tests, when unvented knickpoints are vented, the jet moves away from the vertical face of the knickpoint and undercutting ceases. Depending on the geometry of the knickpoint and the velocity of flow an unvented knickpoint that is vented will remain or gradually become unvented again as the air under the nappe is removed.

j. The diameter of the reverse roller portion of the jet remains relatively constant for the dimensions of the knickpoint and flow conditions.

k. For the reverse roller to undercut effectively, the erodible layer has to be at least as thick as the diameter of the reverse roller. When the thickness of the erodible layer exceeds the diameter of the reverse roller, mass failure mechanisms such as slumping play an important role.

l. The similarity between the Froude numbers in many of the spillway flows examined in the field and the Froude numbers generated in the flume studies suggest that the principles of hydraulic similitude can be applied.

m. Approximations of the velocities of turbulent water under an overfall can be accomplished by measuring the velocities of particles in the reverse roller by using a video camera and stop action.

Recommendations

123. Based on this research dealing with the effect of stratigraphic variability and venting of headcutting in layered rocks, the following recommendations are made:

a. Acquire detailed geologic information at spillway sites where flow has occurred or is expected to occur.

b. Instrument and monitor field sites where knickpoints already exist to determine the extent of the unvented condition.

c. Begin the design of devices to vent naturally occurring knickpoints after the extent of unvented knickpoint problems in the field is determined. Preventive devices and devices that could be used during flood event should also be evaluated.

d. Conduct additional flume studies to better understand the pressure differentials at the knickpoint in relation to the rate of headcutting in various geologic materials.

e. Carry out large-scale flume and field investigations to quantify the relationship between the thickness of the lower erodible layer and the diameter of the reverse roller.

f. Initiate studies to determine the application of hydraulic similitude to modeling of knickpoint prototypes.

g. Incorporate the mechanisms causing unvented scour into a recently developed discrete element computer model for transport of eroded material.

h. Analyze current reservoir discharge practices in regard to the past peak headcutting phenomena.

i. Conduct studies to determine equations for turbulent flow velocities using a video camera.

REFERENCES

American Geological Institute. 1980. Glossary of Geology, American Geological Institute, Washington, DC.

Berg, R. R. 1986. Reservoir Sandstones, Prentice-Hall, Inc., Englewood Cliffs, NJ.

Blaisdell, F. W. 1983. Analysis of Scour Observations at Cantilever Outlets, US Department of Agriculture, Miscellaneous Publication No. 1427, US Department of Agriculture, Washington, DC.

Blaisdell, F. W., and Anderson, C. L. 1984. "Pipe Spillway Plunge Pool Design Equations," Proceedings, Conference on Water Resource Development, American Society of Civil Engineers, Hydraulics Division, pp 390-396.

Brush, L. M., and Wolman, M. G. 1960. "Knickpoint Behavior in Noncohesive Material: A Laboratory Study," Bulletin of the Geological Society of America, Vol 71, No. 1, pp 59-74.

Cameron, C. P., Cato, K. D., McAneny, C. C., and May, J. H. 1986. "Geotechnical Aspects of Rock Erosion in Emergency Spillway Channels," Technical Report REMR-GT-3, US Army Engineer Waterways Experiment Station, Vicksburg, MS.

Cameron, C. P., Patrick, D. M., Cato, K. D., and May, J. H. 1988a. "Geotechnical Aspects of Rock Erosion in Emergency Spillway Channels; Report 2: Analysis of Field and Laboratory Data," Technical Report REMR-GT-3, US Army Engineer Waterways Experiment Station, Vicksburg, MS.

Cameron, C. P., Patrick, M., Bartholomew, C. O., Hatheway, A. W., and May, J. H. 1988b. "Geotechnical Aspects of Rock Erosion in Emergency Spillway Channels; Report 3: Remediation," Technical Report REMR-GT-3, US Army Engineer Waterways Experiment Station, Vicksburg, MS.

Clemence, K. T. 1987. Influence of Stratigraphy and Structure on Knickpoint Erosion, unpublished Undergraduate Fellow Thesis, Texas A&M University, Department of Geology, College Station, TX.

Fletcher, B. P. 1982. "Los Esteros Spillway, Pecos River, New Mexico; Hydraulic Model Investigation," Technical Report HL-82-24, US Army Engineer Waterways Experiment Station, Vicksburg, MS.

Grissinger, E. H., and Bowie, A. . 1984. "Material and Site Controls of Stream Bank Vegetation," Transactions of the American Society of Agriculture Engineers, St. Joseph, MI, Vol 27, No. 6, pp 1829-1835.

Guy, H. P., Simons, D. B., and Richardson, E. V. 1966. "Summary of Alluvial Channel Data from Flume Experiments, 1956-61," US Geological Survey Professional Paper 462-I, US Geological Survey, Washington, DC.

Henderson, F. M. 1966. Open Channel Flow, Macmillan, Inc., New York.

Hjulstrom, F. 1939. "Transportation of Detritus by Running Water," in Trask, P. D. (editor), Recent Marine Sediments, Dover, New York, pp 5-29.

Mason, P. J. 1984. "Erosion of Plunge Pools Downstream of Dams Due to the Action of Free-Trajectory Jets," Proceedings of the Institution of Civil Engineers, Paper 8734, Vol 76, pp 523-537.

Moore, W. L. 1943. "Energy Loss at the Base of a Free Overfall," Transactions of the American Society of Civil Engineers, Vol 108, p 1343, with discussions by White, M. P., p 1361, Rouse, H., p 1381, and others.

Paek, Y. K., and Heller, L. W. 1968. "Gelatin Modeling Methods for the Study of Foundation Dynamics, Ground Motion and Seismic Phenomena," Miscellaneous Paper No. 4-969, US Army Engineer Waterways Experiment Station, Vicksburg, MS.

Perry, E. B. 1982. "Erosion Tests on Rock from Spillway at Lewisville Dam," US Army Engineer Waterways Experiment Station, Geotechnical Laboratory, Vicksburg, MS.

Pettigrew, R. J. 1986. Analysis of A Knickpoint Migration on the Spillway of a Small Lake Near Waco, Texas, unpublished Bachelor of Science Thesis, Department of Geology, Baylor University, Waco, TX.

Piest, R. F., Bradford, J. M., and Wyatt, G. M. 1975. "Soil Erosion and Sediment Transport from Gullies," Journal of the Hydraulics Division, American Society of Civil Engineers, pp 65-80.

Pugh, C. A., and Gray, E. W., Jr. 1984. "Fuse Plug Embankments in Auxiliary Spillways-Developing Design Guidelines and Parameters," US Bureau of Reclamations, Engineering and Research Center, Denver, CO.

Rehbinder, G. 1980. "A Theory About Cutting Rock with a Water Jet," Rock Mechanics, Springer Verlag, Vol 12, No. 3-4, pp 247-257.

Reinius, E. 1986 (Jun). "Rock Erosion," Water Power and Dam Construction, pp 43-48.

Robinson, R. F. 1987. "Stress Distribution at an Overfall," Draft report, US Department of Agriculture, Soil Conservation Service, Stillwater, OK.

Schumm, S. A. 1973. "Geomorphic Thresholds and Complex Response of Drainage Systems, Fluvial Geomorphology," Morisawa, M. (editor), Proceedings, Fourth Annual Geomorphology Symposium, State of New York, Binghamton, NY, pp 299-310.

__________. 1985. "Experimental Studies of the Fluvial System, Report No. 6," Colorado State University, Fort Collins, CO.

Simonson, C. P. S. 1979. Hydraulic Model Studies-Scour Velocity of Rock, File 1202-EWB, Reference No. MM188/79, (Translation from Russian), US Army Engineer Waterways Experiment Station, Vicksburg, MS.

Smith, L. M., and Patrick, D. M. 1979. "Engineering Geology and Geomorphology of Streambank Erosion: Report 1, Eel River Basin, California," Technical Report GL-79-7, US Army Engineer Waterways Experiment Station, Vicksburg, MS.

Soil Conservation Service. 1973. "A Guide for Design and Layout of Earth Emergency Spillways as Part of Emergency Spillway Systems for Earth Dams, Technical Release No. 52," US Department of Agriculture, Washington, DC.

__________. 1984a. "Rock Material Field Classification Procedure, Technical Release No. 71," US Department of Agriculture, Washington, DC.

__________. 1984b. "Arkansas, December 1982 Spillway Performance Report, National Bulletin No. 210-4-14," US Department of Agriculture, Washington, DC.

__________. 1985a. "Virginia Spillway Damage Report, North River Virginia, Informal Report," US Department of Agriculture, Washington, DC.

Soil Conservation Service. 1985b. "1985 Soil and Water Conservation, Research and Education Progress and Needs," US Department of Agriculture, Washington, DC.

_________. 1985c. "Mississippi, December 1982 Spillway Performance Report, National Bulletin No. 210-5-16," US Department of Agriculture, Washington, DC.

_________. 1986. "June 1986 Spillway Performance Report, National Bulletin No. 210-6-13," US Department of Agriculture, Washington, DC.

Spurr, K. J. W. 1985 (Jul). "Energy Approach to Estimating Scour Downstream of a Large Dam," Water Power and Dam Construction, pp 81-89.

Temple, D. M. 1980. "Tractive Design of Vegetated Channels," Transactions of the American Society of Agricultural Engineers, St. Joseph, MI, Vol 23, No. 4, pp 884-890.

_________. 1982. "Flow Retardance of Submerged Grass Channel Linings," Transactions of the American Society of Agricultural Engineers, St. Joseph, MI, Vol 25, No. 5, pp 1300-1303.

_________. 1983. "Design of Grass-Lined Open Spillways," Transactions of the American Society of Agricultural Engineers, St. Joseph, MI, Vol 26, No. 4, pp 1064-1069.

_________. 1984. "Erosionally Effective Soil Stress in Grass-Lined Open Channels," American Society of Agricultural Engineers, Paper No. SWR84-102, St. Joseph, MI.

_________. 1986. "Distribution Coefficients for Grass-Lined Channels," Journal of Hydraulic Engineering, American Society of Civil Engineers, Paper No. 20435, Vol 112, No. 3, pp 193-205.

US Army Corps of Engineers. 1970. Hydraulic Design of Flood Control Channels, Engineering Manual 1110-2-1601, Office, Chief of Engineers, US Army Corps of Engineers, Washington, DC.

US Army Engineer District, Fort Worth. 1971. "Lake Brownwood: Modification of Spillway, Design Memorandum No. 2," US Army Engineer District, Fort Worth, Corps of Engineers, Fort Worth, TX.

US Army Engineer District, Rock Island. 1962. "Spillway, Saylorville Reservoir, Design Memorandum No. 10," US Army Engineer District, Rock Island, Corps of Engineers, Rock Island, IA.

_________. 1984. "Saylorville Dam: Initial Overflow of Spillway, Supplement to Periodic Inspection Report No. 7," US Army Engineer District, Rock Island, Corps of Engineers, Rock Island, IA.

Whitten, C. B., and Patrick, D. M. 1981. "Engineering Geology and Geomorphology of Streambank Erosion: Report 2, Yazoo River Basin Uplands, Mississippi," Technical Report GL-79-7, Geotechnical Laboratory, US Army Engineer Waterways Experiment Station, Vicksburg, MS.

Vieux, B. E. 1986. "Plunge Pool Erosion in Cohesive Soils at Two Dams in Kansas," Draft report, US Department of Agriculture, Soil Conservation Service, Washington, DC.

APPENDIX A

LABORATORY DATA SHEETS

HYDRAULIC FLUME EXPERIMENTS

TESTED BY GWJ
CHECKED BY SDM, JHM

DATE: 2-18-87

FLUME EXPERIMENT NO. 2 | RUN NO. 1 | FLOW COMMENCED AT 1342 HRS. | FLOW TERMINATED AT 1515 HRS. | TOTAL DURATION OF FLOW: 97 MIN.

SAMPLE COMPOSITION: (INCLUDE DATE SAMPLE WAS MADE)

LAYER 1: PLEXIGLASS 0.5" THICK
LAYER 2: GELATIN/H_2O; RATIO BY WEIGHT:
+ GRAVEL (<1/2")

SAMPLE CONFIGURATION:
TOTAL WEIGHT: 92.016; 41.8 Kg

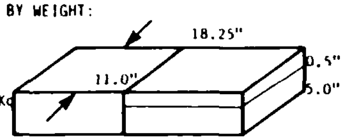

FLUME CONFIGURATION:
LEVEL

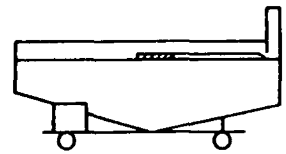

TIME	HEADWATER FLOW CHAR.	HEADWATER DEPTH (IN.)	TAILWATER FLOW CHAR.	TAILWATER DEPTH (IN.)	PRESSURE DIFFERENTIAL	FLOW CHAR. AT SAMPLE	OBSERVATIONS
1347	LF	1.25	MTF	1.0	(?) 63 * RANGE 47-87	LF	'MODERATE' RATE OF UNDERCUTTING MASS WASTING - NO AIRPOCKET
1358	LF	0.75	MTF	0.75	1.42	LF	SLOWER RATE OF UNDERCUTTING - AIRPOCKET PRESENT
1408	LF	1.1	MTF	1.0	1.22	LF	DISSOLVING OF GELATIN CAUSING SLOPE FAILURE
1416	LF	1.1	MTF	1.0	1.20	LF	CONTINUED SLOPE FAILURE
1441	LF	1.25	MTF	0.75	1.27	SW	MANY STANDING WAVES IN HEADWATERS

U = UPSTREAM
D = DOWNSTREAM
SW = STANDING WAVES
LF = LAMINAR FLOW
TF = TURBULENT FLOW
MTF = MODERATELY TURBULENT FLOW

STF = SLIGHTLY TURBULENT FLOW
AP = AIRPOCKET
T_O = INITIAL WATER TEMPERATURE (°C)
T_F = FINAL WATER TEMPERATURE (°C)

HYDRAULIC FLUME EXPERIMENTS

TESTED BY CPC
CHECKED BY SDM, JHM

DATE: 8-6-86

FLUME EXPERIMENT NO. 2

RUN NO. 1

FLOW COMMENCED AT 1415 HRS.

FLOW TERMINATED AT 1620 HRS.

TOTAL DURATION OF FLOW: 125 MIN.

SAMPLE COMPOSITION: (INCLUDE DATE SAMPLE WAS MADE)
GRAVEL, LIME, CEMENT, AND WATER - MIXES JM-1G and JM2G.
POURED 8-1-86

SAMPLE CONFIGURATION:

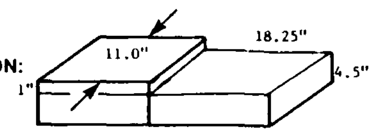

FLUME CONFIGURATION:
LEVEL

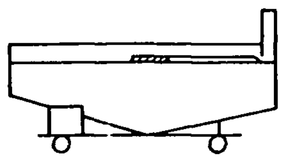

TIME	HEADWATER FLOW CHAR.	HEADWATER DEPTH (IN.)	TAILWATER FLOW CHAR.	TAILWATER DEPTH (IN.)	PRESSURE DIFFERENTIAL	FLOW CHAR. AT SAMPLE	OBSERVATIONS
1415	LF	1.0	--	--	--		--
1421		1.0			110 (0.01 PSI)		WATER LEVEL DROPPED SLOWLY TO 0.5" U.S., RAISED TO 1.0" AGAIN
1427	SW	2.7	--	--	--		FLOW INCREASED TO 2.7"
1428	LF	1.2	TF	--	--		FLOW DECREASED
1437	LF	3.5	TF	1.5	425 (0.04 PSI)		FLOW INCREASED
1440	LF	1.0	STF	0.75	080(0.008 PSI)		FLOW DECREASED. TRANSDUCER READING AT CONSTANT WATER FLOW INCREASED TO 112 (0.01 PSI)
1600	LF	1.0	STF	0.75	0.95 (0.01 PSI)		A SMALL AMOUNT OF EROSION HAS TAKEN PLACE
1620	--	--	--	--	--		STOP RUN 1
							PICTURES 1, 2, AND 3 TAKEN BEFORE RUN 1, 4, AND 5 TAKEN AFTER RUN 1. FILM ROLL 7, (SECOND ROLL KODACHROME)

U = UPSTREAM
D = DOWNSTREAM
SW = STANDING WAVES
LF = LAMINAR FLOW
TF = TURBULENT FLOW
MTF = MODERATELY TURBULENT FLOW

STF = SLIGHTLY TURBULENT FLOW
AP = AIRPOCKET
T_O = INITIAL WATER TEMPERATURE (°C)
T_F = FINAL WATER TEMPERATURE (°C)

HYDRAULIC FLUME EXPERIMENTS

TESTED BY GWJ
CHECKED BY SDM, JHM

DATE: 4-2-87

FLUME EXPERIMENT NO. 2

RUN NO. 1A

FLOW COMMENCED AT 1021 HRS.

FLOW TERMINATED AT 1032 HRS.

TOTAL DURATION OF FLOW: 11 MIN.

NOTE: COMPRESSION INDUCED FROM PLACING PLEXIGLASS ON TOP OF SAMPLE CAUSED BULGING WHEN THE FRONT PANEL WAS REMOVED; SOME GAP BETWEEN THE GELATIN AND PLEXIGLASS EXISTS

SAMPLE COMPOSITION: (INCLUDE DATE SAMPLE WAS MADE)
- 0.45" PLEXIGLASS ON TOP (A)
- 0.0131 GELATIN/H_2O SOLUTION + GRAVEL (R)

SAMPLE CONFIGURATION:

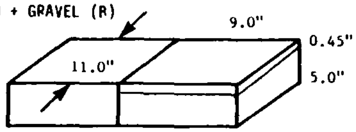

FLUME CONFIGURATION:
LEVEL

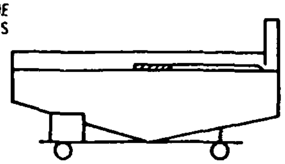

TIME	HEADWATER FLOW CHAR.	HEADWATER DEPTH (IN.)	TAILWATER FLOW CHAR.	TAILWATER DEPTH (IN.)	PRESSURE DIFFERENTIAL	FLOW CHAR. AT SAMPLE	OBSERVATIONS
							* SLUMPING OCCURRED AT REMOVAL OF FRONT PANEL. ESTIMATED VOLUME: 10 ml
							- FURTHER SLUMPING WHEN FLOW COMMENCED, WATER ENTERED AREA BEHIND SAMPLE
							- TERMINATED FLOW

U = UPSTREAM
D = DOWNSTREAM
SW = STANDING WAVES
LF = LAMINAR FLOW
TF = TURBULENT FLOW
MTF = MODERATELY TURBULENT FLOW
STF = SLIGHTLY TURBULENT FLOW
AP = AIRPOCKET
T_O = INITIAL WATER TEMPERATURE (°C)
T_F = FINAL WATER TEMPERATURE (°C)

HYDRAULIC FLUME EXPERIMENTS

TESTED BY GWJ
CHECKED BY SDM, JHM

DATE: 4-7-87

FLUME EXPERIMENT NO. 2 RUN NO. 2 FLOW COMMENCED AT 1050 HRS. FLOW TERMINATED AT 1124 HRS. TOTAL DURATION OF FLOW: 34 MIN.

SAMPLE COMPOSITION: (INCLUDE DATE SAMPLE WAS MADE)
LAYER 2: GEL/GRAVEL RATIO: 0.014 (WEIGHT)

LAYER 1: PLEXIGLASS

SAMPLE CONFIGURATION:

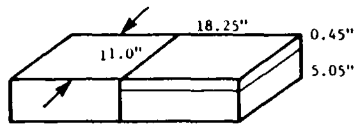

FLUME CONFIGURATION:
LEVEL

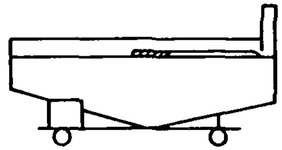

TIME	HEADWATER FLOW CHAR.	HEADWATER DEPTH (IN.)	TAILWATER FLOW CHAR.	TAILWATER DEPTH (IN.)	PRESSURE DIFFERENTIAL		FLOW CHAR. AT SAMPLE	OBSERVATIONS
1051	STF	4.0	TF	2.0	0.49	0.82		* ESTIMATED VOLUME DUE TO SLUMPING BEFORE FLOW BEGAN: 90 ml
1053	LF	1.7	TF	0.6	0.15	0.45		AIRPOCKET DEVELOPED INCREASED Q TO ELIMINATE AIRPOCKET
1057	LF	2.0	TF	0.7	0.19	0.51		10:57 WATERFALL SLOPE NEAR VERTICAL, LITTLE EROSION DUE TO RECESSION OF GRAVEL LAYER UNDER PLEXIGLASS
1101	LF	1.6	MTF	0.6	0.14	0.44		11:01 SMALL AIRPOCKET SLOPE OF WATER FALL OVER-TURNED, POINTING TOWARD BASE OF KNICKPOINT - THICKNESS OF AIRPOCKET: 0.70"
1107	LF	1.6	MTF	0.6	0.14	0.44		LARGE AIRPOCKET, BUT NO SIGNIFICANT EROSION
1110	LF	1.3	TF	0.5	0.10	0.37		2.0"
1122	LF	1.6	TF	0.6	0.14	0.44		SLUMPING OCCURS IN THE SUBMERGED PART OF LAYER 2. DEPTH OF RECESSION: 2.3" FROM FACE OF ORIGINAL KNICKPOINT
								VOLUME ERODED: 2619 ml

U = UPSTREAM
D = DOWNSTREAM
SW = STANDING WAVES
LF = LAMINAR FLOW
TF = TURBULENT FLOW
MTF = MODERATELY TURBULENT FLOW

STF = SLIGHTLY TURBULENT FLOW
AP = AIRPOCKET
T_O = INITIAL WATER TEMPERATURE (°C)
T_F = FINAL WATER TEMPERATURE (°C)

HYDRAULIC FLUME EXPERIMENTS

TESTED BY GWJ
CHECKED BY CPC, JHM

DATE: 4-10-87

FLUME EXPERIMENT NO. 2

RUN NO. 3

FLOW COMMENCED AT 0841 HRS.

FLOW TERMINATED AT 0917 HRS.

TOTAL DURATION OF FLOW: 36 MIN.

SAMPLE COMPOSITION: (INCLUDE DATE SAMPLE WAS MADE)
(1) GEL/H_2O: 0.01406 + GRAVEL <1/2"

(2) PLEXIGLASS

SAMPLE CONFIGURATION:

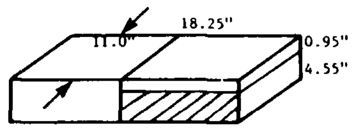

FLUME CONFIGURATION:
LEVEL

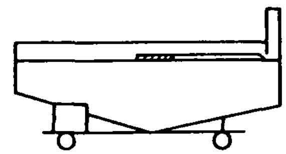

TIME	HEADWATER FLOW CHAR.	HEADWATER DEPTH (IN.)	TAILWATER FLOW CHAR.	TAILWATER DEPTH (IN.)	PRESSURE DIFFERENTIAL (× .1 PSI)	VELOCITY	FLOW CHAR. AT SAMPLE	OBSERVATIONS
0843	LF	1.7	TF	0.75	0.14	0.44 M/S	LOW SW	NO AIRPOCKET; SOME REMOVAL OF SLUMPED MATERIAL
0848	LF	1.6	TF	0.6	0.15	0.45	LF	REMOVAL OF SLUMPED MATERIAL CAUSES REMOVAL OF SUPPORT AT BASE OF SAMPLE, CONTINUED SLUMPING.* EFFECT OF SHEAR EROSION OCCURS ONLY UNTIL ABOUT 3.0" FROM FACE OF SAMPLE:
0855	LF	1.5	MTF	0.5	0.13	0.42	LF	AIRPOCKET FORMS 1.5" HIGH
0905	LF	1.3	MTF	0.4	0.12	0.41	LF	GRAVEL APPROACHING ANGLE OF REPOSE
								Q. CAN EROSION IN SPILLWAYS BE A COMBINATION OF SLUMPING, SHEARING, AND UNDERCUTTING?
0912	LF	1.7	TF	0.6	0.17	0.48	LF, SW	LITTLE SIGNIFICANT EROSION
								* SOME SLUMPING AND REMOVAL OF GRAVEL OCCURRED AFTER PUMP TURNED OFF - WATER THAT WAS SUPPORTING GRAVEL BEHIND THE WATERFALL DRAINED OUT, CARRYING SOME GRAVEL WITH IT
								VOLUME ERODED = 3216 ml

U = UPSTREAM
D = DOWNSTREAM
SW = STANDING WAVES
LF = LAMINAR FLOW
TF = TURBULENT FLOW
MTF = MODERATELY TURBULENT FLOW

STF = SLIGHTLY TURBULENT FLOW
AP = AIRPOCKET
T_O = INITIAL WATER TEMPERATURE (°C)
T_F = FINAL WATER TEMPERATURE (°C)

HYDRAULIC FLUME EXPERIMENTS

TESTED BY GWJ
CHECKED BY CPC, JHM

DATE: 4-15-87

FLUME EXPERIMENT NO. 2 | RUN NO. 4 | FLOW COMMENCED AT 8:24 HRS. | FLOW TERMINATED AT 905 HRS. | TOTAL DURATION OF FLOW: 41 MIN.

SAMPLE COMPOSITION: (INCLUDE DATE SAMPLE WAS MADE)
(1) SAMPLE POURED 1710 (4-14-87) GEL/H_2O = 0.01406 (+ GRAVEL)

(2) PLEXIGLASS

SAMPLE CONFIGURATION:

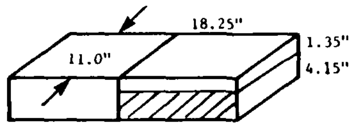

FLUME CONFIGURATION:
LEVEL

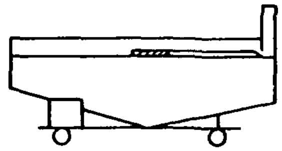

TIME	HEADWATER FLOW CHAR.	HEADWATER DEPTH (IN.)	TAILWATER FLOW CHAR.	TAILWATER DEPTH (IN.)	PRESSURE DIFFERENTIAL	FLOW CHAR. AT SAMPLE	OBSERVATIONS
8:26	LF	3.3	TF	1.8	0.083 PSI	LF	AIRPOCKET ELIMINATED
8:29	LF	1.3	TF	0.7	0.042	LF	SMALL AP - (1.5")
8:36	LF	1.0	TF	0.6	0.035	LF	LARGER AP - 2.5", SLUMPING, NOT MUCH UNDERCUTTING
8:49	FLOW STOPPED						ESTIMATED VOL. LOSS - 1/2(4.8)(4.1)(11.0)
	FLOW STARTED						
8:54	LF	3.0	TF	1.6	0.073	LF	ELIMINATE AP - NO SLUMPING - ϕ = 35°
8:58	LF	1.2	TF	0.6	0.042	LF	SMALL AP - 1.4" - CHURNING OF LOOSE GRAVEL, BUT NONE CARRIED AWAY, NO FURTHER SLUMPING, DISTANCE TOP OF LAYER (1) ERODED BACK - 5.3"
							VOLUME LOST = 2500 ml
							VOLUME SLUMPED (BEFORE FLOW) = 230 ml
							VOLUME ERODED = 2270 ml

U = UPSTREAM
D = DOWNSTREAM
SW = STANDING WAVES
LF = LAMINAR FLOW
TF = TURBULENT FLOW
MTF = MODERATELY TURBULENT FLOW

STF = SLIGHTLY TURBULENT FLOW
AP = AIRPOCKET
T_O = INITIAL WATER TEMPERATURE (°C)
T_F = FINAL WATER TEMPERATURE (°C)

HYDRAULIC FLUME EXPERIMENTS

TESTED BY GWJ
CHECKED BY CPC, JHM
DATE: 4-16-87

FLUME EXPERIMENT NO. 2
RUN NO. 5
FLOW COMMENCED AT 802 HRS.
FLOW TERMINATED AT 837 HRS.
TOTAL DURATION OF FLOW: 35 MIN.

SAMPLE COMPOSITION: (INCLUDE DATE SAMPLE WAS MADE)
(1) GEL/H_2O = 0.015 + GRAVEL - POURED 4-15-87
(2) PLEXIGLASS

SAMPLE CONFIGURATION:

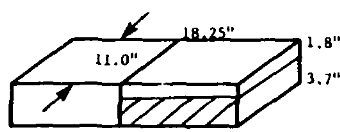

FLUME CONFIGURATION:
LEVEL

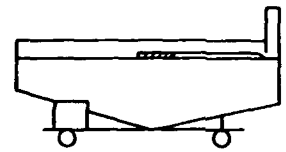

TIME	HEADWATER FLOW CHAR.	HEADWATER DEPTH (IN.)	TAILWATER FLOW CHAR.	TAILWATER DEPTH (IN.)	PRESSURE DIFFERENTIAL	FLOW CHAR. AT SAMPLE	OBSERVATIONS
808	LF	1.25	TF	0.6	0.041	LF	- SOME SLUMPING INITIALLY 150 ml - SMALL AP - 1.3"
816	LF	1.25	TF	0.6	0.041	LF	- SLUMPING NOT AS SEVERE AS BEFORE - ϕ = 43°, MUCH HIGHER THAN FOR GEL/H_2O = 0.01406
8:20	LF	1.0	TF	0.5	0.033	LF	- AP BELOW, UNDERNEATH PLEXIGLASS - 2.4" HIGH; SEEMS TO CAUSE ACCELERATED EROSION, INCREASED TURBULENCE
8:34	LF	1.0	TF	0.5	0.033	LF	- LITTLE SIGNIFICANT EROSION OR SLUMPING VOL. LOST = 1695 ml VOL. SLUMPED 150 ml VOL. ERODED = 1545 ml

U = UPSTREAM
D = DOWNSTREAM
SW = STANDING WAVES
LF = LAMINAR FLOW
TF = TURBULENT FLOW
MTF = MODERATELY TURBULENT FLOW
STF = SLIGHTLY TURBULENT FLOW
AP = AIRPOCKET
T_O = INITIAL WATER TEMPERATURE (°C)
T_F = FINAL WATER TEMPERATURE (°C)

HYDRAULIC FLUME EXPERIMENTS

TESTED BY GWJ
CHECKED BY CPC, JHM

DATE: 4-17-87

FLUME EXPERIMENT NO. 2 | RUN NO. 6 | FLOW COMMENCED AT ______ HRS. | FLOW TERMINATED AT ______ HRS. | TOTAL DURATION OF FLOW: ______ MIN.

SAMPLE COMPOSITION: (INCLUDE DATE SAMPLE WAS MADE)
(1) GEL/H_2O = 0.015 (WEIGHT) + GRAVEL (4-16); ROOM TEMP

(2) PLEXIGLASS

SAMPLE CONFIGURATION:

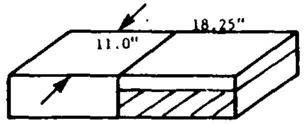

FLUME CONFIGURATION:
LEVEL

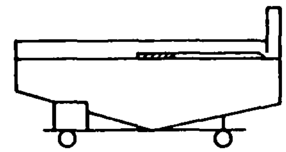

TIME	HEADWATER FLOW CHAR.	HEADWATER DEPTH (IN.)	TAILWATER FLOW CHAR.	TAILWATER DEPTH (IN.)	PRESSURE DIFFERENTIAL	FLOW CHAR. AT SAMPLE	OBSERVATIONS
							SAMPLE NOT SET UP

U = UPSTREAM
D = DOWNSTREAM
SW = STANDING WAVES
LF = LAMINAR FLOW
TF = TURBULENT FLOW
MTF = MODERATELY TURBULENT FLOW

STF = SLIGHTLY TURBULENT FLOW
AP = AIRPOCKET
T_O = INITIAL WATER TEMPERATURE (°C)
T_F = FINAL WATER TEMPERATURE (°C)

HYDRAULIC FLUME EXPERIMENTS

TESTED BY GWJ
CHECKED BY CPC, JHM

DATE: 4-20-87

FLUME EXPERIMENT NO. 2

RUN NO. 7

FLOW COMMENCED AT 1603 HRS.

FLOW TERMINATED AT 1727 HRS.

TOTAL DURATION OF FLOW: 84 MIN.

SAMPLE COMPOSITION: (INCLUDE DATE SAMPLE WAS MADE)
(1) GEL/H_2O = 0.031 + GRAVEL (MADE 4-20-87)
(2) PLEXIGLASS

SAMPLE CONFIGURATION:

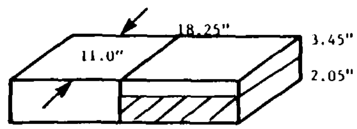

FLUME CONFIGURATION:
LEVEL

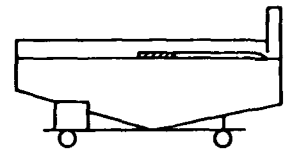

TIME	HEADWATER FLOW CHAR.	HEADWATER DEPTH (IN.)	TAILWATER FLOW CHAR.	TAILWATER DEPTH (IN.)	PRESSURE DIFFERENTIAL	FLOW CHAR. AT SAMPLE	OBSERVATIONS
1604						SW	
1606	SW	3.4	TF	1.0	0.037	SW	ELIMINATE AP
1609	LF	1.6	TF	0.6	0.020	LF	NO APPARENT DISSOLUTION OF GELATIN SOME EROSION, NO SLUMPING
1656	LF	1.6	TF	0.6	0.020	LF	LITTLE SIGNIFICANT EROSION
1713	LF	1.6	TF	0.6	0.020	LF	SOME EROSION, GRADUALLY UNDERCUTTING
							VOL. ERODED = 1000 ml

U = UPSTREAM
D = DOWNSTREAM
SW = STANDING WAVES
LF = LAMINAR FLOW
TF = TURBULENT FLOW
MTF = MODERATELY TURBULENT FLOW

STF = SLIGHTLY TURBULENT FLOW
AP = AIRPOCKET
T_O = INITIAL WATER TEMPERATURE (°C)
T_F = FINAL WATER TEMPERATURE (°C)

HYDRAULIC FLUME EXPERIMENTS

TESTED BY GWJ
CHECKED BY CPC, JHM
DATE: 4-21-87

FLUME EXPERIMENT NO. 2 | RUN NO. 8 | FLOW COMMENCED AT 1609 HRS. | FLOW TERMINATED AT 1751 HRS. | TOTAL DURATION OF FLOW: 102 MIN.

SAMPLE COMPOSITION: (INCLUDE DATE SAMPLE WAS MADE)
(1) GEL/H_2O = 0.031 + GRAVEL (4-21-87)
(2) PLEXIGLASS

SAMPLE CONFIGURATION:

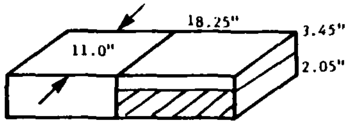

FLUME CONFIGURATION: LEVEL

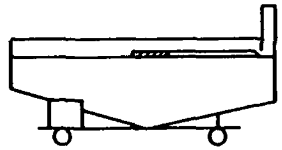

TIME	HEADWATER FLOW CHAR.	HEADWATER DEPTH (IN.)	TAILWATER FLOW CHAR.	TAILWATER DEPTH (IN.)	PRESSURE DIFFERENTIAL	FLOW CHAR. AT SAMPLE	OBSERVATIONS
1610	LF, SW	3.6	TF	1.8	0.053	MTF	ELIMINATE AP
1616	LF	1.6	TF	0.6	0.020	LF	SMALL AP, LITTLE UNDERCUTTING
1620	SW, LF	3.5	TF	1.7	0.054	LF	INCREASED FLOW TO ELIMINATE AP, START DECREASING Q
1625	LF	1.6	TF	0.7	0.021	LF	SMALL AP - 1.75" HIGH
1641	LF	1.6	TF	0.7	0.021	LF	NO SIGNIFICANT EROSION, INCREASED FLOW TO ELIMINATE AP AND START AGAIN
1647	LF	1.5	TF	0.6	0.019	LF	AP IS 1.5" HIGH, NO SIGNIFICANT EROSION
1718	LF	1.5	TF	0.6	0.019	LF	SLIGHTLY ACCELERATED EROSION AP 1.75" HIGH
1751	LF	1.5	TF	0.6	0.019	LF	FLOW TERMINATED: 1.8" UNDERCUTTING
							VOL. ERODED = 901 ml

U = UPSTREAM
D = DOWNSTREAM
SW = STANDING WAVES
LF = LAMINAR FLOW
TF = TURBULENT FLOW
MTF = MODERATELY TURBULENT FLOW

STF = SLIGHTLY TURBULENT FLOW
AP = AIRPOCKET
T_O = INITIAL WATER TEMPERATURE (°C)
T_F = FINAL WATER TEMPERATURE (°C)

HYDRAULIC FLUME EXPERIMENTS

TESTED BY GWJ
CHECKED BY CPC, JHM
DATE: 4-22-87

FLUME EXPERIMENT NO. 2 | RUN NO. 9a | FLOW COMMENCED AT 1543 HRS. | FLOW TERMINATED AT 1710 HRS. | TOTAL DURATION OF FLOW: 87 MIN.

SAMPLE COMPOSITION: (INCLUDE DATE SAMPLE WAS MADE)
(1) GEL/H_2O = 0.031 + GRAVEL (4-22-87)

(2) PLEXIGLASS

SAMPLE CONFIGURATION:

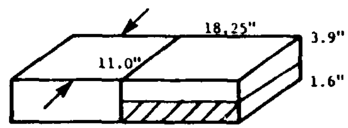

FLUME CONFIGURATION:
LEVEL

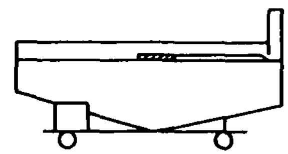

TIME	HEADWATER FLOW CHAR.	HEADWATER DEPTH (IN.)	TAILWATER FLOW CHAR.	TAILWATER DEPTH (IN.)	PRESSURE DIFFERENTIAL	FLOW CHAR. AT SAMPLE	OBSERVATIONS
1544	SW, MTF	3.7	TF	1.7	0.055	LF	INCREASED FLOW TO ELIMINATE AP
1549	LF	1.5	TF	0.6	0.013	LF	AP HEIGHT = 2.2" SIGNIFICANT EROSION INCREASED FLOW TO ELIMINATE AP, START OVER
1600	LF	1.6	TF	0.6	0.014	LF	AP HEIGHT = 2.1" LARGER AP THAN PREVIOUSLY AT SAME HEADWATER DEPTH
1601	LF	1.5	TF	0.5	0.014	LF	AP HEIGHT = 2.4"
1606	LF	2.0	TF	0.7	0.018	LF	NO AP; SIGNIFICANT EROSION; VELOCITY LOWER FOR A HIGHER HEADWATER DEPTH
1638	LF	2.0	TF	0.7	0.018	LF	LITTLE FURTHER EROSION
1710	LF	2.0	TF	0.7	0.018	LF	LITTLE FURTHER EROSION; UNDERCUTTING TO 2.3"
							VOL. ERODED = 288 ml

U = UPSTREAM
D = DOWNSTREAM
SW = STANDING WAVES
LF = LAMINAR FLOW
TF = TURBULENT FLOW
MTF = MODERATELY TURBULENT FLOW

STF = SLIGHTLY TURBULENT FLOW
AP = AIRPOCKET
T_O = INITIAL WATER TEMPERATURE (°C)
T_F = FINAL WATER TEMPERATURE (°C)

HYDRAULIC FLUME EXPERIMENTS

TESTED BY GWJ
CHECKED BY CPC, JHM

DATE: 4-23-87

FLUME EXPERIMENT NO. 2 | RUN NO. 9b | FLOW COMMENCED AT 9:34 HRS. | FLOW TERMINATED AT 10:49 HRS. | TOTAL DURATION OF FLOW: 67 MIN.

SAMPLE COMPOSITION: (INCLUDE DATE SAMPLE WAS MADE)
(1) GEL/H_2O = 0.031 + GRAVEL (4-23-87)

(2) PLEXIGLASS

SAMPLE CONFIGURATION:

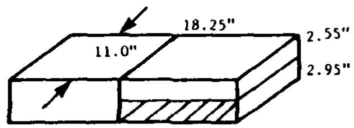

FLUME CONFIGURATION:
LEVEL

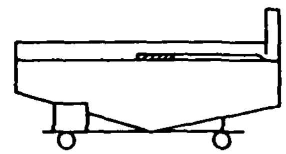

TIME	HEADWATER FLOW CHAR.	HEADWATER DEPTH (IN.)	TAILWATER FLOW CHAR.	TAILWATER DEPTH (IN.)	PRESSURE DIFFERENTIAL	FLOW CHAR. AT SAMPLE	OBSERVATIONS
944	SW	4.0	TF	1.7	0.047	LF	INCREASE FLOW TO ELIMINATE AP
949	LF, SW	1.6	TF	0.6	0.018	LF	AP HEIGHT = 1.5"; H_2O TEMP = 30°C
1022	LF, SW	1.6	TF	0.6	0.019	LF	H_2O TEMP = 33°C
1050	LF, SW	1.6	TF	0.6	0.019	LF	H_2O TEMP = 35°C
							VOL. ERODED = 1127 ml

U = UPSTREAM
D = DOWNSTREAM
SW = STANDING WAVES
LF = LAMINAR FLOW
TF = TURBULENT FLOW
MTF = MODERATELY TURBULENT FLOW

STF = SLIGHTLY TURBULENT FLOW
AP = AIRPOCKET
T_O = INITIAL WATER TEMPERATURE (°C)
T_F = FINAL WATER TEMPERATURE (°C)

HYDRAULIC FLUME EXPERIMENTS

TESTED BY GWJ
CHECKED BY CPC, JHM
DATE: 4-23-87

FLUME EXPERIMENT NO. 2
RUN NO. 10
FLOW COMMENCED AT 1342 HRS.
FLOW TERMINATED AT 1447 HRS.
TOTAL DURATION OF FLOW: 65 MIN.

SAMPLE COMPOSITION: (INCLUDE DATE SAMPLE WAS MADE)
(1) GEL/H_2O = 0.031 (4-23-87) + GRAVEL
(2) PLEXIGLASS

SAMPLE CONFIGURATION:

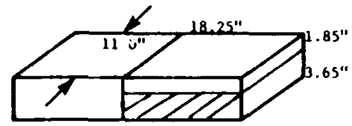

FLUME CONFIGURATION:
LEVEL

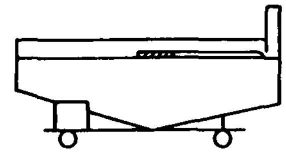

TIME	HEADWATER FLOW CHAR.	HEADWATER DEPTH (IN.)	TAILWATER FLOW CHAR.	TAILWATER DEPTH (IN.)	PRESSURE DIFFERENTIAL	FLOW CHAR. AT SAMPLE	OBSERVATIONS
1343	SW, LF	3.4	TF	1.6	0.034	LF	INCREASED FLOW TO ELIMINATE AP H_2O TEMP = 34°C T_f = 38°C
1347	SW, LF	1.7	TF	0.6	UNRELIABLE	LF	1.5" AP; TRANSDUCER ERRATIC, VALUES POSITIVE AND NEGATIVE, DO NOT AGREE WITH PREVIOUS READINGS FOR SOME HEADWATER DEPTHS
1417	SW, LF	1.7	TF	0.6	0.021	LF	SIGNIFICANT EROSION STOPPED. H_2O TEMP = 36°C
1447	SW, LF	1.7	TF	0.6	0.021	LF	GELATIN DISSOLVING, NO MECHANICAL EROSION FINAL H_2O TEMP = 38°C
							VOL. ERODED = $1/2(5.3)(3.65)(11.0)(2.54)^3$ = 1744 ml

U = UPSTREAM
D = DOWNSTREAM
SW = STANDING WAVES
LF = LAMINAR FLOW
TF = TURBULENT FLOW
MTF = MODERATELY TURBULENT FLOW

STF = SLIGHTLY TURBULENT FLOW
AP = AIRPOCKET
T_O = INITIAL WATER TEMPERATURE (°C)
T_F = FINAL WATER TEMPERATURE (°C)

HYDRAULIC FLUME EXPERIMENTS

TESTED BY GWJ
CHECKED BY CPC, JHM

DATE: 4-24-87

FLUME EXPERIMENT NO. 2 | RUN NO. 11 | FLOW COMMENCED AT 1400 HRS. | FLOW TERMINATED AT 1435 HRS. | TOTAL DURATION OF FLOW: 35 MIN.

SAMPLE COMPOSITION: (INCLUDE DATE SAMPLE WAS MADE)
(1) GEL/H_2O = 0.031 (4-24-87)

(2) PLEXIGLASS

SAMPLE CONFIGURATION:

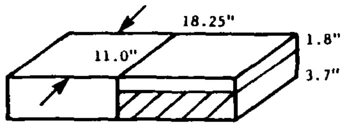

FLUME CONFIGURATION: LEVEL

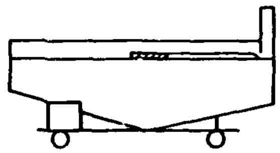

TIME	HEADWATER FLOW CHAR.	HEADWATER DEPTH (IN.)	TAILWATER FLOW CHAR.	TAILWATER DEPTH (IN.)	PRESSURE DIFFERENTIAL	FLOW CHAR. AT SAMPLE	OBSERVATIONS
1401	LF	3.0	TF	1.9	(A) 0.075	LF	ELIMINATED AP (NO STANDING WAVES) TEMP = 22°C
1405	LF	1.3	TF	0.6	(B) 0.029	LF	AP HEIGHT = 1.4"; HIGHER TRANSDUCERS READINGS* AND ABSENCE OF SW MAY INDICATE THAT THE PUMP'S DISCHARGE VARIES SIGNIFICANTLY
1414	LF	1.3	TF	0.6	(C) 0.042	LF	* FOR LOWER HEADWATER DEPTHS THAN BEFORE
1422	LF	1.3	TF	0.6	(D) 0.043	LF	LITTLE SLUMPING, UNDERCUTTING
1430	LF	1.3	TF	0.6	(F) 0.039	LF	TEMP = 28°C
1435	FLOW STOPPED						1.2" UNDERCUT BOTTOM OF PLEXIGLASS, NOT WEDGE SHAPED VOL. ERODED - 810 ml

U = UPSTREAM
D = DOWNSTREAM
SW = STANDING WAVES
LF = LAMINAR FLOW
TF = TURBULENT FLOW
MTF = MODERATELY TURBULENT FLOW

STF = SLIGHTLY TURBULENT FLOW
AP = AIRPOCKET
T_O = INITIAL WATER TEMPERATURE (°C)
T_F = FINAL WATER TEMPERATURE (°C)

HYDRAULIC FLUME EXPERIMENTS

TESTED BY GWJ
CHECKED BY CPC, JHM

DATE: 4-27-87

FLUME EXPERIMENT NO. 2

RUN NO. 12

FLOW COMMENCED AT 1502 HRS.

FLOW TERMINATED AT 1538 HRS.

TOTAL DURATION OF FLOW: 36 MIN.

SAMPLE COMPOSITION: (INCLUDE DATE SAMPLE WAS MADE)
(1) GEL/H_2O = 0.031 + GRAVEL (4-27-87)

(2) PLEXIGLASS

SAMPLE CONFIGURATION:

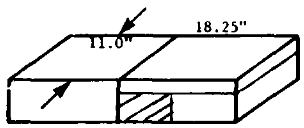

FLUME CONFIGURATION:
LEVEL

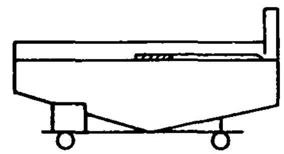

TIME	HEADWATER FLOW CHAR.	HEADWATER DEPTH (IN.)	TAILWATER FLOW CHAR.	TAILWATER DEPTH (IN.)	PRESSURE DIFFERENTIAL	FLOW CHAR. AT SAMPLE	OBSERVATIONS
1503	SW	4.3	TF	2.0	(A) 0.054	LF	ELIMINATED AP TEMP = 24.5°C
1508	LF	1.5	TF	0.6	(B) 0.017	LF	2.0" AP
1527	LF	1.5	TF	0.6	(C) 0.18	LF	NO SLUMPING, LITTLE EROSION 1.75" AP
1530	FLOW STOPPED						

U = UPSTREAM
D = DOWNSTREAM
SW = STANDING WAVES
LF = LAMINAR FLOW
TF = TURBULENT FLOW
MTF = MODERATELY TURBULENT FLOW

STF = SLIGHTLY TURBULENT FLOW
AP = AIRPOCKET
T_O = INITIAL WATER TEMPERATURE (°C)
T_F = FINAL WATER TEMPERATURE (°C)

HYDRAULIC FLUME EXPERIMENTS

TESTED BY GWJ
CHECKED BY CPC, JHM
DATE: 4-28-87

FLUME EXPERIMENT NO. 2 | RUN NO. 13 | FLOW COMMENCED AT 8:59 HRS. | FLOW TERMINATED AT 9:34 HRS. | TOTAL DURATION OF FLOW: 35 MIN.

SAMPLE COMPOSITION: (INCLUDE DATE SAMPLE WAS MADE)
(1) GEL/H_2O = 0.031 + GRAVEL (4-27-87)
(2) 2 PLEXIGLASS PLATES

SAMPLE CONFIGURATION:

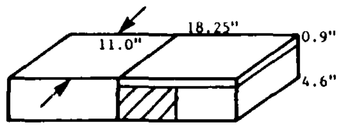

FLUME CONFIGURATION:
LEVEL

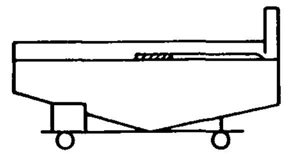

TIME	HEADWATER FLOW CHAR.	HEADWATER DEPTH (IN.)	TAILWATER FLOW CHAR.	TAILWATER DEPTH (IN.)	PRESSURE DIFFERENTIAL	FLOW CHAR. AT SAMPLE	OBSERVATIONS
9:00	SW	3.6	TF	1.7	(A) 0.056	LF	ELIMINATED AP
9:04	LF	ı.5	TF	0.5	(B) 0.018	LF	2.4" AP
9:10	LF	1.6	TF	0.5	(C) 0.018	LF	0.6" AP
9:14	LF	1.6	TF	0.5	(C) 0.018	LF	AP "VENTED ITSELF" NOW IT IS 1.5" HIGH TEMP AT 9:22: 27°C
9:29	LF	1.6	TF	0.5	(D) 0.018	LF	AP 1.0" VERY LITTLE EROSION
9:34	FLOW STOPPED						

U = UPSTREAM
D = DOWNSTREAM
SW = STANDING WAVES
LF = LAMINAR FLOW
TF = TURBULENT FLOW
MTF = MODERATELY TURBULENT FLOW
STF = SLIGHTLY TURBULENT FLOW
AP = AIRPOCKET
T_O = INITIAL WATER TEMPERATURE (°C)
T_F = FINAL WATER TEMPERATURE (°C)

HYDRAULIC FLUME EXPERIMENTS

TESTED BY GWJ
CHECKED BY CPC, JHM
DATE: 4-28-87

FLUME EXPERIMENT NO. 2
RUN NO. 14
FLOW COMMENCED AT 1651 HRS.
FLOW TERMINATED AT 1724 HRS.
TOTAL DURATION OF FLOW: 32 MIN.

SAMPLE COMPOSITION: (INCLUDE DATE SAMPLE WAS MADE)
(1) GEL/H_2O = 0.031 + GRAVEL (4-28-87)
(2) 1 PLEXIGLASS PLATE

SAMPLE CONFIGURATION:

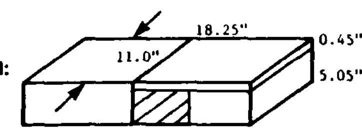

FLUME CONFIGURATION:
LEVEL

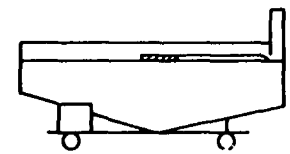

TIME	HEADWATER FLOW CHAR.	HEADWATER DEPTH (IN.)	TAILWATER FLOW CHAR.	TAILWATER DEPTH (IN.)	PRESSURE DIFFERENTIAL	FLOW CHAR. AT SAMPLE	OBSERVATIONS
1652	SW	3.8	TF	1.8	(A) 0.052	LF	ELIMINATED AP
1654	LF, SW	1.6	TF	0.6	(B) 0.022	LF	AP 1.3" HIGH TEMP AT 1707 = 28°C TEMP AT 1718 = 30°C
1721	LF, SW	1.6	TF	0.6	(C) 0.022	LF	LITTLE EROSION
1724	FLOW STOPPED						

U = UPSTREAM
D = DOWNSTREAM
SW = STANDING WAVES
LF = LAMINAR FLOW
TF = TURBULENT FLOW
MTF = MODERATELY TURBULENT FLOW
STF = SLIGHTLY TURBULENT FLOW
AP = AIRPOCKET
T_O = INITIAL WATER TEMPERATURE (°C)
T_F = FINAL WATER TEMPERATURE (°C)

HYDRAULIC FLUME EXPERIMENTS

TESTED BY GWJ
CHECKED BY CPC, JHM

DATE: 4-29-87

FLUME EXPERIMENT NO. 2

RUN NO. 15

FLOW COMMENCED AT 1557 HRS.

FLOW TERMINATED AT 1630 HRS.

TOTAL DURATION OF FLOW: 33 MIN.

SAMPLE COMPOSITION: (INCLUDE DATE SAMPLE WAS MADE)
(1) GEL/H_2O = 0.031
(2) 8 PLATES PLEXIGLASS

SAMPLE CONFIGURATION:

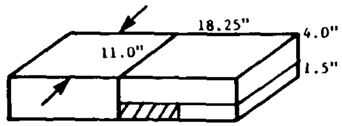

FLUME CONFIGURATION:
LEVEL

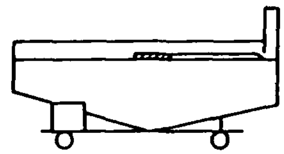

TIME	HEADWATER FLOW CHAR.	HEADWATER DEPTH (IN.)	TAILWATER FLOW CHAR.	TAILWATER DEPTH (IN.)	PRESSURE DIFFERENTIAL	FLOW CHAR. AT SAMPLE	OBSERVATIONS
1558	SW	3.6	TF	1.4	(A) 0.035	LF	TEMP BEFORE FLOW STARTED: 23°C T_f = 26.0°C ELIMINATED AP
1600	SW, LF	1.5	TF	0.5	(B) 0.017	LF	AP 2.5" HIGH, DECREASING
1620	SW, LF	1.5	TF	0.5	(C) 0.016	LF	- DECREASED FLOW MOMENTARILY TO HD = 1.3" LITTLE EROSION
1630	FLOW STOPPED						FLUME WATER 26°C AT 1624

U = UPSTREAM
D = DOWNSTREAM
SW = STANDING WAVES
LF = LAMINAR FLOW
TF = TURBULENT FLOW
MTF = MODERATELY TURBULENT FLOW

STF = SLIGHTLY TURBULENT FLOW
AP = AIRPOCKET
T_O = INITIAL WATER TEMPERATURE (°C)
T_F = FINAL WATER TEMPERATURE (°C)

HYDRAULIC FLUME EXPERIMENTS

TESTED BY GWJ
CHECKED BY CPC, JHM

DATE: 4-30-87

FLUME EXPERIMENT NO. 2

RUN NO. 16

FLOW COMMENCED AT 905 HRS.

FLOW TERMINATED AT 944 HRS.

TOTAL DURATION OF FLOW: 39 MIN.

SAMPLE COMPOSITION: (INCLUDE DATE SAMPLE WAS MADE)
(1) GEL/H_2O = 0.031 (4-29-87)

(2) 7 PLEXIGLASS PLATES

SAMPLE CONFIGURATION:

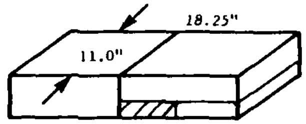

FLUME CONFIGURATION:
LEVEL

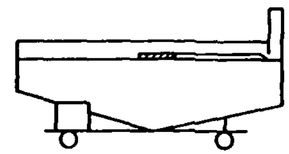

TIME	HEADWATER FLOW CHAR.	HEADWATER DEPTH (IN.)	TAILWATER FLOW CHAR.	TAILWATER DEPTH (IN.)	PRESSURE DIFFERENTIAL	FLOW CHAR. AT SAMPLE	OBSERVATIONS
907	SW	3.8	TF	1.7	(A) 0.056	LF	ELIMINATED AP TEMP AT 9:12: 25°C
912	SW, LF	1.6	TF	0.7	(B) 0.022	LF	AP 0.5" HIGH 9:14: AP VENTED TO 1.5" HIGH
914	SW, LF	1.5	TF	0.6	(C) 0.022	LF	AP 1.3" HIGH
944	SW, LF	1.5	TF	0.6	(D) 0.022	LF	- VENTED TO 2.0" (9:28) TEMP. AT 9:42: 28°C AP 1.6" HIGH NO SIGNIFICANT EROSION (<3 ml) PREVIOUS EROSION MAY HAVE BEEN DUE TO DISTURBANCE AND WEAKENING OF THE FACE OF LAYER (1) DURING REMOVAL OF FRONT PLATE AND/OR IRREGULARITIES CAUSED BY REMOVAL OF CLAY SEAL

U = UPSTREAM
D = DOWNSTREAM
SW = STANDING WAVES
LF = LAMINAR FLOW
TF = TURBULENT FLOW
MTF = MODERATELY TURBULENT FLOW

STF = SLIGHTLY TURBULENT FLOW
AP = AIRPOCKET
T_O = INITIAL WATER TEMPERATURE (°C)
T_F = FINAL WATER TEMPERATURE (°C)

HYDRAULIC FLUME EXPERIMENTS

TESTED BY GWJ
CHECKED BY CPC, JHM

DATE: 4-30-87

FLUME EXPERIMENT NO. 2

RUN NO. 17

FLOW COMMENCED AT 1620 HRS.

FLOW TERMINATED AT 1653 HRS.

TOTAL DURATION OF FLOW: 33 MIN.

SAMPLE COMPOSITION: (INCLUDE DATE SAMPLE WAS MADE)

(1) GEL/H_2O = 0.031 + GRAVEL (4-29-87)

(2) 6 PLATES OF PLEXIGLASS

SAMPLE CONFIGURATION:

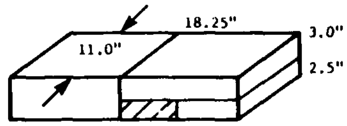

FLUME CONFIGURATION: LEVEL

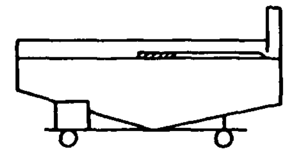

TIME	HEADWATER FLOW CHAR.	HEADWATER DEPTH (IN.)	TAILWATER FLOW CHAR.	TAILWATER DEPTH (IN.)	PRESSURE DIFFERENTIAL	FLOW CHAR. AT SAMPLE	OBSERVATIONS
1621	SW	3.6	TF	1.6	(A) 0.037	LF	TEMP BEFORE TEST: 26.5°C AP ELIMINATED
1623	LF	1.6	TF	0.7	(B) 0.018	LF	1.5" AP, STABLE
1651	LF	1.6	TF	0.7	(C) 0.018	LF	1.8" AP TEMP: 31°C
1653	FLOW STOPPED						

U = UPSTREAM
D = DOWNSTREAM
SW = STANDING WAVES
LF = LAMINAR FLOW
TF = TURBULENT FLOW
MTF = MODERATELY TURBULENT FLOW

STF = SLIGHTLY TURBULENT FLOW
AP = AIRPOCKET
T_O = INITIAL WATER TEMPERATURE (°C)
T_F = FINAL WATER TEMPERATURE (°C)

HYDRAULIC FLUME EXPERIMENTS

TESTED BY GWJ
CHECKED BY CPC, JHM
DATE: 5-1-87

FLUME EXPERIMENT NO. 2 | RUN NO. 18 | FLOW COMMENCED AT 8:10 HRS. | FLOW TERMINATED AT 849 HRS. | TOTAL DURATION OF FLOW: 39 MIN.

SAMPLE COMPOSITION: (INCLUDE DATE SAMPLE WAS MADE)
(1) GEL/H_2O = 0.031 + GRAVEL (4-30)

(2) 7 PLEXIGLASS PLATES

SAMPLE CONFIGURATION:

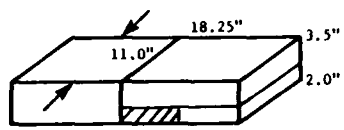

FLUME CONFIGURATION:
LEVEL

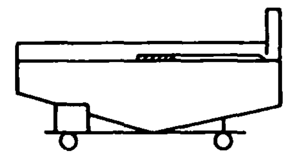

TEMP: 26.5°C, T_f = 30°C

TIME	HEADWATER FLOW CHAR.	HEADWATER DEPTH (IN.)	TAILWATER FLOW CHAR.	TAILWATER DEPTH (IN.)	PRESSURE DIFFERENTIAL	FLOW CHAR. AT SAMPLE	OBSERVATIONS
812	SW	3.5	TF	1.7	(A) 0.061	LF	ELIMINATED AP
813	SW, LF	1.6	TF	0.6	(B) 0.023	LF	AP 1.5" HIGH
819	SW, LF	1.5	TF	0.6	(C) 0.019	LF	AP 1.5"
845	SW, LF	1.5	TF	0.6	(D) 0.018	LF	AP 1.7" TEMP AT 8:47 30°C
849	FLOW STOPPED						

U = UPSTREAM
D = DOWNSTREAM
SW = STANDING WAVES
LF = LAMINAR FLOW
TF = TURBULENT FLOW
MTF = MODERATELY TURBULENT FLOW
STF = SLIGHTLY TURBULENT FLOW
AP = AIRPOCKET
T_O = INITIAL WATER TEMPERATURE (°C)
T_F = FINAL WATER TEMPERATURE (°C)

HYDRAULIC FLUME EXPERIMENTS

TESTED BY GWJ
CHECKED BY CPC, JHM
DATE: 5-1-87

FLUME EXPERIMENT NO. 2 RUN NO. 19 FLOW COMMENCED AT 1643 HRS. FLOW TERMINATED AT 1726 HRS. TOTAL DURATION OF FLOW: 43 MIN.

SAMPLE COMPOSITION: (INCLUDE DATE SAMPLE WAS MADE)
(1) GEL/H_2O = 0.031 + GRAVEL (5-1)
(2) 5 PLEXIGLASS PLATES

SAMPLE CONFIGURATION:

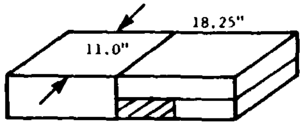

FLUME CONFIGURATION:
LEVEL

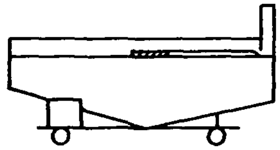

TIME	HEADWATER FLOW CHAR.	HEADWATER DEPTH (IN.)	TAILWATER FLOW CHAR.	TAILWATER DEPTH (IN.)	PRESSURE DIFFERENTIAL	FLOW CHAR. AT SAMPLE	OBSERVATIONS
1644	SW	3.0	TF	1.4	(A) 0.040	LF	TEMP 26.5°C, T_f = 31.0°C
1645	SW	3.5	TF	1.7	(B) 0.045	LF	AP ELIMINATED
1649	SW	1.5	TF	0.6	(C) 0.015	LF	AP 2.0"
1651	SW	4.0	TF	1.8	(D) 0.041	LF	INCREASED FLOW TO ELIMINATE AP, PRODUCED SMALLER AP
1656	LF	1.5	TF	0.6	(E) 0.014	LF	AP 1.5"
1721	LF	1.5	TF	0.6	(F) 0.016	LF	AP 1.5" SIGNIFICANT EROSION TEMP: 31°C

U = UPSTREAM
D = DOWNSTREAM
SW = STANDING WAVES
LF = LAMINAR FLOW
TF = TURBULENT FLOW
MTF = MODERATELY TURBULENT FLOW
STF = SLIGHTLY TURBULENT FLOW
AP = AIRPOCKET
T_O = INITIAL WATER TEMPERATURE (°C)
T_F = FINAL WATER TEMPERATURE (°C)

HYDRAULIC FLUME EXPERIMENTS

TESTED BY GWJ
CHECKED BY CPC, JHM

DATE: 5-4-87

FLUME EXPERIMENT NO. 2 | RUN NO. 20 | FLOW COMMENCED AT 1507 HRS. | FLOW TERMINATED AT 1545 HRS. | TOTAL DURATION OF FLOW: 38 MIN.

SAMPLE COMPOSITION: (INCLUDE DATE SAMPLE WAS MADE)
(1) GEL/H_2O = 0.031 + GRAVEL (5-4-87)

(2) 4 PLEXIGLASS PLATES

SAMPLE CONFIGURATION:

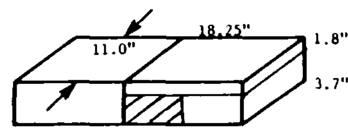

FLUME CONFIGURATION:
LEVEL

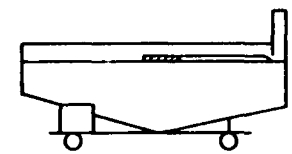

T_o = 25°C, T_f = 29°C

TIME	HEADWATER FLOW CHAR.	HEADWATER DEPTH (IN.)	TAILWATER FLOW CHAR.	TAILWATER DEPTH (IN.)	PRESSURE DIFFERENTIAL*	FLOW CHAR. AT SAMPLE	OBSERVATIONS
1509	SW	3.5	TF	1.7	(A) 0.075	LF	ELIMINATED AP
1515	LF, SW	1.5	TF	0.6	(B) 0.040	LF	AP 1.5" HIGH
1534	LF, SW	1.5	TF	0.6	(C) 0.042	LF	AP 1.5" HIGH T = 28°C
1543	LF, SW	1.5	TF	0.6	(D) 0.050	LF	TRANSDUCER READING INCREASING T_f = 29°C
1545	FLOW STOPPED						
							VOL. ERODED: 657 ml

* WHEN ZEROING THE TRANSDUCER, READING WAS ~ 0.021 PSI, AFTER ADJUSTMENT TO ZERO, THE READINGS SEEM TO BE ABOUT 0.021 HIGHER THAN IN PREVIOUS TESTS

U = UPSTREAM
D = DOWNSTREAM
SW = STANDING WAVES
LF = LAMINAR FLOW
TF = TURBULENT FLOW
MTF = MODERATELY TURBULENT FLOW
STF = SLIGHTLY TURBULENT FLOW
AP = AIRPOCKET
T_O = INITIAL WATER TEMPERATURE (°C)
T_F = FINAL WATER TEMPERATURE (°C)

HYDRAULIC FLUME EXPERIMENTS

TESTED BY GWJ
CHECKED BY CPC, JHM
DATE: 5-7-87

FLUME EXPERIMENT NO. 2 | RUN NO. 21 | FLOW COMMENCED AT 1350 HRS. | FLOW TERMINATED AT 1423 HRS. | TOTAL DURATION OF FLOW: 32 MIN.

SAMPLE COMPOSITION: (INCLUDE DATE SAMPLE WAS MADE)

(1) GEL/H_2O = 0.031 + GRAVEL (5-7-87)

(2) 7 PLEXIGLASS PLATES

SAMPLE CONFIGURATION:

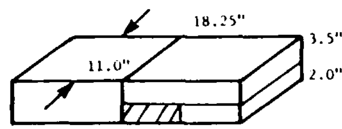

FLUME CONFIGURATION:

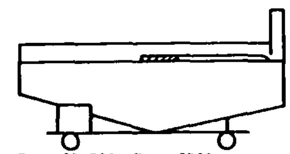

T_o = 23.5°C, T_f = 27°C

TIME	HEADWATER FLOW CHAR.	HEADWATER DEPTH (IN.)	TAILWATER FLOW CHAR.	TAILWATER DEPTH (IN.)	PRESSURE DIFFERENTIAL	FLOW CHAR. AT SAMPLE	OBSERVATIONS
1351	SW	3.5	TF	1.5	(A) 0.045	LF	ELIMINATED AP
1353	LF	1.5	TF	1.1*	(B) 0.018	LF	AP 1.5" HIGH
1420	LF	1.5	TF	1.1*	(C) 0.017	LF	AP 1.5" HIGH: VERY LITTLE EROSION
1423	FLOW STOPPED						
							VOL. ERODED: 163 ml

* A SMALL SW WAS PRESENT AT POINT OF MEASUREMENT, AVERAGE DEPTH: 0.6"

U = UPSTREAM
D = DOWNSTREAM
SW = STANDING WAVES
LF = LAMINAR FLOW
TF = TURBULENT FLOW
MTF = MODERATELY TURBULENT FLOW
STF = SLIGHTLY TURBULENT FLOW
AP = AIRPOCKET
T_O = INITIAL WATER TEMPERATURE (°C)
T_F = FINAL WATER TEMPERATURE (°C)

HYDRAULIC FLUME EXPERIMENTS

TESTED BY GWJ
CHECKED BY CPC, JHM

DATE: 5-8-87

FLUME EXPERIMENT NO. 2

RUN NO. 22

FLOW COMMENCED AT 1401 HRS.

FLOW TERMINATED AT 1436 HRS.

TOTAL DURATION OF FLOW: 35 MIN.

SAMPLE COMPOSITION: (INCLUDE DATE SAMPLE WAS MADE)
(1) GEL/H_2O = 0.031 + GRAVEL (5-8-87)

(2) 7 PLEXIGLASS PLATES

SAMPLE CONFIGURATION:

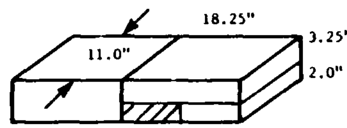

FLUME CONFIGURATION:
LEVEL

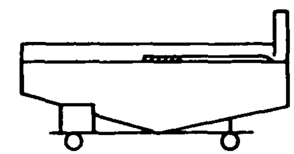

T_o = 25°C, T_f = 28.5°C

TIME	HEADWATER FLOW CHAR.	HEADWATER DEPTH (IN.)	TAILWATER FLOW CHAR.	TAILWATER DEPTH (IN.)	PRESSURE DIFFERENTIAL	FLOW CHAR. AT SAMPLE	OBSERVATIONS
1402	SW	3.7	TF	1.6	(A) 0.048	LF	AP ELIMINATED
1406	LF, SW	1.5	TF	0.6	(B) 0.019	LF	AP 1.5" HIGH
1433	LF, SW	1.5	TF	0.6	(C) 0.019	LF	AP 1.7" HIGH
1436	STOPPED						
							VOL. ERODED: <10 ml

U = UPSTREAM
D = DOWNSTREAM
SW = STANDING WAVES
LF = LAMINAR FLOW
TF = TURBULENT FLOW
MTF = MODERATELY TURBULENT FLOW

STF = SLIGHTLY TURBULENT FLOW
AP = AIRPOCKET
T_O = INITIAL WATER TEMPERATURE (°C)
T_F = FINAL WATER TEMPERATURE (°C)

HYDRAULIC FLUME EXPERIMENTS

TESTED BY GWJ
CHECKED BY CPC, JHM

DATE: 5-12-87

FLUME EXPERIMENT NO. 3 RUN NO. 1 FLOW COMMENCED AT 821 HRS. FLOW TERMINATED AT 850 HRS. TOTAL DURATION OF FLOW: 29 MIN.

SAMPLE COMPOSITION: (INCLUDE DATE SAMPLE WAS MADE)
(1) GEL/H_2O = 0.025 + GRAVEL (5-11-87)

(2) 1 PLEXIGLASS PLATE

SAMPLE CONFIGURATION:

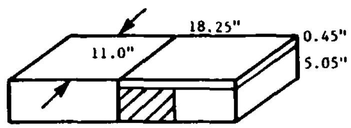

FLUME CONFIGURATION:
LEVEL

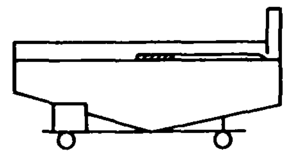

T_o = 25°C, T_f = 28°C

TIME	HEADWATER FLOW CHAR.	HEADWATER DEPTH (IN.)	TAILWATER FLOW CHAR.	TAILWATER DEPTH (IN.)	PRESSURE DIFFERENTIAL	FLOW CHAR. AT SAMPLE	OBSERVATIONS
824	SW	4.2	TF	1.9	(A) 0.051	LF	ELIMINATED AP
830	SMALL SW, LF	1.5	TF	0.6	(B) 0.018	LF	1.5" AP MUCH SCOUR DURING ESTABLISHMENT OF DESIRED DISCHARGE - SIGNIFICANT EROSION OCCURRED BEFORE THE TIME SEGMENT
850	FLOW STOPPED						A LARGE BLOCK FELL AFTER FLOW STOPPED

U = UPSTREAM
D = DOWNSTREAM
SW = STANDING WAVES
LF = LAMINAR FLOW
TF = TURBULENT FLOW
MTF = MODERATELY TURBULENT FLOW

STF = SLIGHTLY TURBULENT FLOW
AP = AIRPOCKET
T_O = INITIAL WATER TEMPERATURE (°C)
T_F = FINAL WATER TEMPERATURE (°C)

HYDRAULIC FLUME EXPERIMENTS

TESTED BY GWJ
CHECKED BY CPC, JHM
DATE: 5-14-87

FLUME EXPERIMENT NO. 3 | RUN NO. 2 | FLOW COMMENCED AT 808 HRS. | FLOW TERMINATED AT 840 HRS. | TOTAL DURATION OF FLOW: 32 MIN.

SAMPLE COMPOSITION: (INCLUDE DATE SAMPLE WAS MADE)
(1) GEL/H_2O = 0.025 (5-14-87)

(2) 1 PLEXIGLASS PLATE

SAMPLE CONFIGURATION:

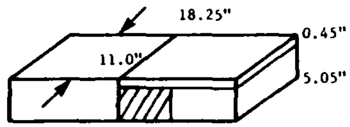

FLUME CONFIGURATION:
LEVEL

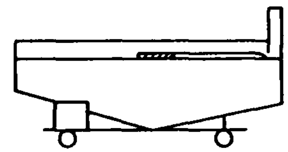

T_o = 24.5°C, T_f = 28°C

TIME	HEADWATER FLOW CHAR.	HEADWATER DEPTH (IN.)	TAILWATER FLOW CHAR.	TAILWATER DEPTH (IN.)	PRESSURE DIFFERENTIAL	FLOW CHAR. AT SAMPLE	OBSERVATIONS
809	SW	4.3	TF	1.9	(A) 0.041	LF	ELIMINATED AP; NO INITIAL EROSION
813	LF	1.5	TF	0.6	UNRELIABLE* TRANSDUCER	LF	PHASE W/NO AP; FLOW CLOSE TO KNICKPOINT FACE VENTED ITSELF
817	SW	4.0	TF	1.9	(B) 0.054	LF	ELIMINATED AP AGAIN
8:20	LF	1.7	TF	0.6	UNRELIABLE* TRANSDUCER	LF	NO AP, SLOPE OF WATERFALL NEAR VERTICAL 8:37 VERY SMALL AP DEVELOPED, 0.4" HIGH

* READINGS WERE <.005 PSI, SOME NEGATIVE

U = UPSTREAM
D = DOWNSTREAM
SW = STANDING WAVES
LF = LAMINAR FLOW
TF = TURBULENT FLOW
MTF = MODERATELY TURBULENT FLOW
STF = SLIGHTLY TURBULENT FLOW
AP = AIRPOCKET
T_O = INITIAL WATER TEMPERATURE (°C)
T_F = FINAL WATER TEMPERATURE (°C)

HYDRAULIC FLUME EXPERIMENTS

TESTED BY GWJ
CHECKED BY CPC, JHM

DATE: 5-15-87

FLUME EXPERIMENT NO. 3
RUN NO. 3
FLOW COMMENCED AT 917 HRS.
FLOW TERMINATED AT 1014 HRS.
TOTAL DURATION OF FLOW: 57 MIN.

SAMPLE COMPOSITION: (INCLUDE DATE SAMPLE WAS MADE)
(1) $GEL/H_2O = 0.025$ + GRAVEL (5-14-87)
(2) 2 PLEXIGLASS PLATES

SAMPLE CONFIGURATION:

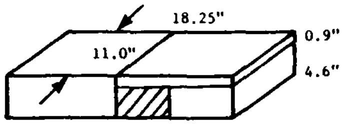

FLUME CONFIGURATION:
LEVEL

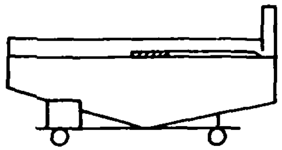

T_o = 24.5°C, T_f = 28.0°C

TIME	HEADWATER FLOW CHAR.	HEADWATER DEPTH (IN.)	TAILWATER FLOW CHAR.	TAILWATER DEPTH (IN.)	PRESSURE DIFFERENTIAL	FLOW CHAR. AT SAMPLE	OBSERVATIONS
918	SW	3.9	TF	1.8	(A) 0.052	LF	ELIMINATED AP DECREASED FLOW, AIRPOCKET FORMED; INCREASED FLOW TO ELIMINATE AP
927	LF	1.8	TF	0.7	(B) 0.018	LF	NO AP, VERTICAL SLOPE OF WATER ON KNICKPOINT FACE
934							WATERFALL VENTED ITSELF, INCREASED FLOW TO ELIMINATE AP
936	SW	3.8	TF	1.7	(C) 0.049		NO AP, NO EROSION YET T = 20°C
944	SW	1.8	TF	0.7	(D) 0.017		
1004							VERY LITTLE EROSION, <30 ml T = 30°C DISSOLUTION OF GELATIN CAUSES PARALLEL RETREAT OF KNICKPOINT FACE
1014	FLOW STOPPED						

U = UPSTREAM
D = DOWNSTREAM
SW = STANDING WAVES
LF = LAMINAR FLOW
TF = TURBULENT FLOW
MTF = MODERATELY TURBULENT FLOW

STF = SLIGHTLY TURBULENT FLOW
AP = AIRPOCKET
T_O = INITIAL WATER TEMPERATURE (°C)
T_F = FINAL WATER TEMPERATURE (°C)

HYDRAULIC FLUME EXPERIMENTS

TESTED BY GWJ
CHECKED BY CPC, JHM

DATE: 5-19-87

FLUME EXPERIMENT NO. 3 | RUN NO. 4 | FLOW COMMENCED AT 1650 HRS. | FLOW TERMINATED AT 1717 HRS. | TOTAL DURATION OF FLOW: 27 MIN.

SAMPLE COMPOSITION: (INCLUDE DATE SAMPLE WAS MADE)
(1) GEL/H_2O = 0.025 + GRAVEL (5-19-87)

(2) 1 PLEXIGLASS PLATE

SAMPLE CONFIGURATION:

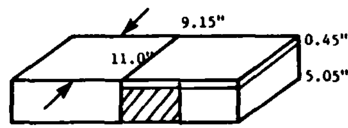

FLUME CONFIGURATION:
LEVEL

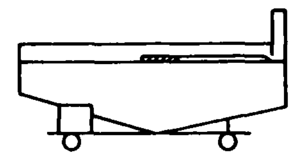

T_o = 25°C, T_f = 27°C

TIME	HEADWATER FLOW CHAR.	HEADWATER DEPTH (IN.)	TAILWATER FLOW CHAR.	TAILWATER DEPTH (IN.)	PRESSURE DIFFERENTIAL	FLOW CHAR. AT SAMPLE	OBSERVATIONS
1651	SW	3.3	TF	1.5	(A) 0.050	LF	ELIMINATED AP
1654	SW, LF	1.7	TF	0.7	(B) 0.023	LF	NO AP INITIALLY, VENTED ITSELF TO FORM A 0.3" AP
							1707 - BEGAN TO VENT ITSELF, BUT I INCREASED Q AND *PREVENTED IT, THEN DECREASED Q TO THE PRIOR LEVEL*
1709	SW, LF	1.8	TF	0.6	(C) 0.021	LF	
1717	FLOW STOPPED						WITHIN ONE MINUTE AFTER TURNING OFF PUMP, COVER PLATE REPLACED IN SAMPLE - SOME SLUMPING OCCURRED IMMEDIATELY AFTER PUMP WAS TURNED OFF (WHILE DISCHARGE WAS DECREASING)
							VOL. ERODED - 1316 ml

U = UPSTREAM
D = DOWNSTREAM
SW = STANDING WAVES
LF = LAMINAR FLOW
TF = TURBULENT FLOW
MTF = MODERATELY TURBULENT FLOW

STF = SLIGHTLY TURBULENT FLOW
AP = AIRPOCKET
T_O = INITIAL WATER TEMPERATURE (°C)
T_F = FINAL WATER TEMPERATURE (°C)

HYDRAULIC FLUME EXPERIMENTS

TESTED BY GWJ
CHECKED BY CPC, JHM

DATE: 5-20-87

FLUME EXPERIMENT NO. 3

RUN NO. 5

FLOW COMMENCED AT 1559 HRS.

FLOW TERMINATED AT 1625 HRS.

TOTAL DURATION OF FLOW: 26 MIN.

SAMPLE COMPOSITION: (INCLUDE DATE SAMPLE WAS MADE)
(1) GEL/H_2O = 0.025 + GRAVEL (5-20-87)

(2) 2 PLEXIGLASS PLATES

SAMPLE CONFIGURATION:

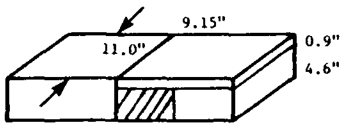

FLUME CONFIGURATION:
LEVEL

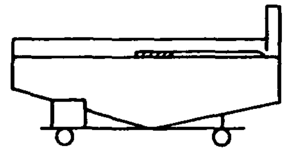

T_o = 26°C, T_f = 29°C

TIME	HEADWATER FLOW CHAR.	HEADWATER DEPTH (IN.)	TAILWATER FLOW CHAR.	TAILWATER DEPTH (IN.)	PRESSURE DIFFERENTIAL	FLOW CHAR. AT SAMPLE	OBSERVATIONS
1601	SW	3.5	TF	1.6	(A) 0.042	LF	ELIMINATED AP
1602	SW	1.7	TF	0.6	(B) 0.024	LF	AP = 0.3"; SAMPLE APPEARS TO BE DISSOLVING MUCH QUICKER
1625	FLOW STOPPED						NEARLY ALL EROSION WAS DUE TO DISSOLVING OF GELATIN; WAS EITHER TOO WEAK OR HAD NOT SET UP VOL. ERODED - 1580 ml

U = UPSTREAM
D = DOWNSTREAM
SW = STANDING WAVES
LF = LAMINAR FLOW
TF = TURBULENT FLOW
MTF = MODERATELY TURBULENT FLOW

STF = SLIGHTLY TURBULENT FLOW
AP = AIRPOCKET
T_O = INITIAL WATER TEMPERATURE (°C)
T_F = FINAL WATER TEMPERATURE (°C)

HYDRAULIC FLUME EXPERIMENTS

TESTED BY GWJ
CHECKED BY CPC, JHM
DATE: 5-21-87

FLUME EXPERIMENT NO. 3 — RUN NO. 6 — FLOW COMMENCED AT 1518 HRS. — FLOW TERMINATED AT 1546 HRS. — TOTAL DURATION OF FLOW: 28 MIN.

SAMPLE COMPOSITION: (INCLUDE DATE SAMPLE WAS MADE)
(1) GEL/H_2O = 0.025 + GRAVEL (5-21-87)

(2) 2 PLEXIGLASS PLATES

SAMPLE CONFIGURATION:

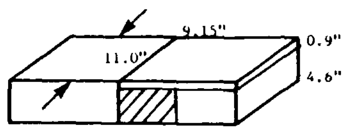

FLUME CONFIGURATION:
LEVEL

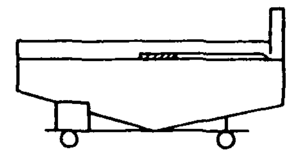

T_o = 24°C, T_f = 27°C

TIME	HEADWATER FLOW CHAR.	HEADWATER DEPTH (IN.)	TAILWATER FLOW CHAR.	TAILWATER DEPTH (IN.)	PRESSURE DIFFERENTIAL	FLOW CHAR. AT SAMPLE	OBSERVATIONS
1520	SW, TF	4.5	TF	1.8	(A) 0.047	LF	ELIMINATED AP
1523	SW, LF	1.8	TF	0.7	(B) 0.024	LF	NO AP; MUCH INITIAL EROSION
1546	SW, LF	1.8	TF	0.7	(C)		UNDERCUTTING IN GELATIN LAYER CAUSED COLLAPSE OF OVERLYING MATERIAL
	FLOW STOPPED						VOL. ERODED - 906 ml

U = UPSTREAM
D = DOWNSTREAM
SW = STANDING WAVES
LF = LAMINAR FLOW
TF = TURBULENT FLOW
MTF = MODERATELY TURBULENT FLOW

STF = SLIGHTLY TURBULENT FLOW
AP = AIRPOCKET
T_O = INITIAL WATER TEMPERATURE (°C)
T_F = FINAL WATER TEMPERATURE (°C)

HYDRAULIC FLUME EXPERIMENTS

TESTED BY GWJ
CHECKED BY CPC, JHM
DATE: 5-22-87

FLUME EXPERIMENT NO. 3
RUN NO. 7
FLOW COMMENCED AT 1543 HRS.
FLOW TERMINATED AT 1608 HRS.
TOTAL DURATION OF FLOW: 25 MIN.

SAMPLE COMPOSITION: (INCLUDE DATE SAMPLE WAS MADE)
(1) GEL/H_2O = 0.025 + GRAVEL (5-22-87)

(2) 3 PLEXIGLASS PLATES

SAMPLE CONFIGURATION:

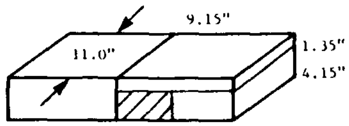

FLUME CONFIGURATION:
LEVEL

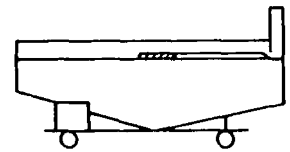

T_o = 24°C, T_f = 27°C

TIME	HEADWATER FLOW CHAR.	HEADWATER DEPTH (IN.)	TAILWATER FLOW CHAR.	TAILWATER DEPTH (IN.)	PRESSURE DIFFERENTIAL	FLOW CHAR. AT SAMPLE	OBSERVATIONS
1544	SW	4.0	TF	1.7	(A) 0.066	LF	AP ELIMINATED
1545	SW, LF	1.8	TF	0.7	(B) 0.022	LF	NO AP
1608	FLOW STOPPED						A PROCESS WHICH HAPPENS DURING UNDERCUTTING: GRAVEL IS REMOVED FROM BASE OF KNICKPOINT AND THE MATERIAL UPWARD IS ERODED OUT IMMEDIATELY AFTER AND SEQUENTIALLY UPWARD VOL. ERODED - 760 ml

U = UPSTREAM
D = DOWNSTREAM
SW = STANDING WAVES
LF = LAMINAR FLOW
TF = TURBULENT FLOW
MTF = MODERATELY TURBULENT FLOW

STF = SLIGHTLY TURBULENT FLOW
AP = AIRPOCKET
T_O = INITIAL WATER TEMPERATURE (°C)
T_F = FINAL WATER TEMPERATURE (°C)

HYDRAULIC FLUME EXPERIMENTS

TESTED BY GWJ
CHECKED BY CPC, JHM

DATE: 5-26-87

FLUME EXPERIMENT NO. 3

RUN NO. 8

FLOW COMMENCED AT 1609 HRS.

FLOW TERMINATED AT 1635 HRS.

TOTAL DURATION OF FLOW: 26 MIN.

SAMPLE COMPOSITION: (INCLUDE DATE SAMPLE WAS MADE)
(1) GEL/H_2O = 0.025 + GRAVEL (5-26-87)

(2) 4 PLEXIGLASS PLATES

SAMPLE CONFIGURATION:

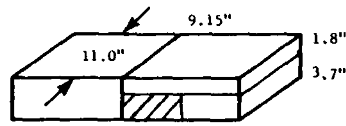

FLUME CONFIGURATION:
LEVEL

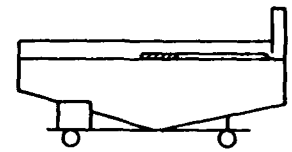

T_o = 24°C, T_f = 27.5°C

TIME	HEADWATER FLOW CHAR.	HEADWATER DEPTH (IN.)	TAILWATER FLOW CHAR.	TAILWATER DEPTH (IN.)	PRESSURE DIFFERENTIAL	FLOW CHAR. AT SAMPLE	OBSERVATIONS
1610	SW	4.3	TF	1.6	(A) 0.051	LF	ELIMINATED AP
1612	LF	1.8	TF	0.7	(B) 0.018	LF, SW	NO AP
1635	FLOW STOPPED						
							VOL. ERODED - 156 ml

U = UPSTREAM
D = DOWNSTREAM
SW = STANDING WAVES
LF = LAMINAR FLOW
TF = TURBULENT FLOW
MTF = MODERATELY TURBULENT FLOW

STF = SLIGHTLY TURBULENT FLOW
AP = AIRPOCKET
T_O = INITIAL WATER TEMPERATURE (°C)
T_F = FINAL WATER TEMPERATURE (°C)

HYDRAULIC FLUME EXPERIMENTS

TESTED BY GWJ
CHECKED BY CPC, JHM

DATE: 5-27-87

FLUME EXPERIMENT NO. 3 | RUN NO. 9 | FLOW COMMENCED AT 1544 HRS. | FLOW TERMINATED AT 1616 HRS. | TOTAL DURATION OF FLOW: 32 MIN.

SAMPLE COMPOSITION: (INCLUDE DATE SAMPLE WAS MADE)
(1) GEL/H_2O = 0.025 + GRAVEL (5-27-87)

(2) 5 PLEXIGLASS PLATES*

SAMPLE CONFIGURATION:
* (NOT COUNTING THE THIN PLATE)

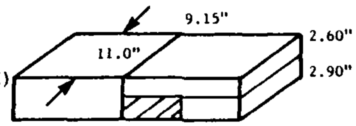

FLUME CONFIGURATION:
LEVEL

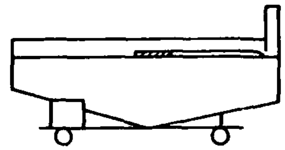

T_o = 24°C, T_f = 27.5°C

TIME	HEADWATER FLOW CHAR.	HEADWATER DEPTH (IN.)	TAILWATER FLOW CHAR.	TAILWATER DEPTH (IN.)	PRESSURE DIFFERENTIAL	FLOW CHAR. AT SAMPLE	OBSERVATIONS
1545	SW	3.4	TF	1.7	(A) 0.069	LF	ELIMINATED AP
1549	SW, LF	1.8 (1.5)	TF	0.7	(B) 0.025	LF	AP DEVELOPED, RAISED D TO ELIMINATE AP
1555	SW, LF	1.6 ABOVE SAMPLE	TF	0.7	(C) 0.022	LF	NO AP, LITTLE EROSION
1608	SW, LF	1.6 (1.4)	TF	0.6	(D) 0.022	LF	LITTLE EROSION
							MOST EROSION OCCURRED AFTER FLOW STOPPED BY "SLACKWATER"
							VOL. ERODED - 164 ml

U = UPSTREAM
D = DOWNSTREAM
SW = STANDING WAVES
LF = LAMINAR FLOW
TF = TURBULENT FLOW
MTF = MODERATELY TURBULENT FLOW
STF = SLIGHTLY TURBULENT FLOW
AP = AIRPOCKET
T_O = INITIAL WATER TEMPERATURE (°C)
T_F = FINAL WATER TEMPERATURE (°C)

HYDRAULIC FLUME EXPERIMENTS

TESTED BY GWJ

CHECKED BY CPC, JHM

DATE: 5-28-87

FLUME EXPERIMENT NO. 3 | RUN NO. 10 | FLOW COMMENCED AT 1330 HRS. | FLOW TERMINATED AT 1400 HRS. | TOTAL DURATION OF FLOW: 30 MIN.

SAMPLE COMPOSITION: (INCLUDE DATE SAMPLE WAS MADE)
(1) GEL/H_2O = 0.025 + GRAVEL (5-28-87)

(2) 6 PLEXIGLASS PLATES

SAMPLE CONFIGURATION:

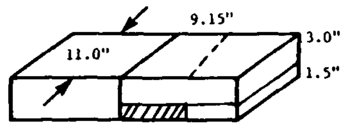

FLUME CONFIGURATION:
LEVEL

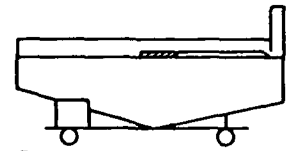

T_o = 24°C, T_f = 27°C

TIME	HEADWATER FLOW CHAR.	HEADWATER DEPTH (IN.)	TAILWATER FLOW CHAR.	TAILWATER DEPTH (IN.)	PRESSURE DIFFERENTIAL	FLOW CHAR. AT SAMPLE	OBSERVATIONS
1331	SW	3.5	TF	1.7	(A) 0.049	LF	ELIMINATED AP; INITIALLY FLOW WAS LF, BUT WITHIN ONE MINUTE SW DEVELOPED
1337	SW	1.8	TF	0.7	(B) 0.024	LF	NO AP, LITTLE INITIAL EROSION
1400	FLOW STOPPED						1350 LITTLE SIGNIFICANT EROSION, BUT APPEARS TO BE INCREASING VOL. ERODED - 171 ml

U = UPSTREAM
D = DOWNSTREAM
SW = STANDING WAVES
LF = LAMINAR FLOW
TF = TURBULENT FLOW
MTF = MODERATELY TURBULENT FLOW
STF = SLIGHTLY TURBULENT FLOW
AP = AIRPOCKET
T_O = INITIAL WATER TEMPERATURE (°C)
T_F = FINAL WATER TEMPERATURE (°C)

HYDRAULIC FLUME EXPERIMENTS

TESTED BY GWJ
CHECKED BY CPC, JHM
DATE: 5-29-87

FLUME EXPERIMENT NO. 3 | RUN NO. 11 | FLOW COMMENCED AT 1156 HRS. | FLOW TERMINATED AT 1223 HRS. | TOTAL DURATION OF FLOW: 27 MIN.

SAMPLE COMPOSITION: (INCLUDE DATE SAMPLE WAS MADE)
(1) GEL/H_2O = 0.025 + GRAVEL (5-29-87)

(2) 7 PLEXIGLASS PLATES

SAMPLE CONFIGURATION:

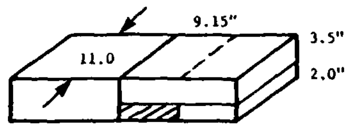

FLUME CONFIGURATION:
LEVEL

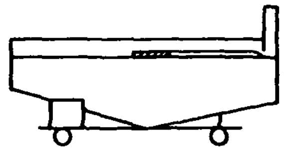

T_o = 24°C, T_f = 27°C

TIME	HEADWATER FLOW CHAR.	HEADWATER DEPTH (IN.)	TAILWATER FLOW CHAR.	TAILWATER DEPTH (IN.)	PRESSURE DIFFERENTIAL	FLOW CHAR. AT SAMPLE	OBSERVATIONS
1156	LF, SW	3.6	TF	1.5	(A) 0.047	LF	ELIMINATED AP
1200	SW	1.7	TF	0.7	(B) 0.028	LF	NO AP, SAME WATERFALL CONFIGURATION AS RUN 10, BUT *HIGHER VELOCITY*
1215	SW	1.7	TF	0.7	(C) 0.025	LF	ERODING FASTER THAN IN PREVIOUS TEST 12:20: ERODING BACK TO 1/2 INCH
1223	FLOW STOPPED						*PARALLEL RETREAT OF LAYER 1*
							VOL. ERODED - 156 ml

U = UPSTREAM
D = DOWNSTREAM
SW = STANDING WAVES
LF = LAMINAR FLOW
TF = TURBULENT FLOW
MTF = MODERATELY TURBULENT FLOW

STF = SLIGHTLY TURBULENT FLOW
AP = AIRPOCKET
T_O = INITIAL WATER TEMPERATURE (°C)
T_F = FINAL WATER TEMPERATURE (°C)

HYDRAULIC FLUME EXPERIMENTS

TESTED BY GWJ
CHECKED BY CPC, JHM

DATE: 5-29-87

FLUME EXPERIMENT NO. 3

RUN NO. 12

FLOW COMMENCED AT 1717 HRS.

FLOW TERMINATED AT 1744 HRS.

TOTAL DURATION OF FLOW: 26.0 MIN.

SAMPLE COMPOSITION: (INCLUDE DATE SAMPLE WAS MADE)
(1) GEL/H_2O = 0.025 + GRAVEL (5-29-87)
(2) 8 PLEXIGLASS PLATES

SAMPLE CONFIGURATION:

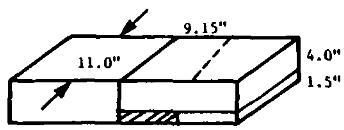

FLUME CONFIGURATION:
LEVEL

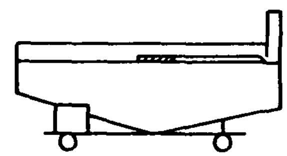

T_o = 25°C, T_f = 28°C

TIME	HEADWATER FLOW CHAR.	HEADWATER DEPTH (IN.)	TAILWATER FLOW CHAR.	TAILWATER DEPTH (IN.)	PRESSURE DIFFERENTIAL	FLOW CHAR. AT SAMPLE	OBSERVATIONS
1718	SW	4.7	TF	1.8	(A) 0.055	LF	ELIMINATED AP, SOME INITIAL EROSION.
1722	SW, LF	1.8	TF	0.7	(B) 0.018	LF	NO AP ERODING MUCH FASTER THAN PREVIOUS RUN (11); PERHAPS DUE TO DISTURBANCE OF GRAVEL AT KNICKPOINT FACE DURING REMOVAL OF PLEXIGLASS DIVIDER
1744	SW, LF	1.0	TF	0.7	(C) 0.0195	LF	- SAME CONFIGURATION OF WATERFALL AS BEFORE, BUT LOWER FLOW VELOCITY
							VOL. ERODED 224 ML

U = UPSTREAM
D = DOWNSTREAM
SW = STANDING WAVES
LF = LAMINAR FLOW
TF = TURBULENT FLOW
MTF = MODERATELY TURBULENT FLOW
STF = SLIGHTLY TURBULENT FLOW
AP = AIRPOCKET
T_O = INITIAL WATER TEMPERATURE (°C)
T_F = FINAL WATER TEMPERATURE (°C)

HYDRAULIC FLUME EXPERIMENTS

TESTED BY GWJ
CHECKED BY CPC, JHM

DATE: 5-18-87

FLUME EXPERIMENT NO. 4 RUN NO. 1 FLOW COMMENCED AT 603 HRS. FLOW TERMINATED AT 612 HRS. TOTAL DURATION OF FLOW: 9 MIN.

SAMPLE COMPOSITION: (INCLUDE DATE SAMPLE WAS MADE)
(1) GEL/H_2O = 0.025 (5-18-87)
(2) NaS: O_4 + H_2O + SET AGENT (CELTITE 55-03) + GRAVEL (5-18-87)

SAMPLE CONFIGURATION:

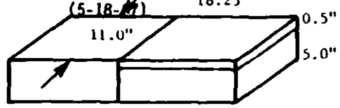

FLUME CONFIGURATION: LEVEL

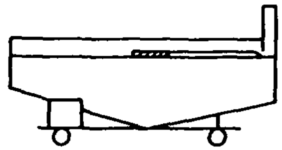

TIME	HEADWATER FLOW CHAR.	HEADWATER DEPTH (IN.)	TAILWATER FLOW CHAR.	TAILWATER DEPTH (IN.)	PRESSURE DIFFERENTIAL	FLOW CHAR. AT SAMPLE	OBSERVATIONS
608	LF	1.3	TF	0.9*	(A) 0.022	LF	ELIMINATED AP, MUCH HEADWARD EROSION NO AP ATT
612							ENTIRE SAMPLE ERODED

* DEBRIS MADE DEPTH UNEVEN

U = UPSTREAM
D = DOWNSTREAM
SW = STANDING WAVES
LF = LAMINAR FLOW
TF = TURBULENT FLOW
MTF = MODERATELY TURBULENT FLOW
STF = SLIGHTLY TURBULENT FLOW
AP = AIRPOCKET
T_O = INITIAL WATER TEMPERATURE (°C)
T_F = FINAL WATER TEMPERATURE (°C)

APPENDIX B

METHOD OF ESTIMATING PARTICLE VELOCITY IN TURBULENT FLOW

1. In order to estimate the velocity of flow in the turbulent reverse roller, a 1-in. grid was placed on the side of the flume in front of the video camera. A stop watch capable of measuring to hundredths of a second was positioned in line with the reverse roller. Using stop action, particles were tracked across the grid and the time recorded. The particles tended to stay in the same plane of rotation once the reverse roller was set in motion. The following table presents the particle velocity data.

Particle Velocity

Particle No.	Distance in.	Time sec	Velocity in./sec
1	1.7	0.22	7.7
2	1.7	0.16	10.6
3	0.9	0.16	5.6
4	1.9	0.16	11.9
5	1.7	0.08	21.3
6	1.9	0.12	15.8
7	1.0	0.12	8.3
8	1.2	0.12	10.0
9	1.6	0.24	6.7
10	1.0	0.14	7.1
11	1.2	0.16	7.5
12	1.7	0.13	13.1
13	1.5	0.22	6.8
14	1.0	0.20	5.0
15	1.8	0.22	8.2
16	1.4	0.20	7.0
17	0.8	0.16	5.0
18	1.7	0.16	10.6
19	0.8	0.16	5.0
20	1.3	0.20	6.5
21	1.3	0.16	8.1
22	1.8	0.28	6.4
23	2.0	0.38	5.3
24	1.8	0.22	8.2
25	1.7	0.16	10.6
26	1.2	0.14	8.6
27	2.2	0.18	12.2
28	1.1	0.12	9.2
29	1.2	0.22	5.5
30	2.1	0.12	17.5
31	1.8	0.18	10.0
32	1.5	0.26	5.8
33	1.9	0.34	5.6
34	1.6	0.26	6.2
35	1.5	0.16	9.4
36	1.1	0.16	6.9
37	2.3	0.16	14.4
38	1.2	0.10	12.0
39	0.9	0.14	6.4
40	1.1	0.12	9.2
41	1.0	0.16	6.2
42	1.9	0.38	5.0
43	1.3	0.22	5.9
44	1.4	0.18	7.8
45	0.8	0.16	5.0
46	1.8	0.16	11.2

(Continued)

Particle Velocity (Concluded)

Particle No.	Distance in.	Time sec	Velocity in./sec
47	1.1	0.22	5.0
48	1.9	0.28	6.8
49	1.0	0.16	6.2
50	1.2	0.16	7.5

Average velocity = 8.5 in./sec.

APPENDIX C

MIX DESIGNS AND PROCEDURES

1. Appendix C contains the mix designs and procedures for the various mixes tested during this study. All the mixes are given because the ones that were not suitable for our particular flume velocities could possibly be useful in future modeling or remedial action efforts.

Cement Mixes (Cellular Concrete)

Mix	Cement lb	Water lb	Foam cu ft	Water Cement	Density lb/cu ft
JM-1(bot)	26.0	20.8	0.535	0.80	47.0
JM-3(top)	36.6	16.9	0.540	0.46	53.5
JM-10(top)	22.0	11.0	0.71	0.50	33.0
JM-11(bot)	12.0	6.0	0.84	0.50	20.0
JM-12(bot)	16.1	7.0	0.81	0.43	24.9
JM-13(top)	25.8	12.7	0.67	0.49	40.0

2. The cellular concrete was prepared by first adding the cement to the water in the mixer. The preformed foam was then added in an amount less than the required theoretical amount. A unit weight determination was made and the remaining amount of foam was calculated and added to the mixture to obtain the required unit weight.

Cement Mixes (Concrete)

Mix	Cement lb	Water lb	Lime Dust lb	Gravel lb	Density lb/cu ft
JM-1G(top)	4.9	9.8	18.4	113.7	146.8
JM-2G(bot)	1.5	9.8	18.8	116.0	146.3

Mix	Cement gr	Water lb	Lime Dust lb	Limestone Cement	Density lb/cu ft
JM-3G(top)	27.0	4.5	2.8	18.0	158.1
JM-4G(bot)	40.0	16.0	10.0	63.0	128.9

3. The limestone aggregate concrete was prepared by mixing the dry components in the mixer and then adding the water until mixing was complete.

Sodium Silicate Mix

Mix	Sodium Silicate ml	Setting Agent ml	Water ml
18(top)	200	40	760
19(bot)	100	50	850
20(top)	150	50	800
21)bot)	60	40	900
22(top)	100	100	800
23(bot)	50	50	900

4. The sodium silicate mix was prepared by adding 25 percent of the total water to the sodium silicate and mixing well. Next, the setting agent was added to the remaining 75 percent of the water in a separate container. The setting agent and water was then added very slowly to the sodium silicate and water and mixed for about 2 min and then poured into the mold containing the dry gravel.

Gelatin

Mix[1]	Water gr	Knox Gelatin gr
0.031	2,500	77.5
0.025	2,500	62.5
0.015	2,500	37.5

[1]Gelatin mix was identified by the gelatin/water ratio.

5. Approximately half of the water was mixed with the gelatin at a temperature of 75° C. The remainder of the water at a temperature of 0° C was added and mixed thoroughly. The mixture was then poured into the mold containing the dry gravel. The setting time was usually 4 to 5 hr.

APPENDIX D

SUMMARY OF FLUME TEST DATA

The following table presents the results of the knickpoint erosion test data for the Gelatin mixtures.

No.	Layer Thickness Top in.	Layer Thickness Bottom in.	Duration min	Vel[1] ft/sec	Volume cu cm	Mix[2]
2-1	0.5	5.0	97.0			0131
2-1A	0.45	5.0	11.0			0131
2-1B	0.45	5.0	42.0		1000	0152
2-2	0.45	5.05	34.0		2619	0140
2-3	0.95	4.55	36.0	1.34-1.57	3216	0140
2-4	1.35	4.15	41.0	1.5 -3.51	2270	0140
2-5	1.80	3.70	35.0	2.21-2.45	1545	0150
2-6	1.80	3.70	--	--	--	0150
2-7	1.80	3.70	84.0	90-2.30	1000	0310
2-8	3.45	2.05	80.0	1.68-2.80	901	0310
29A	3.90	1.60	87.0	1.63-2.86	288	0310
29B	2.55	2.95	67.0	1.68-2.50	1127	0310
2-10	1.85	3.65	65.0	1.60-2.50	1744	0310
2-11	1.80	3.70	35.0	2.50-3.33	810	0310
2-12	1.4	4.1	35.0	1.64-2.83	190	0310
2-13	0.9	4.6	35.0	1.64-2.88	50	0310
2-14	0.45	5.05	32.0	1.81-2.78	250	0310
2-15	4.0	1.50	33.0	1.59-2.28	86	0310
2-16	3.5	2.0	39.0	1.80-2.88	3	0310
2-17	3.0	2.5	33.0	1.64-2.34	390	0310
2-18	3.5	2.0	39.0	1.64-3.01	223	0310
2-19	2.6	2.9	43.0	1.49-2.54	325	0310
2-20	1.8	3.7	35.0	1.60-2.83	657	0310
2-21	3.5	2.0	32.0	1.61-2.58	163	0310
2-22	3.5	2.0	35.0	1.68-2.67	10	0310
3-1	0.45	5.05	29.0	1.62-2.75	--	025
3-2	0.45	5.05	--	--	--	025
3-3	0.9	4.6	57.0	1.60-2.78	600	025
3-4	0.45	5.05	27.0	1.62-2.72	1316	025
3-6	0.9	4.6	28.0	1.89-2.64	906	025
3-7	1.35	4.15	25.0	1.80-3.13	760	025
3-8	1.8	3.7	26.0	1.64-2.75	156	025
3-9	2.6	2.9	32.0	1.85-320	164	025
3-10	3.0	1.5	30.0	1.88-2.70	121	025
3-11	3.5	2.0	27.0	1.93-2.64	156	025
3-12	4.0	1.5	29.0	1.65-2.86	224	025
4-1	0.5	5.0	9.0	1.9	all	N/A